

AD-A035 639

AVCO CORP LOWELL MASS SYSTEMS DIV  
MAGNETIC FLUID DENSITY SEPARATION SYSTEM FOR FINE POWDERS. (U)  
AUG 76 E P MCQUAID

F/G 14/2

F08606-74-C-0064

NL

UNCLASSIFIED

1 OF 2  
ADA035639

FILE  
DATE



FINAL REPORT

MAGNETIC FLUID DENSITY S  
SYSTEM FOR FINE POWD

Phase 1A

AFTAC PA No. VT/5415/-E

Contract No. - F08606-74-

ARPA Order No.

Date of Contract: 1 July 1

Contract Expiration Date: Marc

Prepared For

Headquarters, 1035th Technical O  
(HQ COMD USAF)

AFTAC/TR

Patrick Air Force Base, Flor

Everett P. McQuaid (617-452-8  
AVCO Corporation  
Systems Division  
Lowell, Massachusetts

| REPORT DOCUMENTATION PAGE   |   | READ INSTRUCTIONS BEFORE COMPLETING FORM                       |
|---|---|--|
| 1. REPORT NUMBER<br><i>(6)</i>  | 2. GOVT ACCESSION NO.   | 3. RECIPIENT'S CATALOG NUMBER                                  |
| 4. TITLE (and Subtitle)<br>Magnetic Fluid Density Separation System for Fine Powders  |   | 5. TYPE OF REPORT & PERIOD COVERED<br>Final<br>7/1/74 - 3/1/76 |
| 6. AUTHOR(s)<br><i>(10)</i><br>Everett P. McQuaid   | 7. CONTRACT OR GRANT NUMBER(s)<br><i>(15)</i><br>F08606-74-C-0064 new |  |
| 8. PERFORMING ORGANIZATION NAME AND ADDRESS<br>Avco Corporation<br>Systems Division<br>Lowell, Mass 01851   | 9. PROGRAM ELEMENT, PROJECT, TASK AREA & WORK UNIT NUMBERS<br>VT 5415 |  |
| 10. CONTROLLING OFFICE NAME AND ADDRESS<br>Headquarters, 1035th Technical Operations Gp., AFTAC/TR, Patrick AF Base, Florida 01851  | 11. REPORT DATE<br><i>(11)</i><br>1 Aug. 1976                         |  |
| 12. MONITORING AGENCY NAME & ADDRESS (if different from Controlling Office)<br><i>(9)</i><br>Final rept.<br>1 Jul 74-1 Mar 76   | 13. NUMBER OF PAGES<br>1  |  |
| 14. SECURITY CLASS. (of this report)<br>Unclassified  | 15. DECLASSIFICATION/DOWNGRADING SCHEDULE                             |  |
| 16. DISTRIBUTION STATEMENT (of this Report)<br><i>(12)</i> 131p, unlimited  | 17. APPROVED FOR PUBLIC RELEASE. DISTRIBUTION UNLIMITED.              |  |
| 18. SUPPLEMENTARY NOTES   |   |  |
| 19. KEY WORDS (Continue on reverse side if necessary and identify by block number)<br>Magnetic fluids, ferrofluids, powder separation, fine particles, density separation   |   |  |
| 20. ABSTRACT (Continue on reverse side if necessary and identify by block number)<br>A feasibility study was performed on the separation of mixtures of fine powders (ferrofluids) according to their densities in a gradient magnetic field. Using liquid oxygen and ferrofluids as the separation media, low yield separations of fine particle mixtures at densities up to 4 GM/cm <sup>3</sup> were achieved. A particle interaction force of magnetic origin is considered to be the primary factor influencing the quality of the |   |  |

separations. Additionally the use of ferrofluid as the separation medium alters the apparent density of powders less than about 50 <sup>μm</sup> inversely as their size making an accurate separation by density impossible. Liquid oxygen does not demonstrate this effect and is considered a promising medium for the separation of fine powders.

micrometers

APPROVED FOR PUBLIC  
RELEASE, DISTRIBUTION  
UNLIMITED

|   | <u>Page</u> |
|---|-------------|
|   | 1           |
| 1.0 SUMMARY   | 1           |
| 2.0 INTRODUCTION  | 4           |
| 2.1 Definition of the Problems  | 4           |
| 2.2 Particle Classification by Density                                  | 5           |
| 2.3 Density Separation in Standard Heavy Liquid Media                   | 7           |
| 3.0 MAGNETIC MEDIA DENSITY SEPARATION                                   | 11          |
| 3.1 Theory of Magnetic Fluid Levitation                                 | 11          |
| 3.2 Magnetic Liquids  | 24          |
| 3.2.1 Ferrofluids   | 24          |
| 3.2.2 Liquid Oxygen   | 30          |
| 3.3 Forces on Fine Particles  | 32          |
| 3.3.1 Mechanism of Powder Agglomeration/Conglomeration                  | 32          |
| 3.3.2 Particle Dispersion Mechanisms in a Liquid Phase                  | 36          |
| 3.3.3 Particle Interaction Forces                                       | 37          |
| 3.4 Applications of Ferrofluid Sink-Float Separations Developed by Avco | 40          |
| 3.4.1 Constant Density Separation                                       | 40          |
| 3.4.2 Separator Magnet Design   | 41          |
| 3.4.3 Battelle Laboratory Separator                                     | 42          |
| 3.4.4 Non-Ferrous Scrap Separator                                       | 42          |
| 4.0 EXPERIMENTAL EFFORTS AND RESULTS                                    | 46          |
| 4.1 Ferrofluids   | 46          |
| 4.2 Liquid Oxygen   | 62          |
| 5.0 MAGNET DESIGN   | 74          |
| 6.0 CONCLUSIONS AND RECOMMENDATIONS                                     | 77          |
| 6.1 Conclusions   | 77          |
| 6.2 Recommendations   | 82          |

|                                 |                                     |
|---------------------------------|-------------------------------------|
| ACCESSION REF                   |                                     |
| NTIS                            | White Section                       |
| DOC                             | <input checked="" type="checkbox"/> |
| UNANNOUCED                      | <input type="checkbox"/>            |
| JUSTIFICATION                   |                                     |
| BY                              |                                     |
| DISTRIBUTION/AVAILABILITY CODES |                                     |
| Dist.                           | AVAIL. and/or SPECIAL               |
| A1                              |                                     |

Appendix A - Calculation of the Force on a Magnetic Dipole in a Magnetic Field by Wm. Harrold

Appendix B - Second Order Effects in Fluidmagnetic Buoyancy by R.A. Curtis

Appendix C - High Gradient Magnet Design

LIST OF ILLUSTRATIONS

| <u>Figure</u> |   | <u>Page</u> |
|---------------|---|-------------|
| 3.1.1         | Coordinate System for Powder Separation Magnet  | 12          |
| 3.1.2         | Forces on a Non-Magnetic Object in a Gradient Magnetic Field  | 13A         |
| 3.1.3         | Direction Vectors for Particles Released Within Magnetic Liquid in a Constant Gradient Magnetic Field.<br>$\Delta P = .05$          | 18          |
| 3.1.4         | Direction Vectors for Particles Released Within Magnetic Liquid in a Constant Gradient Magnetic Field.<br>$\Delta P = .10$          | 19          |
| 3.1.5         | Direction Vectors for Particles Released Within Magnetic Liquid in a Constant Gradient Magnetic Field.<br>$\Delta P = .15$          | 20          |
| 3.1.6         | Particle Trajectories for Particles Released from Several Locations Within a Magnetic Liquid in a Constant Gradient Magnetic Field. | 21          |
| 3.2.1         | Normalized Magnetization Curve for a Typical Ferrofluid.  | 25          |
| 3.2.2         | Magnetization Characteristic for Liquid Oxygen  | 31          |
| 4.1.1         | Size Distribution Histograms  | 50          |
| 4.1.2         | Flotation Characteristics of Glass Microbeads<br>$E_v = .003$   | 51          |
| 4.1.3         | Flotation Characteristics of Glass Microbeads<br>$E_v = .012$   | 52          |
| 4.1.4         | Fine Particle Separation Apparatus for Low Particle Concentration   | 58          |
| 4.1.5         | Float Fractions   | 59          |
| 4.1.6         | Sink Fractions and Microscope Calibration   | 60          |
| 4.2.1         | Liquid Oxygen Separation Apparatus  | 63          |
| 4.2.2         | Magnetization Data for Liquid Oxygen  | 64          |
| 4.2.3         | Measured Field Intensity of Laboratory Magnet   | 65          |
| 4.2.4         | Apparent Density at Top and Bottom of Working Volume in Liquid Oxygen   | 66          |

| <u>Figure</u>   | <u>Page</u> |
|---|-------------|
| 4.2.5 Results of the Separation in Liquid Oxygen of Aluminum Oxide Particles and Glass Microbeads | 70          |
| 4.2.6 Results of the Separation in Liquid Oxygen of Diamond Particles and Glass Microbeads        | 71          |
| 4.2.7 Mixture "A"   | 72          |
| 4.2.8 Results of Separation of Mixture "A"  | 73          |
| 5.1.1 Separation Magnet Specifications  | 75          |

LIST OF TABLES

| <u>Table</u> |  | <u>Page</u> |
|--------------|--|-------------|
| I            | Densities of Common Metal Oxides         | 6           |
| II           | Heavy Liquids for Mineral Separation     | 10          |
| III          | Separation of Zinc Alloy and Brass Scrap | 45          |

## 1.0 SUMMARY

This report presents the results of a study examining the feasibility of using magnetic liquids operating in a gradient magnet field to separate mixtures of fine powders according to their densities. The majority of the efforts concentrated on evaluating separation systems using a colloidal suspension of very fine magnetic particles. These suspensions, called ferrofluids have been applied successfully by Avco in the separation by density of mixtures of large items, such as the non-ferrous portion of automobile scrap. Now, in applying these techniques to the separation of fine particles (1 to 100  $\mu$ m) several factors whose effects were insignificant in working with large objects became controlling elements in obtaining successful separations of mixture of fine particles.

In any sink/float separation process it is necessary that the materials to be separated are physically separated and dispersed throughout the separation medium. The use of magnetic liquids for fine particle separations introduces several factors which tend to favor particle agglomeration and resulting misclassification.

The presence of non-magnetic particles in a magnetic liquid distorts the magnetic field around the particles in such a way that the particles are attracted to each other. This force of attraction is directly related to the strength of the magnetic fluid and particle size and inversely proportional to interparticle spacing. Thus for any particular separation system involving particles having a narrow size distribution the particle interaction force is minimized by operating with fluid of low magnetization and at low volumetric concentration of the particles.

A modified hyperbolic quadripole magnet is used to generate a magnetic field having a linear vertical gradient. At any point not on the axis of the magnet the magnetic field also possesses a horizontal magnetic gradient which, in the magnetic fluid, results in a horizontal force on all particles. This force tends to propel the particles toward the center of the magnet thereby increasing the particle concentration and opportunities for particle agglomeration and misclassification. The ratio of the horizontal magnetic force to the vertical magnetic force on a particle is a function of the location of that particle within the magnetic gap in the magnetic liquid.

Thus to minimize the undesirable centering force on particles it is necessary to operate at a low vertical gradient or to operate low in the magnet gap, a situation which also limits the maximum gradient attainable.

The apparent density of a magnetic liquid operating in a gradient magnetic field is proportional to the product of the magnetization of the fluid and the gradient of the field. Therefore the conflicting requirements for minimum particle interaction of low fluid magnetization and small magnetic gradients must be compromised and optimized to attain desired apparent density of the medium. In any case the quality of separation is enhanced by operating at low particle concentration at the expense of particle separation rate.

Ferrofluids have demonstrated an undesirable characteristic of increasing the effective density of fine particle thus requiring an increased fluid apparent density to levitate fine particles. This results in separation by size as well as density which is an undesirable characteristic. This phenomenon has been

tentatively attributed to the inhomogeneous nature of the ferrofluid and to a force of attraction between the ferrite particles of the ferrofluid and the particles to be separated. It appears that a layer of ferrite particles is deposited on the particles to be separated conferring on them magnetic properties such that the particles respond in the separator as if they are of a different density than they actually are. This effect is especially pronounced in particles below  $10 \mu m$  in size and is insignificant for particles larger than about  $100 \mu m$ . This behavior is peculiar to ferrofluids and was not found when operating with liquid oxygen as the magnetic medium.

Some moderate degree of success in density separations has been obtained with ferrofluids and liquid oxygen on particles as small as several microns in size by operating at very low particle concentrations. With ferrofluids the effects of particle interaction and centering forces were circumvented by injecting the particles, essentially one at a time, into the center of the separation chamber wherein, it is assumed, each particle floats or sinks uninfluenced by other particles. This injection technique has not been tried in liquid oxygen but it should work as well in this medium while eliminating the undesirable modification to the effective density of the particles experienced with ferrofluids.

At the conclusion of this program, the agglomeration and related particle handling techniques had not been sufficiently developed to provide practical, large quantity separations. Further refinement of these techniques using liquid oxygen as the separation medium appeared to be promising avenues for further evaluation.

## 2.0 INTRODUCTION

### 2.1 Definition of the Problem

The analysis of particles released to the environment from industrial facilities is hindered because any collected sample will contain many foreign particles in addition to the particles of interest. The collected particles, which are usually small in size, are often combined with others in the form of agglomerates or conglomerates. If the particles of interest are small, and represent only a small fraction of the total particle population in the collected sample, finding and selectively analyzing all particles of interest in the sample represents a formidable task.

The study of particulate emissions can be carried out successfully only if the particles of interest have a characteristic property which allows them to be identified and then separated from the bulk of the sample for subsequent analysis. Specialized identification techniques exist for limited classes of particles, but these are so specific that many other particles of interest are not identified and thus often not analyzed. A general method of sample preparation is required that would not only separate all particles of interest from contaminating particles, but, if required, classify the particles of interest in various characteristic groups. Such a process would also have to be absolute, in that it could not result in the loss or misclassification of any particles of interest.

Any method of general applicability would have to be keyed to a basic intrinsic physical property. The values of this intrinsic property for the particles of interest as a class must be significantly different than the values of this property exhibited by the foreign contaminating particles. In order to sub-classify the particles of interest, this intrinsic property should be different for the various classes of materials one wishes to examine.

The method must be able to classify the particles smaller than  $20 \mu m$  in size which are characteristically found in environmental samples. While a capacity to classify particles smaller than  $1 \mu m$  in size would be desirable, major emphasis should be placed on the classification of particles larger than  $1 \mu m$  in size that are of principal analytical interest. The method should also account for the particles that are combined as agglomerates and/or conglomerates. It must incorporate provisions for dispersing the agglomerated materials into separate particles without irreversible physical or chemical changes. The method should, furthermore, be practical and operable in a standard laboratory environment.

## 2.2 Particle Classification by Density

Density is one of the most commonly measured intrinsic physical properties of a material. There are large differences in the densities of various classes of solid materials. In particular, the densities of particles of interest released to the environment from industrial facilities are significantly higher than the densities of the bulk of the unwanted foreign particles also present in the sample. Particles of interest are characteristically metal oxides that have a relatively high density. As shown in Table I, the density of these materials is characteristically in excess of  $3 \text{ gr/cm}^3$ . The density of the principal contaminants in the collected sample are characteristically less than  $3 \text{ gr/cm}^3$ . These contaminants consist mainly of vegetable origin that have a density of approximately  $1 \text{ gr/cm}^3$ , of carbonaceous products (e.g., soot) that has a density of about  $1.8 \text{ gr/cm}^3$ , and of common minerals, principally silicates (e.g., sand) or alumino-silicates (clays), that have characteristic densities of less than  $3 \text{ gr/cm}^3$ . Examples include: Quartz,  $\text{SiO}_2$ ,  $\rho = 2.65 \text{ gr/cm}^3$ , and kaolinite,  $\text{Al}_2\text{O}_3 \cdot 2 \text{ SiO}_2 \cdot 2 \text{ H}_2\text{O}$ ,  $\rho = 2.60 \text{ gr/cm}^3$ .

TABLE I  
DENSITIES OF COMMON METAL OXIDES

| <u>Compound</u>            | <u>Formula</u>                 | <u>Density, gr/cm<sup>3</sup></u> |
|----------------------------|--------------------------------|-----------------------------------|
| Aluminum Oxide             | Al <sub>2</sub> O <sub>3</sub> | 3.98                              |
| Chromium Sesqui-Oxide      | Cr <sub>2</sub> O <sub>3</sub> | 5.21                              |
| Cobalt Oxide               | Co <sub>2</sub> O <sub>3</sub> | 5.18                              |
| Copper Oxide               | CuO                            | 6.40                              |
| Ferric Oxide               | Fe <sub>2</sub> O <sub>3</sub> | 5.24                              |
| Lead Oxide                 | PbO                            | 9.53                              |
| Magnesium Oxide            | MgO                            | 3.65                              |
| Mercury Oxide              | HgO                            | 11.14                             |
| Nickel Oxide               | NiO                            | 7.45                              |
| Silver Oxide               | Ag <sub>2</sub> O              | 7.14                              |
| Stannic Oxide              | SnO <sub>2</sub>               | 6.95                              |
| Titanium Oxide<br>(rutile) | TiO <sub>2</sub>               | 4.26                              |
| Zinc Oxide                 | ZnO                            | 5.47                              |

The examination and analysis of particulate pollutants would be greatly simplified if a preparatory method were available that would classify particles into three density cuts:

Cut I      Particles of density of less than 4 gr/cm<sup>3</sup>

Cut II      Particles of densities ranging from about 4 gr/cm<sup>3</sup> to about 7 gr/cm<sup>3</sup>

Cut III      Particles of densities greater than about 7 gr/cm<sup>3</sup>

The first cut would contain the unwanted particles and should be free of particles of interest. The second cut and third cut would be concentrated samples of different types of particles of interest. The technique should be accurate to within 10%, i.e., a 10% density overlap between cuts would be allowable.

### 2.3 Density Separation in Standard Heavy Liquid Media

There exists standard laboratory methods of separating two or more solids which depend on the differences in the densities of the components. The most common method involves sink-float separation in a liquid medium. Sink-float separation operates on the principle that when two objects of different density are immersed in a fluid of intermediate density, the less dense will float and the more dense will sink. The separation is completed by individually removing the two solid fractions. This method and its applications have been reviewed by Browning. While simple in principle, solid separation by the classical sink-float method has a number of severe experimental shortcomings. These include:

- a. Pure liquids or solutions do not cover the range of densities of interest. Most liquids have low densities whereas most solids have high densities. There are very few materials that are liquid at ambient temperature and exhibit a density greater than 2 gr/cm<sup>3</sup>. Commonly used heavy liquids for mineral separation are listed in Table II. Note that these liquids all have a density below 5 gr/cm<sup>3</sup>.
- b. An accurate sink-float separation is obtained only if there is complete liberation of the different particles in the solid mixture. If one is dealing with very fine particles, it is necessary to ensure that the sample is well-dispersed in the sink-float medium. Otherwise, the agglomerates will behave as particles with a density intermediate between those of the ultimate particles, thereby resulting in misclassification of the ultimate particles. Browning reports that fine powders tend to "ball up" in the dense liquids listed in Table II, indicating extensive flocculation.<sup>2</sup> This is the opposite of the basic requirement of a high degree of dispersion.
- c. The density of a given liquid is a constant value which is not readily varied. Changes in temperature will only result in small variations in the liquid density. In order to obtain different density cuts, it is necessary to carry out a series of sink-float separations in different liquids of varying densities. In order to prevent contamination of the different liquids, it is necessary that the solids be completely dried after each separation.

d. There is an unfortunate correlation between the toxicity and density of liquid media. Whereas carbon tetrachloride is only mildly toxic, acetylene bromide and methylene iodide are considered toxic, and the thallium salts are extremely toxic and poisonous to the touch. Their use requires extreme caution and special protective equipment.

A variation of sink-float separation in a liquid of constant density is the classification of particles according to their densities in a density gradient column. In a density gradient column, the density of the liquid increases with depth; the liquid at the top of the pool is less dense than the liquid at the bottom of the pool. A density gradient can be established either by imposing a temperature gradient on a pure liquid, adding heat at the top of the pool and removing it at the bottom, or by having a concentration gradient. In the latter case, two miscible liquids of different density are added in variable proportions along the length of the column. The concentration of the denser liquid increases with column depth. Density gradient columns have been mainly used as a method of measuring the density of an unknown solid sample. By calibrating the column with reference objects of known density, the density of the liquid at any depth is known. A solid object introduced into a column will be in neutral buoyancy at a depth where its density and that of the liquid are equal. The equilibrium position of the solid in the column is, therefore, a direct measure of its density.

TABLE II  
HEAVY LIQUIDS FOR MINERAL SEPARATION

| <u>Liquid</u>  | <u>Density (25°C)</u> | <u>Hazard</u>          |
|--|-----------------------|------------------------|
| Water  | 1.00                  | None                   |
| Carbon Tetrachloride   | 1.58                  | Mildly Toxic           |
| Tetrabromoethane (sym)<br>(Acetylene Tetrabromide)                     | 2.96                  | Toxic                  |
| Methylene Iodide   | 3.32                  | Toxic                  |
| Thallium Formate, Aqueous<br>Solution                                  | 3.5*                  | Extremely<br>hazardous |
| Saturated Thallium Malonate -<br>Thallium Formate, Aqueous<br>Solution | 4.9*                  | Extremely<br>hazardous |

\*Can be diluted with water to provide liquids of lower density

Density gradient columns have limited use as a means of separating the components of a particulate mixture according to their densities.

Density gradient classification, in addition to having the same drawbacks as sink-float separation, presents additional difficulties: a) any mixing or turbulence destroys the density gradients, irreversibly in the case of columns based on a concentration gradient; b) preparing and maintaining a gradient column is not easy and requires considerable art. Introducing and removing the solid particles without upsetting the gradient presents severe problems.

In conclusion, standard methods of sink-float density separation have severe limitations which preclude their use as a method of separating the components of a particulate mixture. An improved separation process is required to successfully exploit the differences in the densities of different particles in a collected sample in order to obtain complete and efficient separation of the particles of interest.

### 3.0 MAGNETIC MEDIA DENSITY SEPARATION

#### 3.1 Theory of Magnetic Fluid Levitation

A schematic presentation of the coordinate system used for the powder separation magnet is given in Fig. 3.1.1.

An object immersed in a liquid experiences a force,  $F_g$ , due to the gravitational attraction of the earth and a buoyant force,  $F_b$  proportional to the volume and density of the liquid displaced:

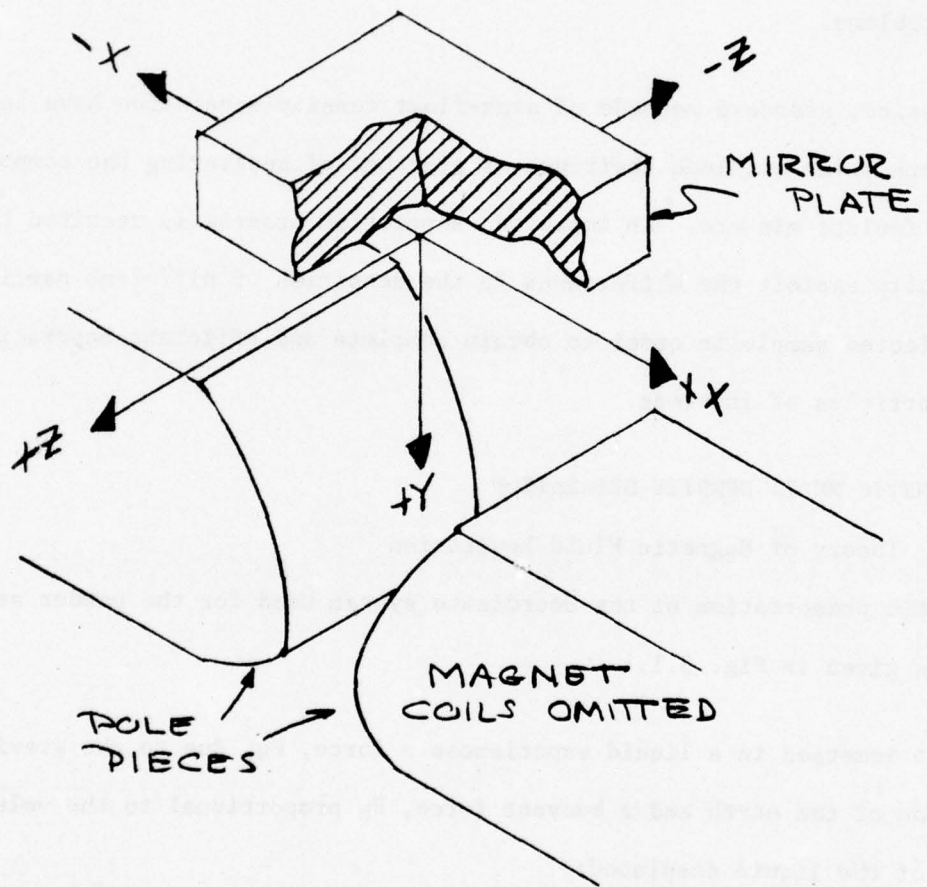
$$F_g = -\rho g V \text{ dynes}$$

$$F_b = +\rho_f g V \text{ dynes}$$

where  $\rho$  is the density of the object in  $\text{gm/cm}^3$

$\rho_f$  is the density of the liquid in  $\text{gm/cm}^3$

FIG 3.1.1. COORDINATE SYSTEM FOR  
POWDER SEPARATION MAGNET



$g$  is a vector in the gravity direction with a magnitude equal to the gravitational constant,  $980 \text{ cm/sec.}^2$

and  $V$  is the volume of the object,  $\text{cm}^3$ .

The minus sign indicates a force that is vertically downward.

A magnetic body force is generated when a magnetic liquid is placed in a non-uniform magnetic field. Under these circumstances there is a net magnetic force on the fluid which tends to drive it, like all magnetizable objects, toward the region of highest magnetic field intensity. The magnetic body force,  $F_m'$ , is, to a first approximation, equal to the product of the induced magnetic dipole moment,  $M$ , the applied field gradient,  $\nabla$ , and the volume  $V$  of the fluid.

$$F_m' = M \nabla V$$

When a non-magnetic object is immersed in a magnetic liquid in the presence of a magnetic field gradient, there is a magnetic force,  $F_m$ , on the object which tends to expel it to a region of minimum field. This magnetic field gradient is aligned to be parallel to the direction of the gravity the magnetic body force can be adjusted to augment the natural buoyancy of the fluid and cancel the gravitational force on a nonmagnetic object. In this manner an object of high density will float in a magnetic liquid of low natural density as shown in Fig. 3.1.2.

When the object immersed in the magnetic liquid is itself magnetic, the above treatment must be modified. If the dipole moment of the object is smaller than that of the ferrofluid, it is still forced from the region of high field to a region of low field. The magnitude of the force is smaller, however, than it would have been if the object were completely non-magnetic. The object behaves as if it were an object of higher density than its true density. If the magnitude of the magnetic dipole

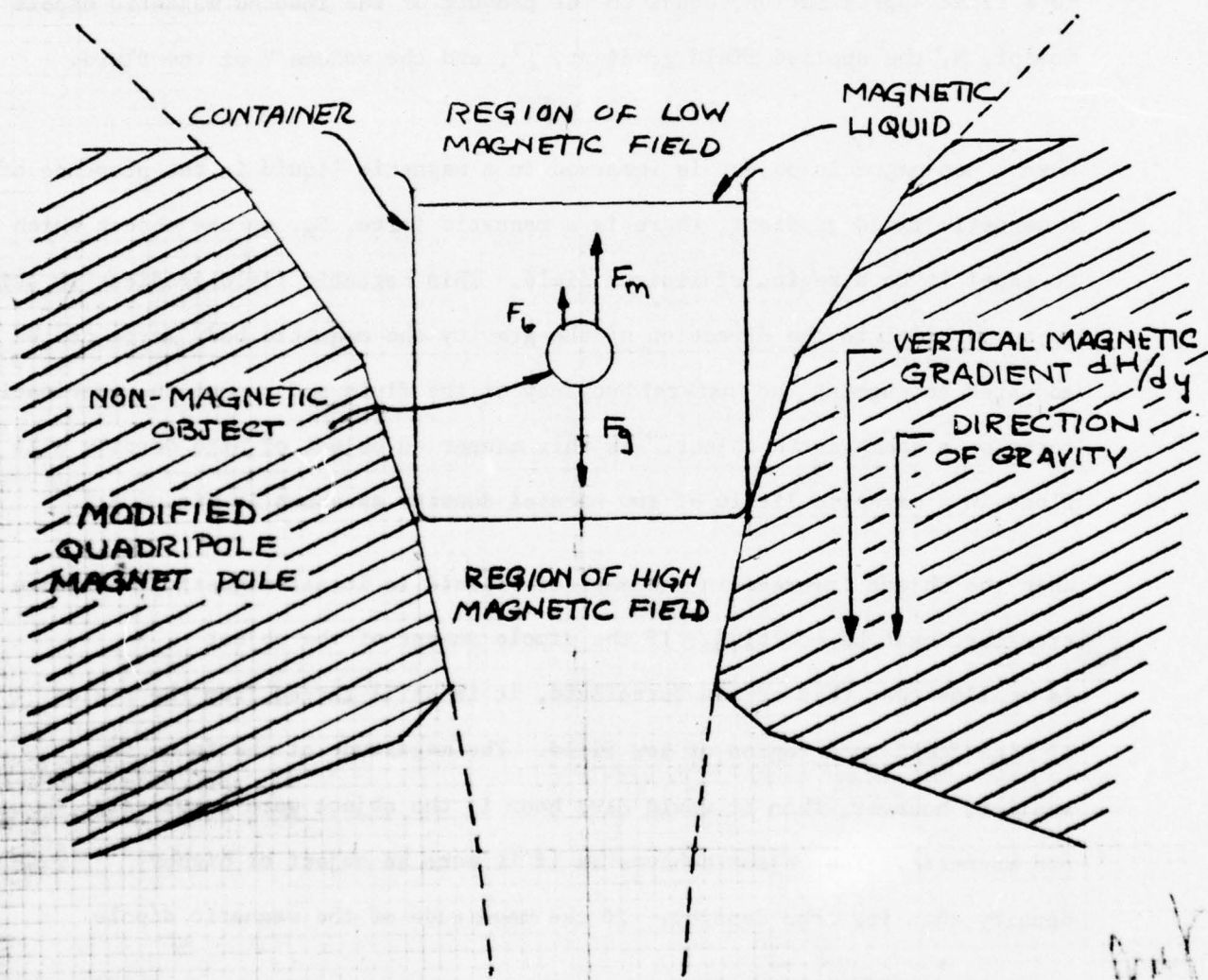


FIG 3.1.2 FORCES ON A NON MAGNETIC OBJECT IN A GRADIENT MAGNETIC FIELD

moment of the object is greater than that of the magnetic liquid the object will move to the region of highest magnetic field and displace the magnetic liquid to a region of lower magnetic field. Such object cannot be floated in a ferrofluid.

The net force on an object is

$$\underline{F} = (\rho_f - \rho) g V + M \underline{T} V$$

where vector notation is introduced to accommodate the magnetic gradient vector  $\underline{T}$  which has components other than vertical which are important to the separation of objects of different densities.

At equilibrium the gravitational force on the object is exactly balanced by the fluid buoyancy and vertical magnetic forces such that

$$\begin{aligned} \sum F_y &= 0 \\ \text{and } \rho_g V &= \rho_f g V + M T_y V \\ \text{or } \rho &= \rho_f + \frac{M T_y}{g} = \rho_a \end{aligned}$$

Now, since the particle is at equilibrium, the apparent density of the magnetic medium,  $\rho_a$  may be defined as equal to the density of the particle.

A constant vertical magnetic gradient,  $T$ , is generated by a modified hyperbolic quadripole magnet. Two of the poles of the quadripole arrangement are eliminated by substituting a "mirror plate" of magnetic material at a plane of zero magnetic potential. For space and material reasons the lower portions of the hyperbola, well removed from the region of interest, are truncated. A coordinate system is established in which X is the lateral

direction between pole faces, with  $X = 0$  being the center of the gap  $Y$  is the vertical direction increasing in a positive sense downward with  $Y = 0$  being at the mirror plate and  $Z$  the horizontal direction parallel to the pole faces, orthogonal to  $X$  and  $Y$ .  $Z = 0$  is the mid point of the pole face.

For infinite  $Z$  the magnetic field,  $H$ , between the poles and below the mirror plate is given by:

$$H = T_x \hat{e}_x + T_y \hat{e}_y$$

where  $\hat{e}_x$  and  $\hat{e}_y$  are unit vectors and  $T$  is the magnetic field gradient along the  $Y$  axis.

Also:  $H = |\vec{H}| = T (x^2 + y^2)^{\frac{1}{2}}$

The gradient of the magnetic field strength is

$$\begin{aligned} \nabla H &= T \left[ \frac{x}{(x^2 + y^2)^{1/2}} \hat{e}_x + \frac{y}{(x^2 + y^2)^{1/2}} \hat{e}_y \right] \\ &= T_x \hat{e}_x + T_y \hat{e}_y \end{aligned}$$

Of interest also is the ratio of the horizontal component of the gradient,  $T_x$ , to the vertical component of the gradient,  $T_y$ :

$$\frac{T_x}{T_y} = \frac{x}{y}$$

The force on an object may now be expressed as:

$$F = [(P_f - P) g V + M T_y V] \hat{e}_y + M T_x V \hat{e}_x$$

In a separation of objects of densities differing by say, 10% the  $M T$  product is adjusted such that the upward force on a light object,  $P_f g V + M T_y V$  is about 5% greater than the gravitational force on the object,  $- P_f V$  and the downward force on a heavy object is 5% less than the gravitational

force. The net vertical force, upward or downward, is rather small.

The horizontal magnetic force,  $MT_x V$ , is directed inward toward  $X = 0$  and is related to the vertical magnetic force by:

$$F_x = MT_x V = \frac{x}{y} F_y$$

And is thus seen to be a function of the location of the object within the magnet poles. In the center of the magnet the horizontal force is zero; at any other location it can be quite significant.

As an example, consider the forces on a particle located at X-Y coordinates (1, 2) which is near the surface of the magnetic liquid near the pole face within the "working volume" of the magnet. For these calculations let  $\rho_f = 1 \text{ gm/cm}^3$ ,  $\rho = 3 \text{ gm/cm}^3$  and let the net vertical force,  $F_y$ , be less than the gravitational force on the particle by 5%.

$$\text{i.e. } \rho_f g + MT_y = .95 \rho g$$

$$\text{and } F_y = .05 \rho g = -147 \text{ dynes/cm}^3$$

The vertical component of the magnetic force is

$$\begin{aligned} F_{my} &= MT_y = (.95 \rho - \rho_f)g \\ &= 1813 \text{ dynes/cm}^3 \end{aligned}$$

The horizontal component of the magnetic force is

$$F_{mx} = \frac{x}{y} F_{my} = \frac{1}{2} F_{my} = 906 \text{ dynes/cm}^3$$

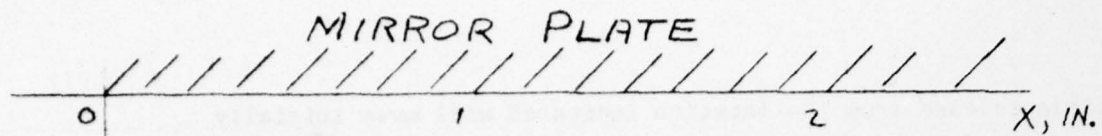
A particle release from the location indicated will move initially toward the center of the magnet at an angle  $\theta = \tan^{-1} \frac{F_x}{F_y}$  with respect to the horizontal.

In this case  $\theta = \tan^{-1} \frac{147}{906} = 9^\circ$

Additional particle direction vectors have been calculated and are shown in Figures 3.1.3, 3.1.4 and 3.1.5 for  $\Delta \rho$ 's of .05, .10 and .15 gm/cm<sup>3</sup> which would correspond to particle density differences of 10, 20 and 30% respectively in a separation in which the apparent density of the magnetic medium is set midway between the densities of the component to be separated.

Figure 3.1.6 is a plot of the trajectories of particles released from several locations within the magnetic liquid for conditions approximating those of the laboratory experiments. The particle trajectories from points A and B are for a  $\Delta \rho$  of 10% and from points C & D of 15%. It may be seen that the horizontal force on a particle is predominant for particles well removed from the centerline of the magnet such that the particles initially move to the center of the magnet more rapidly than they sink. The particles then approach the centerline asymptotically where they descent in a line in this case or a narrow sheet if one considers the third dimension of the magnet.

It should be noted that for the density differences cited, which represent realistic separation situations, the particles have moved to a very narrow band within the first inch of the "working height" thereby greatly increasing the particle concentration and opportunities for particle agglomeration.



Q

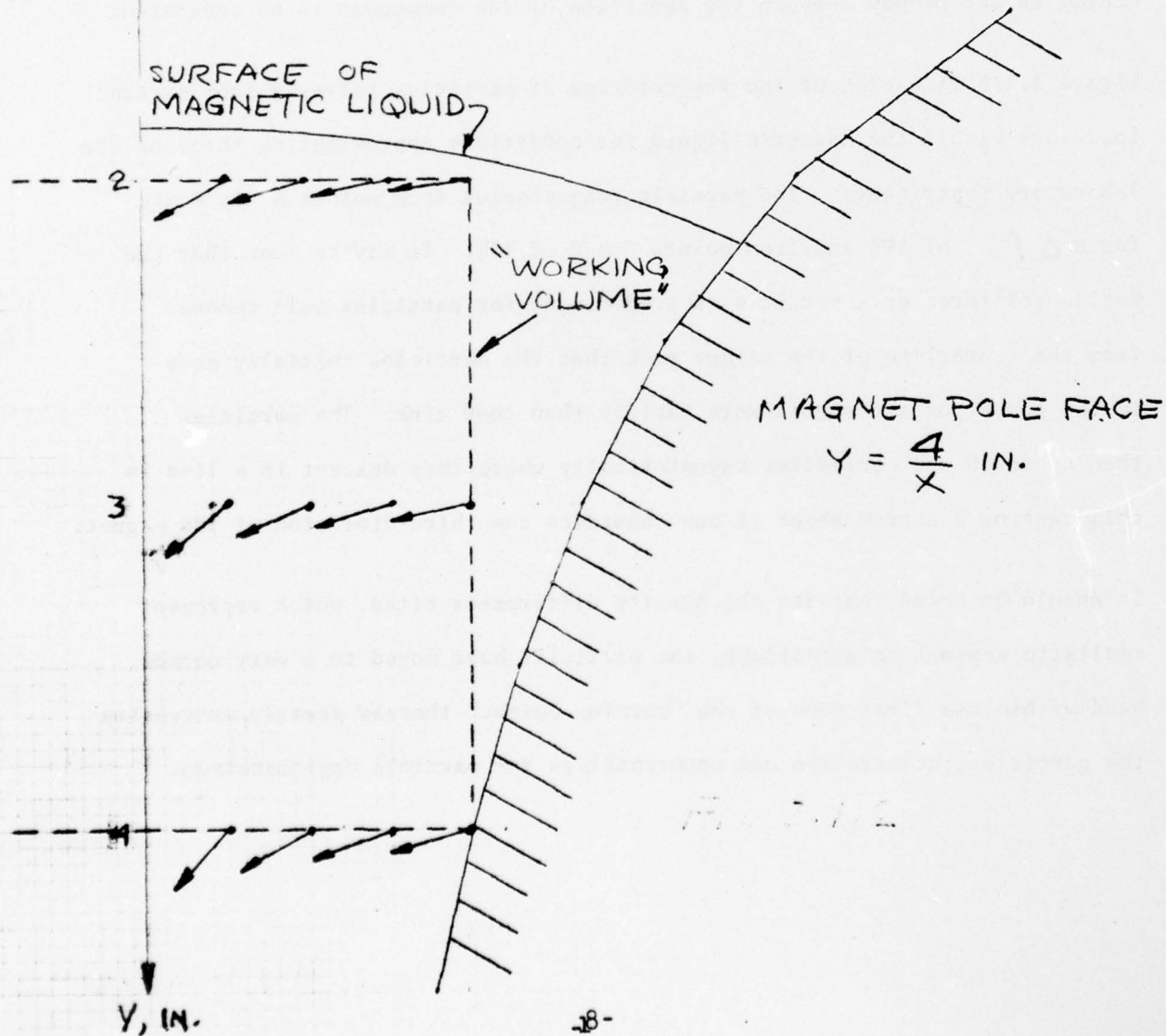
FIG 3.1.3

DIRECTION VECTORS FOR PARTICLES  
RELEASED WITHIN MAGNETIC  
LIQUID IN A CONSTANT GRADIENT  
MAGNET FIELD

$$\rho_0 = 3 \text{ GM/CM}^3$$

$$\rho_p = 1 \text{ GM/CM}^3$$

$$\Delta\rho = \rho_0 - \rho_p = .05 \rho_0$$



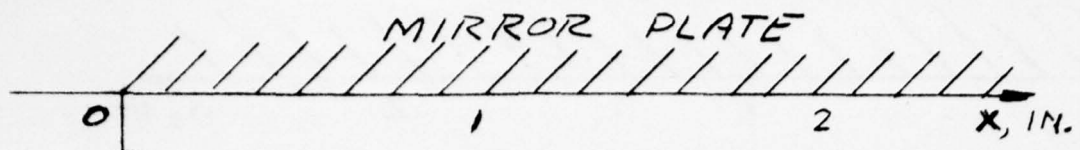


FIG 3.1.4

DIRECTION VECTORS FOR PARTICLES  
RELEASED WITHIN MAGNETIC  
LIQUID IN A CONSTANT GRADIENT  
MAGNETIC FIELD

$$\rho_0 = 3 \text{ GM/CM}^3$$

$$\rho_f = 1 \text{ GM/CM}^3$$

$$\Delta\rho = \rho_0 - \rho_f = \underline{.10 \rho_0}$$

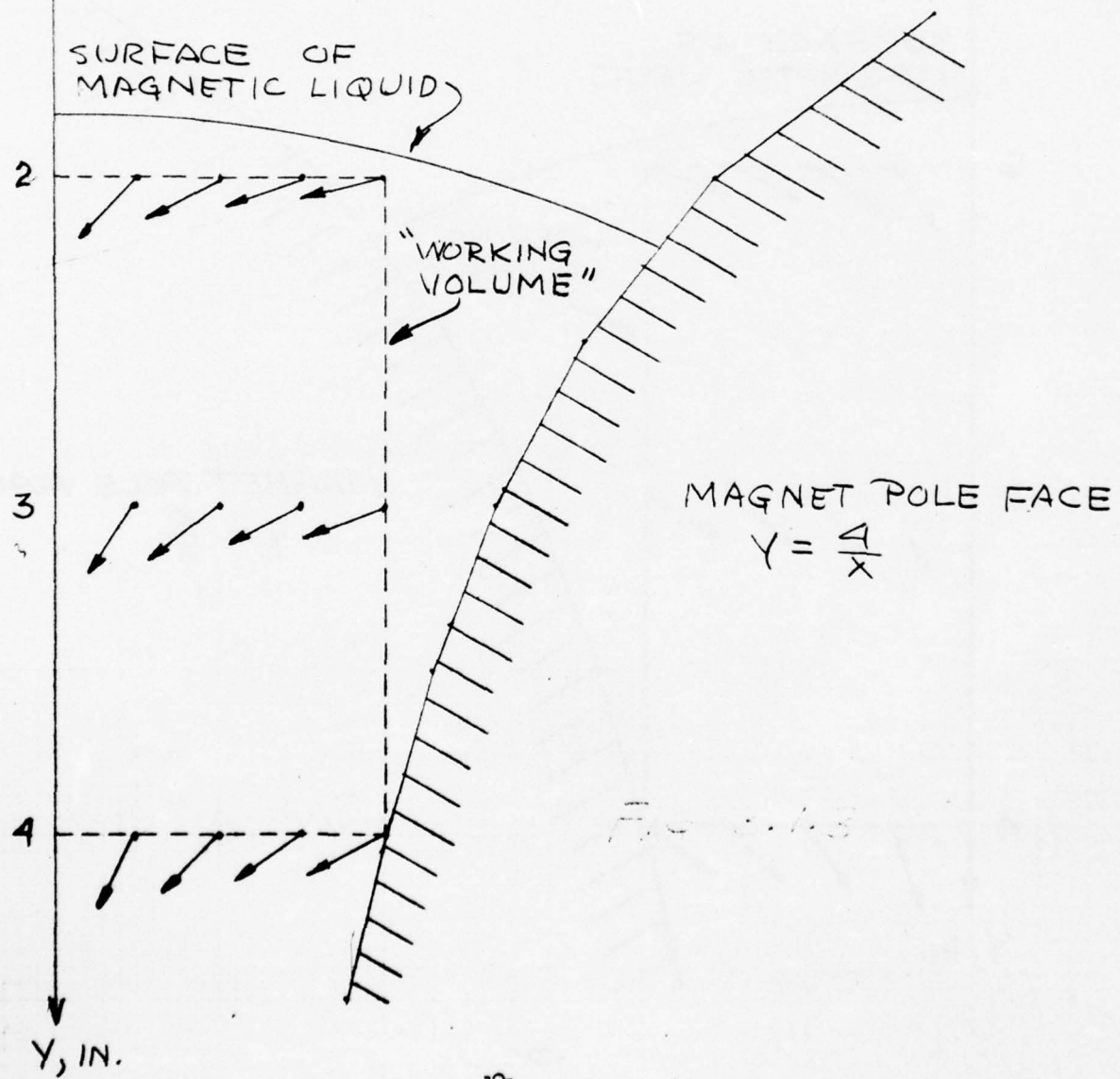


FIG 3.1.5

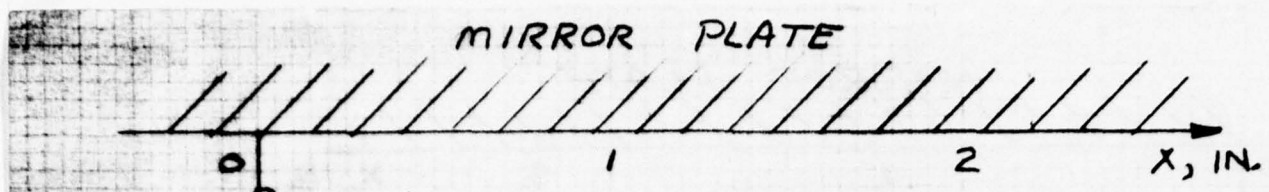


FIG 3.1.5

DIRECTION VECTORS FOR PARTICLES  
RELEASED WITHIN MAGNETIC  
LIQUID IN A CONSTANT GRADIENT  
MAGNETIC FIELD

$$\rho_0 = 3 \text{ GM/CM}^3$$

$$\rho_f = 1 \text{ GM/CM}^3$$

$$\Delta \rho = \rho_0 - \rho_f = .15 \rho_0$$

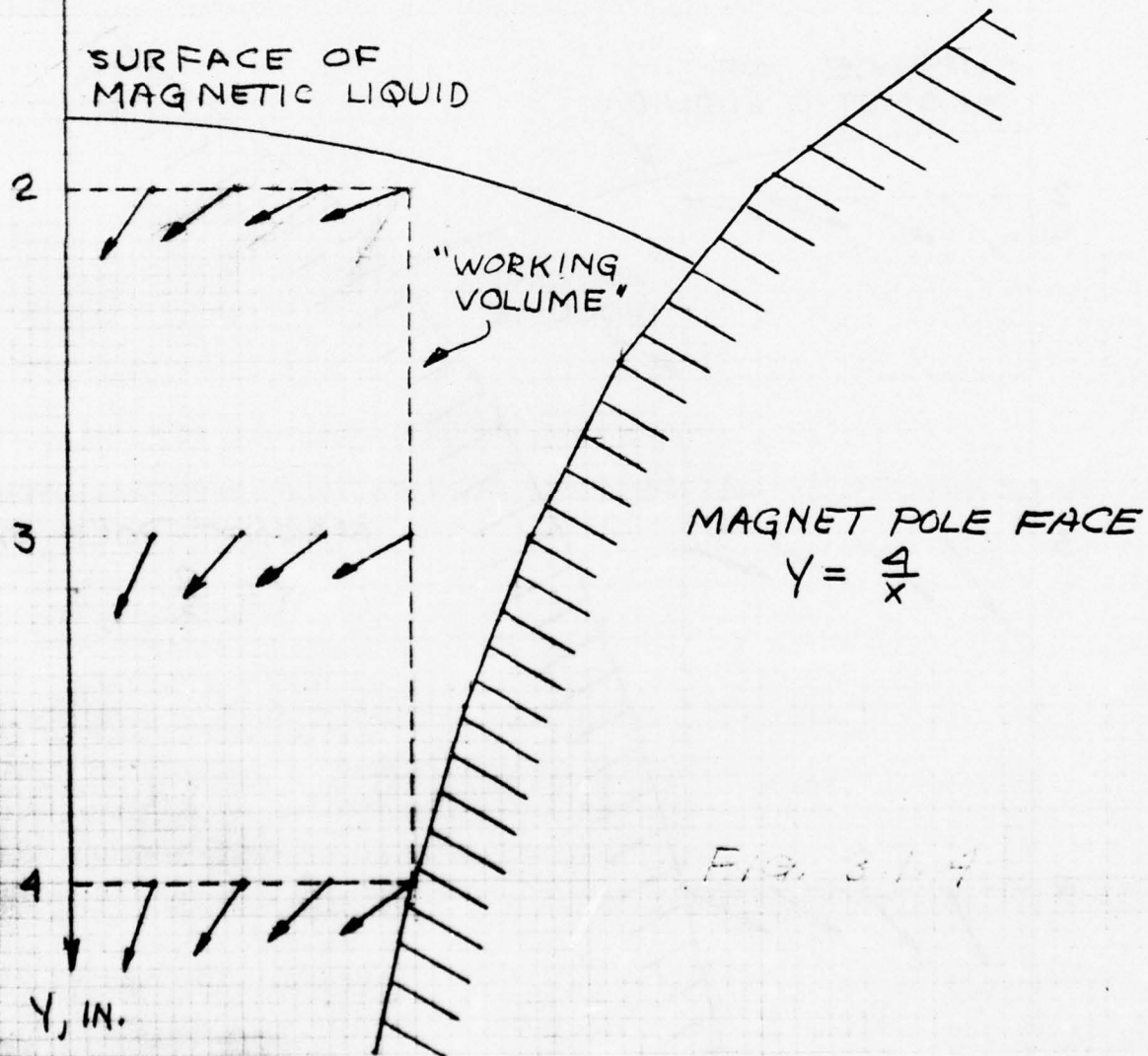


FIG 3.1.6

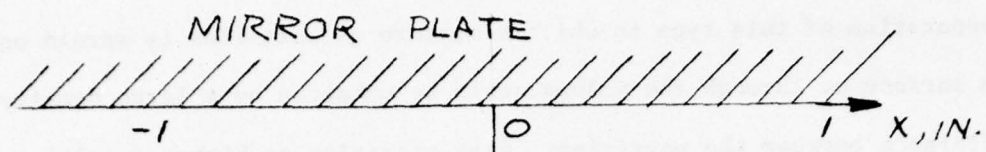
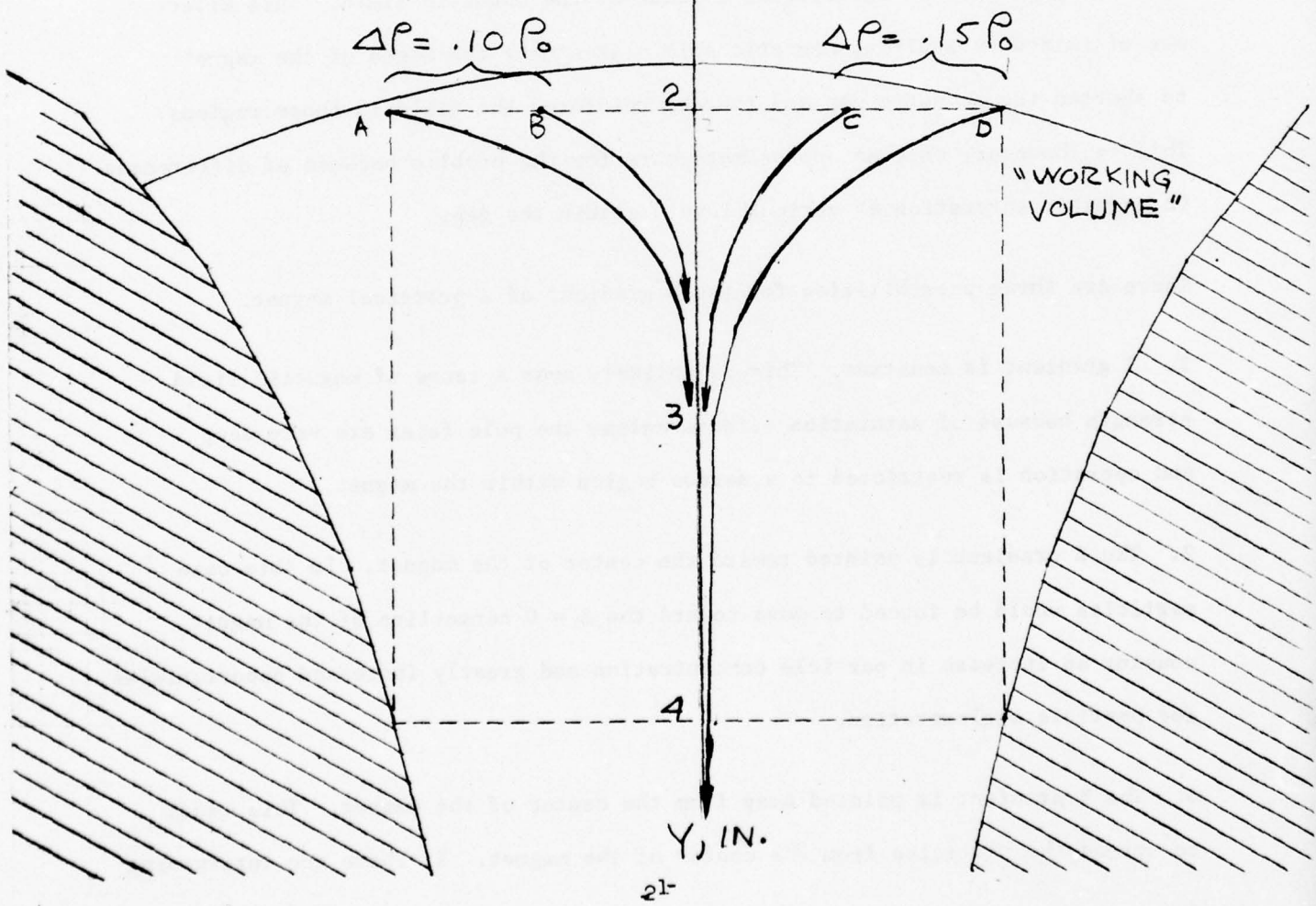


FIG 3.1.6

PARTICLE TRAJECTORIES  
FOR PARTICLES RELEASED  
FROM SEVERAL LOCATIONS  
WITHIN A MAGNETIC  
LIQUID IN A CONSTANT  
GRADIENT MAGNETIC FIELD

$$\rho_0 = 3 \text{ GM/CM}^3$$

$$\rho_f = 1 \text{ GM/CM}^3$$



A separation of this type in which a mixture of particles is spread on the surface or through the volume would be enhanced by a large density difference between the particles. Also operating at higher densities the natural buoyant contribution of the fluid is proportionately less with the result that horizontal centering force will be significantly increased.

For a magnet of infinite or large pole face dimension the magnetic field gradient in the Z-direction is zero. In a practical situation there are Z magnetic gradients which must be accounted for. In the rather narrow laboratory magnet used in the experiments of this project there were pronounced magnetic gradients due to the weakening of the magnetic field near the edges of the magnet because of fringing effects of the magnetic field. This effect was minimized by applying magnetic shim plates near the edges of the magnet to shorten the magnetic gap and thereby reinforce the field in those regions. This is, however, only an approximate cure for the problem because of differences in magnetic saturation at various levels within the gap.

There are three possibilities for the Z gradient of a practical magnet.

1. Z gradient is constant. This is unlikely over a range of magnetic field strength because of saturation effects unless the pole faces are very deep and operation is restricted to a narrow region within the magnet.
2. The Z gradient is pointed toward the center of the magnet. In this case particles would be forced to move toward the  $Z = 0$  centerline of the magnet causing an increase in particle concentration and greatly increased opportunities for particle agglomeration.
3. The Z gradient is pointed away from the center of the magnet. This tends to spread the particles from the center of the magnet. If there are intervening

walls then the particle could tend to gather on these walls preventing proper separation. If there are no walls the outward force may be used to removed particles from the separation area.

There is not a mathematical expression to describe the Z gradient and force. However its effect on particles has been observed and its magnitude may be described as relatively small compared to the centering X-forces. Nevertheless it is a force which must be considered if successful separations are to be performed.

### 3.2 Magnetic Liquids

#### 3.2.1 Ferrofluids

Ferrofluids are very stable dispersions of single domain magnetic particles. The suspended particles are so small (typically less than 150 Å) that they do not settle under gravity or interact even in the presence of a strong magnetic field. The magnetic response of a ferrofluid results from the coupling of individual particles with a substantial volume of the bulk liquid. This coupling is facilitated by a stabilizing agent which adsorbs on the particle surface and is also solvated by the surrounding liquid. This solvated layer is also responsible for the stability of the suspension. By proper choice of stabilizing agent, magnetic properties can be conferred to many liquids including fluorocarbons.

The magnetic properties of a ferrofluid can best be described by considering the particles in a ferrofluid to behave as an assembly of non interacting magnets. Their magnetic properties have been successfully correlated by superparamagnetic theory, taking into account the composition, size distribution, volume concentration and domain magnetization of the particles in suspension. In the absence of a magnetic field, they are randomly oriented and the ferrofluid has no net magnetization. In a magnetic field, the particles tend to align with the field resulting in a net induced fluid magnetization,  $M$ . The magnetization increases with increasing field until a saturation value is observed as shown in Figure 3.2.1. Under these conditions the particle magnetic moments are all aligned in the direction of the applied field. As soon as the magnetic field is removed, the particles become randomly oriented again because of thermal motion. The ferrofluid, therefore, has no residual magnetization and does not exhibit hysteresis.

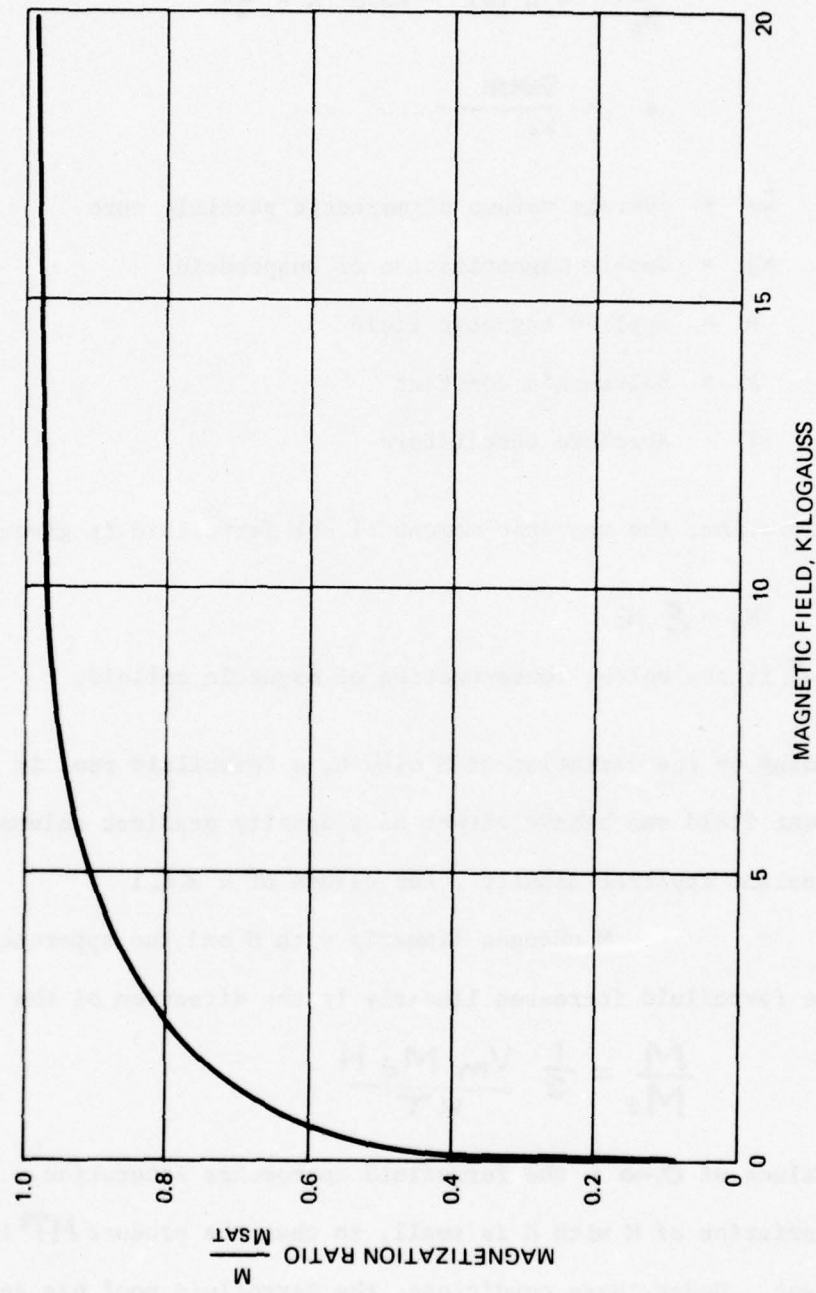


Figure 3.2.1 NORMALIZED MAGNETIZATION CURVE FOR A  
TYPICAL FERROFLUID

The magnetic moment,  $M$ , of a ferrofluid can be expressed by a Langevin function.

$$\frac{M}{M_s} = L(a) = \coth a - \frac{1}{a}$$

where  $a = \frac{v_m M_d H}{kT}$

and  $v_m$  = average volume of magnetic particle core

$M_d$  = domain magnetization of suspendoid

$H$  = applied magnetic field

$k$  = Boltzman's constant

$T$  = absolute temperature

At saturation, the magnetic moment of the ferrofluid is given by:

$$M_s = \epsilon M_d$$

where  $\epsilon$  is the volume concentration of magnetic colloid.

Depending on the variation of  $M$  with  $H$ , a ferrofluid pool in a constant gradient field can behave either as a density gradient column or as a liquid of constant apparent density. For values of  $a \ll 1$

$M$  changes linearly with  $H$  and the apparent density of the ferrofluid increases linearly in the direction of the gradient:

$$\frac{M}{M_s} = \frac{1}{3} \frac{v_m M_d H}{kT}$$

For values of  $a \rightarrow 1$  the ferrofluid approaches saturation. In high fields the variation of  $M$  with  $H$  is small, so that the product  $MH$  is essentially constant. Under these conditions, the ferrofluid pool has an essentially

constant apparent density

$$\frac{M}{M_s} = 1 - \frac{KT}{V_m M_d H}$$

Thus the mode of operation of the ferrofluid pool, as a constant density or density gradient column can be affected by proper selection of the particle size of the suspensoid, large particle size giving saturation at low fields and constant density while smaller particles delay magnetic saturation and yield a gradient density column.

The saturation magnetization of a ferrofluid can be adjusted by varying the concentration of colloidal magnetite. Stable ferrofluids with saturation magnetizations,  $4\pi M_s$  ranging from less than 1 gauss to over 1000 gauss have been prepared at Avco.

A ferrofluid remains a liquid in a magnetic field because the particles do not interact. A minor increase in viscosity (which can be made as small as desired) is noted because of the interaction of the particles with the field. It is to be emphasized that ferrofluids are very different from classical magnetic clutch fluids which become solid in a magnetic field because they are composed of micron size particles which interact when aligned by the field.

Even though the superparamagnetic particles in a ferrofluid do not interact in a magnetic field, there is a tendency for these particles to migrate under the influence of a strong field gradient. For most applications in which a ferrofluid is exposed to a gradient field for short periods of time (of the order of hours) and in which mixing of the ferrofluid may occur as a result of some convective mechanism, there are no noticeable spatial

variations in ferrofluid properties, even if the ferrofluid is used in magnetic fields high enough to provide saturation of the magnetization. This is because the rate of migration of the particles is very small.

The magnetic equivalent of Stokes Law for the sedimentation rate of a stabilized magnetic particle in a field gradient,  $\mathbf{T}$ , is expressed by the following equation<sup>7</sup>:

$$V_m = \frac{d_m^2}{18 \eta_o (1 + \frac{2S}{d_m})} (M_d \mathbf{T})$$

where

$V_m$  = settling velocity of ferrofluid particle

$d_m$  = diameter of magnetic particle core

$S$  = thickness of the non-magnetic layers of a solvated particle (stabilizing particle film and the non-magnetic outer shell of the particle)

$M_d$  = magnetic moment of particle

$\mathbf{T}$  = applied gradient field

$\eta_o$  = carrier liquid viscosity

For example, the velocity of a  $100^\circ \text{A}$  magnetite particle, stabilized by a solvated layer  $50^\circ \text{A}$  thick, is about  $3.6 \times 10^{-7}$  cm/sec. in a kerosene base ferrofluid ( $\eta_o = 0.02$  cp) such as the one shown in Figure 3.2.1 in a local magnetic field of  $H = 5000$  oe, and  $\mathbf{T} = 1000$  oe/cm.

In applications where the fluid is exposed to a gradient field for an extensive period of time ( $>10^6$  sec., for example) under quiescent, isothermal conditions, the effect of migration of the colloidal magnetic particles has to be taken into consideration. This effect can be minimized to any desired extent by decreasing the size of the suspended particles. With small enough particles, thermal diffusion becomes an effective mixing mechanism. For example, a local magnetic field with  $M = 5000$  oe and  $T = 1000$  oe/cm will result in a concentration gradient at equilibrium of less than a 2% change in particle concentration per cm for magnetite particles that have an effective magnetic diameter of  $30 \text{ } \text{\AA}^{\circ}$ . The time needed to approach equilibrium will also be very long because of the extremely slow migration velocity which is about  $6 \times 10^{-9}$  cm/sec. for the case considered above.

### 3.2.2 Liquid Oxygen

Liquid oxygen is a pale blue transparent liquid having a density of 1.14 gm/cm<sup>3</sup> and which boils at 183°C. Because of its unique electron configuration liquid oxygen exhibits magnetic properties. Unlike ferrofluids, however, liquid oxygen is a paramagnetic and does not saturate. Its magnetization increases in proportion to field strength according to the expression

$$M = \chi H$$

where  $\chi$  is the magnetic susceptibility of the liquid oxygen given in the International Critical Tables (Vol. VI p 355) as  $2.79 \times 10^{-4}$ .

The magnetization curve for liquid oxygen is plotted in Figure 3.2.2.

Because of the paramagnetic property of liquid oxygen, the expression for the apparent density of the magnetic medium must be modified. Previously, the apparent density was defined as

$$\rho_a = \rho_f + \frac{M\Gamma}{g}$$

Now, however,  $\rho_a$  is a function of  $H$  which is in turn a function of  $Y$ . Thus

$$\rho_a = \rho_f + \frac{\chi T^2 |y|}{g}$$

The liquid oxygen acts as a density gradient column. The magnetic contribution to the apparent density  $\chi T^2 |y|/g$  increases linearly from  $y=0$  at the mirror plate to a maximum value at the apex of the magnet. To this must be added the term representing the natural density of the liquid.

A valuable characteristic of liquid oxygen is its low viscosity of about .2 centipoise as compared to a viscosity of from 2-5 centipoise for ferrofluids. This low viscosity results in reasonably short transit times for micron sized particle. As an example, a 1  $\mu$  m sized particle in liquid oxygen requires about 5 hours to move a distance of an inch with a  $\Delta P$  of 0.5 gm/cm.

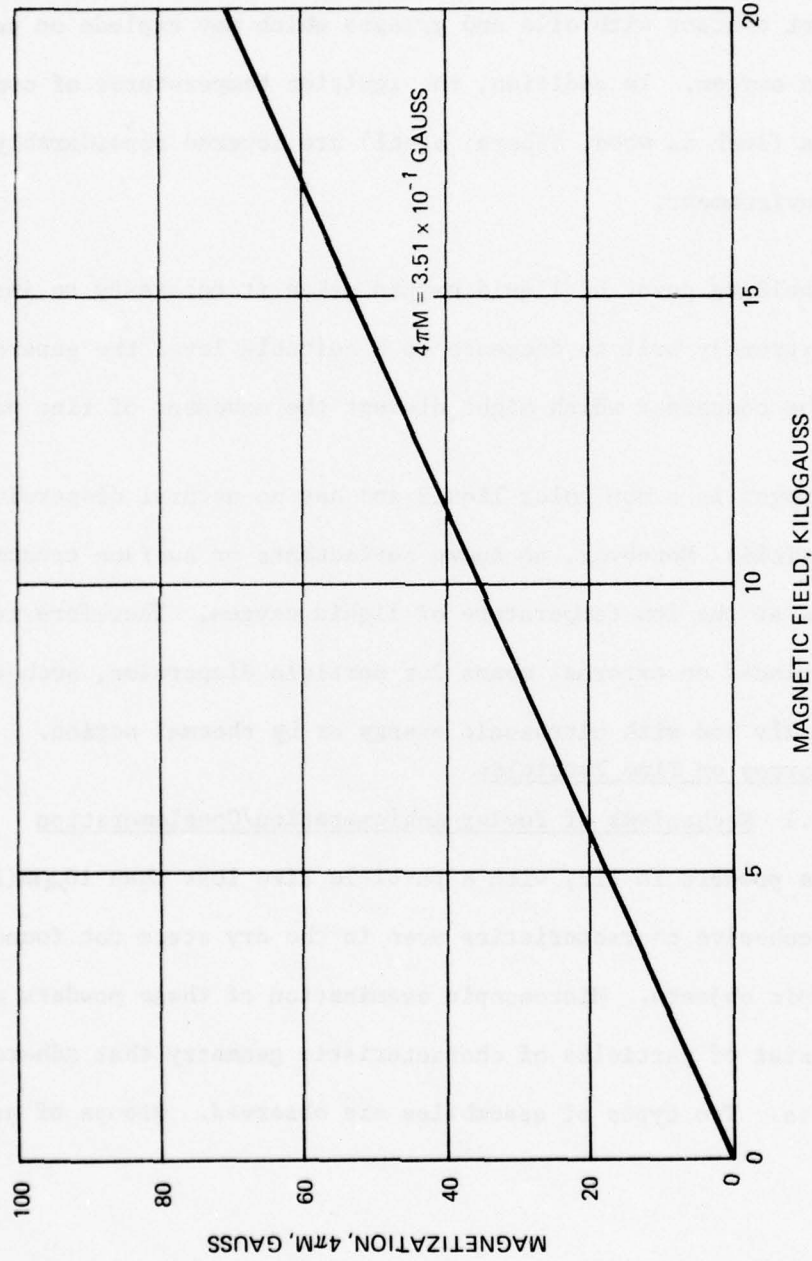


Figure 3.2.2 MAGNETIZATION CHARACTERISTIC FOR LIQUID OXYGEN DATA  
FROM INTERNATIONAL CRITICAL TABLES VOL. VI P. 355

Comparable times with ferrofluids would be 10 to 25 times longer.

Another important feature of liquid oxygen is that it eliminates the necessity of cleaning the separated fractions.

Proper safety precautions must be taken with liquid and gaseous oxygen to prevent contact with oils and greases which may explode on contact with pure oxygen. In addition, the ignition temperatures of combustible materials (such as wood, fibers, steel) are lowered considerably in a pure oxygen environment.

The low boiling point of liquid oxygen makes it necessary to insulate the holding vessel extremely well to decrease to a suitable level the generation of bubbles within the container which might disrupt the movement of fine particles.

Liquid oxygen is a non polar liquid and has no natural dispersive power for fine particles. Moreover, no known surfactants or surface treatments are effective at the low temperature of liquid oxygen. Therefore, reliance must be placed on external means for particle dispersion, such as stirring mechanically and with ultrasonic energy or by thermal action.

### 3.3 Forces on Fine Particles

#### 3.3.1 Mechanisms of Powder Agglomeration/Conglomeration

Ultrafine powders in air, with a particle size less than  $10\text{ }\mu\text{m}$  ( $10^{-3}\text{ cm}$ ), exhibit cohesive characteristics even in the dry state not found with macroscopic objects. Microscopic examination of these powders reveals that they consist of particles of characteristic geometry that adhere to form firm assemblies. Two types of assemblies are observed. Groups of particles

can be fused together to form aggregates, bonded by primary valence (chemical) bonds. There is no distinguishable surface between the particles forming the primary aggregates. These aggregates are usually formed during the deposition of the ultimate particles.

These aggregates in turn are found to adhere by physical forces (Van der Waals Forces) to form agglomerates. (The term conglomerate is used in the case where all the particles in the agglomerate do not have the same composition and origin). This agglomerate formation becomes increasingly more apparent as the size of the ultimate particles or aggregates decreases. Agglomeration of fine powders becomes especially significant when the particles are smaller than 1 micron in diameter.

Agglomerates differ from aggregates in that there is a discontinuous surface zone between the constituting particles or aggregates. Actual contact of two adjacent particles is prevented by the presence of layers of adsorbed molecules on the particle surfaces. Such layers will always be present under atmospheric conditions. Either physical adsorption or chemical adsorption may occur. These adsorbed films can greatly alter the magnitude of the interaction between fine particles since any interaction between two solids decays rapidly with increasing distance of separation of their surfaces.

Fine particle agglomeration is considered to be mainly due to secondary valence interaction between the particles. The concept of an attraction between two neutral atoms or molecules was introduced in 1873 by Van der Waals in order to explain deviations of real gases from the perfect gas law. In 1932, in order

to take into account the coagulation of colloidal dispersions, Kallmann and Willstatter suggested that secondary valence forces or Van der Waals forces could also be an effective and universal force of attraction between macroscopic solids. At the present time, it is generally considered that these forces are responsible for the so-called "spontaneous" adhesions of finely divided solids.

General explanations for the nature of Van der Waals forces were first proposed by London in 1930 and more recently by Lifschitz. These explanations were both based on quantum theory which considers that all atoms, even in their ground state, possess rapidly fluctuating dipole moments which lead to an attraction between these atoms. The force between two solid objects, which are viewed as assemblies of many atoms, is obtained from the summation of the individual interactions of all the atoms in the two bodies with the force between any two atoms being considered independent of the presence of other atoms. According to Lifschitz, the secondary valence force,  $F$ , between two spheres of diameter,  $d$ , whose surfaces are separated by a distance,  $a$ , can be expressed as follows:

$$F = \frac{-Bd}{36a^3}$$

In the above equation,  $B$  is a characteristic material constant, whose value will depend on composition of the particles and the surrounding phase. According to Dejohgh, the value of  $B$  is approximately  $10^{-19}$  ergs/cm for particles of polar materials in a vacuum. It is to be noted that the interaction decreases as the third power of separation.

In air, agglomerate formation occurs in fine particle systems because the thickness of the adsorbed layers is small, of the order of  $10 \text{ \AA}$ . Under these conditions, the Van der Waals interaction between two particles separated by this distance, is significantly higher than the potential energy of disruptive mechanisms namely thermal energy,  $kT$ , where  $k$  is Boltzmann's constant and  $T$  is the absolute temperature, or inertial effects proportional to the volume of the particles which are proportional to the volume of the particles. Thus, although the attractive force between two solids increases with diameter, the effect of Van der Waals forces becomes insignificant with macroscopic objects (e.g. particles greater than  $10 \mu\text{m} - 20\mu\text{m}$ ) in air since inertial effects increase with mass and are thus proportional to the third power diameter.

Electromagnetic interactions, other than secondary valence forces, that can be considered are forces due to induced electrostatic charges and magnetic dipole interaction. Electrostatic charges can be induced in many powders and can result in significant transient forces. However, because of either bulk or surface conductivity due to moisture, the electrostatic potential will leak away and hence will have no lasting effects. An exception is the case of an electret, such as aminoazobenzene, where there is a charge retention. In a similar manner, magnetic dipole-dipole interaction is important only in materials that have a significant magnetic coercitivity, such as magnetic iron oxide. Mechanical interlocking occurs in systems which contain very irregularly shaped particles. Liquid particle bridging due to surface tension forces may also occur as a result of capillary condensation of a liquid (water). Solid particle bridging is a reflection of the origin of the particles and is representative of aggregation rather than agglomeration.

### 3.3.2 Particle Dispersion Mechanisms in a Liquid Phase

As in the gas phase, solid particles in a liquid phase are also subject to secondary valence forces which lead to agglomeration. While there are no obvious techniques of dispersing sub-micron particles in the gas phase, it is standard technology to disperse particles in the liquid phase.

It is possible to disperse sub-micron particles in liquid systems because it is possible to generate repulsion forces which prevent close approach of two particles.

Two repulsive mechanisms exist which result in stabilization of a liquid phase colloid, namely, double layer electrostatic repulsion or entropic repulsion of interacting molecules adsorbed on the particle surfaces. The first mechanism results from the adsorption of charged species on and around the particle surfaces to form the well-known electrostatic double-layer. Stabilization occurs because of the electrostatic repulsion of two charged particles. The stability of hydrosols (aqueous colloidal dispersions) is usually due to electrostatic stabilization.

The second mechanism of entropic repulsion results from the adsorption on the particle surface of large molecules that solvate with the liquid. This results in the formation of thick film of essentially bound liquid, so thick that when two particles collide, the particle surface to particle surface interaction becomes negligible, at the distance of separation equal to twice the solvated film thickness, in comparison to the thermal energy of these particles. The mechanism of entropic repulsion predominates in colloid suspensions in non-polar media which are poor electrical conductors. In these liquids, it is possible to stably suspend solid particles by adding polar molecules that can both adsorb at the particle surfaces and be solvated by the carrier liquid. Carbon black is a typical example of a finely divided solid material with a characteristic particle size of less than 1  $\mu\text{m}$ . The particles will not disperse in the gas

phase but can be made to form stable suspensions in an immiscible liquid phase. Similar statements can be made for many other materials of widely diverse chemical structure and origin (titanium dioxide, zinc oxide, bentonite, organic dyes, etc.).

### 3.3.3 Particle Interaction Forces

In actual separation practice, the magnetic liquid may contain many non-magnetic objects which are being separated from each other. The presence of these objects introduces perturbations in the externally applied magnetic field and its gradient.

These perturbations result in particle-to-particle interaction forces. In particular, it is predicted that there is an attractive force between two spherical particles immersed in a ferrofluid when the line of centers of the particles is parallel to the direction of the applied magnetic field.

The interaction force is given by the following equation:

$$F_{ss} = \frac{(4\pi M)^2}{96} \frac{D^6}{a^4} \quad (1)$$

where

$a$  = center to center spacing between particles

$D$  = diameter of the particles

$M$  = magnetic dipole moment per unit volume of ferrfluid

When the spheres consist of the two types that are to be separated by magnetic levitation, then half the difference in the net levitation force between the spheres must be greater than the above attraction force if separation is to take place. Half the difference in levitation force,  $F_1$ , between two spheres of identical volume,  $V$ , but different densities situated in a ferrofluid pool is given by

$$F_1 = \frac{1}{2} (\rho_2 - \rho_1) g V \quad (2)$$

where

$\rho_2$  = density of the more dense sphere

$\rho_1$  = density of the less dense sphere

$g$  = acceleration of gravity

The dimensionless ratio  $F_{ss}/F_1$ , given by the following equation, should be an index of whether or not particle separation according to density will occur.

$$\frac{F_{ss}}{F_1} = \frac{1}{8\pi} \left[ \frac{(4\pi M)^2}{(\rho_2 - \rho_1)g} \right] \left[ \frac{D^3}{a^4} \right] \quad (3)$$

This ratio should be as small as practical for good separation to occur. Consider the worst case, where the spheres touch and therefore  $a = D$ ,

$$\frac{F_{ss}}{F_1} = \frac{1}{8\pi} \left[ \frac{(4\pi M)^2}{(\rho_2 - \rho_1)g D} \right] \quad (4)$$

This relation shows that for a fixed value of the ratio  $F_{ss}/F_1$  the magnetization of the ferrofluid must be reduced as the size of the spheres is reduced. A direct result of this requirement is that the magnetic field gradient must be increased to compensate for the reduction of ferrofluid magnetization in order to attain a given apparent ferrofluid density sufficient to float the less dense objects.

The force ratio  $F_{ss}/F_1$  can also be calculated using the average interparticle distance as the measure of particle separation. The average interparticle distance ( $a$ ) can be expressed in terms of the volume concentration of powder particles ( $\mathcal{E}_v$ ) by:

$$\frac{a}{D} = \left( \frac{\pi}{6\mathcal{E}_v} \right)^{1/3} \quad (5)$$

assuming a cubic particle array. Thus, Equation 3 becomes, when a is equated to d:

$$\frac{F_{ss}}{F_1} = \left[ \frac{(4\pi M)^2}{8\pi(\rho_2 - \rho_1) g D} \right] \left[ \frac{6\epsilon_v}{\pi} \right]^{1/3} \quad (6)$$

Equation 5 indicates that in actual practice particle concentration could have a significant effect on the quality of separation. This is a less severe criterion than Equation 4.

### 3.4 Application of Ferrofluid Sink-Float Separation Developed by Avco

#### 3.4.1 Constant Density Separation

Avco has reduced the ferrofluid sink-float separation concept to practice.

The resulting system comprises one or more separation modules, and means for removing and recovering ferrofluid adhering to the separated particles.

An Avco separation module consists of an electromagnet with a regulated power supply designed to generate a region of constant, specified apparent density within a pool of ferrofluid held between the magnet poles. After a sizing operation to remove oversized ( 2 inch) and undersized ( 1/8 inch) particles the solid mixture to be separated is introduced into the pool. Objects less dense than the apparent density of the ferrofluid float to the top, while those more dense sink to the bottom of the ferrofluid pool, resulting in a physical separation. The separation can be carried out on a batch or continuous basis. Mixtures of three or more components can be separated by making two or more passes through the separator during which the apparent density of the ferrofluid is adjusted to produce one pure component per pass. Such mixtures could also be separated by a sequence of separators operating at appropriate apparent density levels, with partly separated mixtures being conveyed from one separator to the next until all separations are achieved. By such means it is possible to accurately separate materials differing in density by as little as 10%, the separation being essentially independent of the size or shape of the objects.

The final processing step is removal of the ferrofluid covering the separated objects. This ferrofluid is easily removed by washing the product streams with a volatile solvent miscible with the ferrofluid being used.

Residual traces of solvent are easily removed from the separated objects by evaporation. Solvent in the wash solution can similarly be separated from the non-volatile ferrofluid by evaporation thus allowing both to be recycled.

#### 3.4.2 Separator Magnet Design

An iron yoke electromagnet with a modified rectangular hyperboloid pole configuration has been found to be a practical design for the field source of the separation modules built to date.

This design configuration results in a constant gradient in the direction of gravity. The magnet is operated so as to provide a minimum magnetic field level sufficient to result in a significant approach to saturation of the ferrofluid placed in the working volume. The magnetization of the ferrofluid will thus not change significantly over the height of the working volume. As a result, the apparent density of the ferrofluid in the working volume is essentially constant. The apparent density of the ferrofluid is changed by increasing the gradient field. This is accomplished by increasing the current to the electromagnet.

With this design there is easy horizontal access to the pool of ferrofluid. Since magnetic forces also retain the ferrofluid in the gap of the magnet, conveyors or other means of introducing the feed or removing the separated products, can be introduced directly into the ferrofluid pool without fluid leakage or sealing problems.

Avco has built a number of separators of different scale based on the magnet configuration described above. In addition to experimental separators built for in-house use, Avco has also built a laboratory separator for Battelle Northwest Laboratories, Richland, Washington, and an industrial scale

separator for NASA Technology Utilization Office, Langley Research Center, Hampton, Virginia, under Contract NAS 1-11793. A wide variation of granulated mixtures of solids, ranging in size from about 0.2 cm to 5 cm, and differing in density by as little as 10% have been successfully separated in these devices.

#### 3.4.3 Battelle Laboratory Separator

A laboratory separator was delivered to Battelle N.W. The separator consists of an electromagnet with 4-inch poles, a small separation vessel that can be positioned between the poles of the magnet and a supply of four ferrofluids of different magnetization. The four ferrofluids supplied, when used with this magnet, can achieve apparent densities of between 2.5 gr/cm<sup>3</sup> and 22 gr/cm<sup>3</sup>. In the working volume of the separator (approximately a 2-inch cube) of about 130 gm<sup>3</sup>, there is less than 10% difference in apparent density when the magnet is operated at minimum current of 80 amps. Under these conditions the magnetic field in the working volume always exceeds 2500 oe. The coils can be operated at currents of up to about 350 amperes when cooling water flow is 2 gpm. At this current, this magnet can generate a vertical magnetic field gradient that approaches 1000 oe/cm.

#### 3.4.4 Nonferrous Scrap Separator

A much larger separator was built for NASA Technology Utilization Office to demonstrate the applicability of aerospace technology to solid wastes management. This separator was designed to separate regranulated nonferrous automobile scrap into its major components according to their densities at a rate of 1 ton/hour on a continuous basis.

This scrap separator consists of:

- a. An electromagnet designed to generate a region of constant apparent density within a pool of ferrofluid held within the magnet poles.

A kerosene base ferrofluid with 500 gauss saturation magnetization, such as the one described in Figure 3.2.1, will have an apparent density of nearly  $12 \text{ gr/cm}^3$  when the magnet is operated at a maximum power input 63 KW which generates a field gradient of 250 oe/cm.

This density level is sufficient to float all common industrial metals of interest.

- b. Conveyors for introducing into the ferrofluid the scrap to be separated and removing the separated products. Objects less dense than the apparent density of the ferrofluid float to the top of the ferrofluid pool where they are removed by an upper conveyor while those more dense sink and are removed by a lower conveyor. The separation process is thus continuous. Since magnetic forces also retain the ferrofluid in the gap of the magnet, conveyors can be introduced directly into the pool without fluid leakage or sealing problems. The conveyors of the materials handling system have been found capable of moving typical automobile scrap at rates of over 5000 lb/hr.

The behavior of non-magnetic objects within the separator has been found to be essentially a function of density and independent of the size or shape of the objects. The effect of object size was

studied on cubes ranging in size from 5 cm to 0.6 cm on a side.

The separation of well characterized scrap mixtures has been evaluated in the separator in order to obtain information on the effects of operating parameters on the purity of the recovered fractions. Typical of the results obtained are those presented in Table III. The first three tests show the effect of varying the apparent density of the ferrofluid pool. Test 2 shows that when the apparent density is close to that of brass (8.4 vs. 8.5) some of the brass starts to contaminate the zinc. Similarly, Test 1 shows that as the apparent density of the ferrofluid pool is lowered, a small amount of zinc appears with the brass fraction. Test 3 carried out at the intermediate density level of 7.9, resulted in complete separation. Test 4 shows that an increase in feed rate to 5,100 lb/hr. resulted in only a slight decrease in product purity.

These test results demonstrate conclusively that very high separation rates are achievable by ferrofluid sink-float separation. With optimal adjustment of operating parameters, the separation is virtually error free.

Avco has also performed a number of separation runs of mixtures of aluminum, zinc and copper derived from automobile shredding. The object is to separate the mixtures of these metals into their separate categories, each of which may then be sold to the appropriate secondary metal smelting industry. The results of these separation runs have been excellent. Samples of the separated fractions of the two metals occurring in the greatest proportion in automobile shredder scrap - aluminum and zinc - have been sent to the respective smelters for analysis, and each fraction has been reported to be well within specification limits and of a purity which can command a premium price on the secondary metals market.

TABLE III  
SEPARATION OF ZINC ALLOY AND BRASS SCRAP

Feed Characteristics

Size of Scrap - 2 inches to 1/4 inch

Composition - 50% Zinc Alloy, 50% Brass

Densities - Zinc Alloy  $6.6 \text{ gr/cm}^3$   
 Brass Alloy  $8.5 \text{ gr/cm}^3$

| <u>Test No.</u> | <u>Feed Rate to Separator lb/hr.</u> | <u>Average Apparent Density of Ferrofluid, gr/cm<sup>3</sup></u> | <u>Purity of Zinc Fraction</u> | <u>Purity of Brass Fraction</u> |
|-----------------|--------------------------------------|--|--------------------------------|---------------------------------|
| 1               | 2,600                                | 7.4  | 100.0%                         | 99.5%                           |
| 2               | 3,100                                | 8.4  | 98.7%                          | 100.0%                          |
| 3               | 3,700                                | 7.9  | 100.0%                         | 100.0%                          |
| 4               | 5,100                                | 7.9  | 99.6%                          | 100.0%                          |

#### 4.0 Experimental Efforts and Results

##### 4.1 Ferrofluids

The initial efforts in this program consisted of acquiring suitable candidate fine powders, the preparation and characterization of ferrofluids and the development of techniques for analysis of the results of experimentation.

A necessary requirement for the evaluation of a sink/float separation system is the ability to determine the identity of the contents of the various fraction. With large sized particles, say  $> 100 \mu\text{m}$ , it is possible to select candidate powders with distinctive colors which may be detected under a low power microscope. Particles smaller than this however, tend to lose their color clues and other means of identification must be found. The use of powders of different densities and different indices of refraction similar to that of one of the candidate powders was supposed to cause those particles to extinguish optically while not effecting the visibility of the other material.

A Millipore  $\pi$  MC Particle Measurement Computer System was used in conjunction with a Leitz microscope to provide a rapid means of measuring and counting the particles of a separation sample. The use of the index of refraction liquid with the particles often left ghost images which the  $\pi$  MC Counter treated very erratically and unpredictably making the data unuseable.

The  $\pi$  MC Counter was very useful, however, in determining the size distribution of particles of a single species for analysis.

The most effective means of identifying the results of a separation test was the use of a globular bead as one of the participants in a separation study. These so called microbeads are available in a wide range of closely graded sizes with densities of 2.42, 2.99 and  $3.99 \text{ gm/cm}^3$ .

Other powders which were used with the glass microbeads and which were easily distinguished by their granular shape included silica,  $\text{SiO}_2$ ,  $\rho = 2.65 \text{ gm/cm}^3$  silicon carbide,  $\text{SiC}$ ,  $\rho = 3.18 \text{ gm/cm}^2$ , diamond dust,  $\rho = 3.5 \text{ gm/cm}^3$  and aluminum oxide,  $\text{Al}_2\text{O}_3$ ,  $\rho = 3.98 \text{ gm/cm}^3$ .

Because the  $\text{PT}$  MC particles counter could not distinguish these shapes it was necessary to estimate the efficiency and quality of a separation by visual identification of the components.

Using ferrofluids of low magnetization to minimize the particle interaction effects and limited by maximum available magnetic gradient of about 1000 oe/cm, the maximum apparent density,  $\rho_a$ , attainable was about  $4 \text{ gm/cm}^3$ . Initially a fluorocarbon-based ferrofluid was used but later a more easily prepared kerosene based ferrofluid was used after determining that there was no difference in separation efficiency.

A plastic ball valve was used for the first separation chamber. One opening of the valve was plugged making a chamber  $1/2''$  diameter and about  $2''$  long which could be divided into three separate chambers by closing the valve after the separation. Calibration of the magnetic fluid apparent density as a function of magnet current was accomplished originally by observing the point at which item of known density floated and sank in the fluid. Later the calibration consisted of measuring the hydraulic head created by the magnetic pressure in the ferrofluid. In practice, the ball valve was about half filled with ferrofluid, then placed in the magnetic field. The powders to be separated were then dispersed in a small quantity of the same ferrofluid and added to the ball valve. Finally the ball valve was

filled with ferrofluid. Typical particle volumetric concentration ratios,  $C_V$ , were about .001 based on the total volume of the chamber. After a suitable time based on particle size, fluid viscosity and density difference, the ball valve was closed preventing mixing of the separated fractions. At first only the upper and lower fractions were recovered but later it was discovered that there was often a significant quantity of material in the middle fraction and thereafter the middle fraction was examined also.

Recovery of the fractions involved first pouring the ferrofluid and then rinsing with a suitable solvent through a millipore filter with a pore diameter of  $0.8 \mu m$ . For microscopic analysis of the results the filter was cleared. In some cases the fractions were subject to gravimetric analysis requiring that the weight of each filter disc be determined beforehand.

The separation experiments were generally operated at an apparent density midway between the densities of the two components to be separated using 50-50 mixtures by volume of the particles. The particles ranged in size from  $2-40 \mu m$ . In most cases only a small percentage of the total input material was found in the float fraction with most of the material recovered in the sink fraction. Neither fraction was perceptibly enriched. All aspects of the separation system were checked with nothing found to be wrong.

Next, a series of experiments was performed to determine the flotation characteristics of individual powders as a function of particle size. It was found that fine particles required a considerably higher apparent density to float than do larger particles of the same material and that there is a definite transition point from sinking to floating. For example glass

microbeads having a density of  $2.99 \text{ gm/cm}^3$  and particle size distributions as shown in Figure 4.1.1, required an apparent density of approximately  $3.1 \text{ gm/cm}^3$  to float particles with an average size of  $45 \mu\text{m}$ ;  $38 \mu\text{m}$  and  $28 \mu\text{m}$  particles of the same material required apparent densities of  $3.5 \text{ gm/cm}^3$  and  $3.9 \text{ gm/cm}^3$  respectively to float. These data are shown in Figure 4.1.2 and 4.1.3 for two values of particle concentration.

Several theoretical models were proposed to explain this relationship between particle size and the apparent density required to float the particle. It was first proposed that for very small particles the ferrofluid had ceased to behave as a fluid continuum with the result that small particles may fall through the spaces between the ferrit particles. A calculation for the average magnetic particle spacing for the ferrofluids used gave a value of about  $.1 \text{ m}$  assuming a uniform cubic array of the particles. To test the possibility of conglomerations of magnetic particles, the viscosity, magnetization, and optical density (as a measure of iron content) were measured before and after passing the ferrofluid through  $0.8 \mu\text{m}$  and  $0.22 \mu\text{m}$  filer discs with and without the influence of a strong magnetic field. No significant changes in these properties were discovered. Based on the above evidence it was tentatively concluded that magnetic particle spacing was not a factor contributing to the aberrant behavior of fine particles.

As an alternative it was postulated that by some unknown mechanism the fine magnetic particles were coupling to the non-magnetic materials, thereby conferring magnetic properties on the non-magnetic particles increasing the apparent or effective density of the particle by generating a magnetic force of attraction to the area of strongest field. If it may be further assumed that the layer of adsorbed magnetic particles is of somewhat constant thickness then the relationship between particle size and increased apparent density of the magnet medium required to float a particle may be readily explained. The volume of

FIG 4.1 SIZE DISTRIBUTION HISTOGRAMS

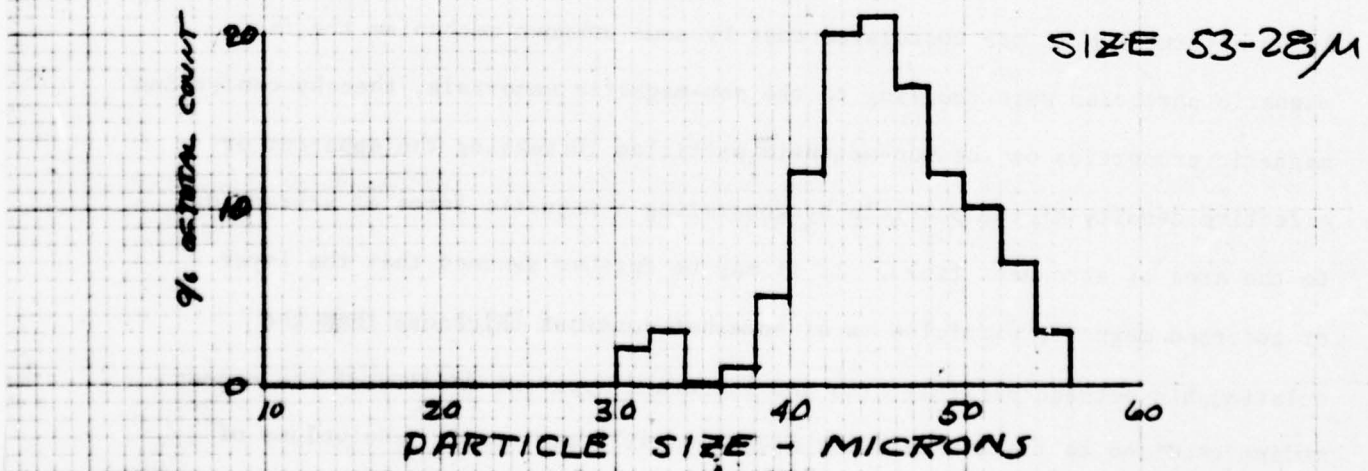
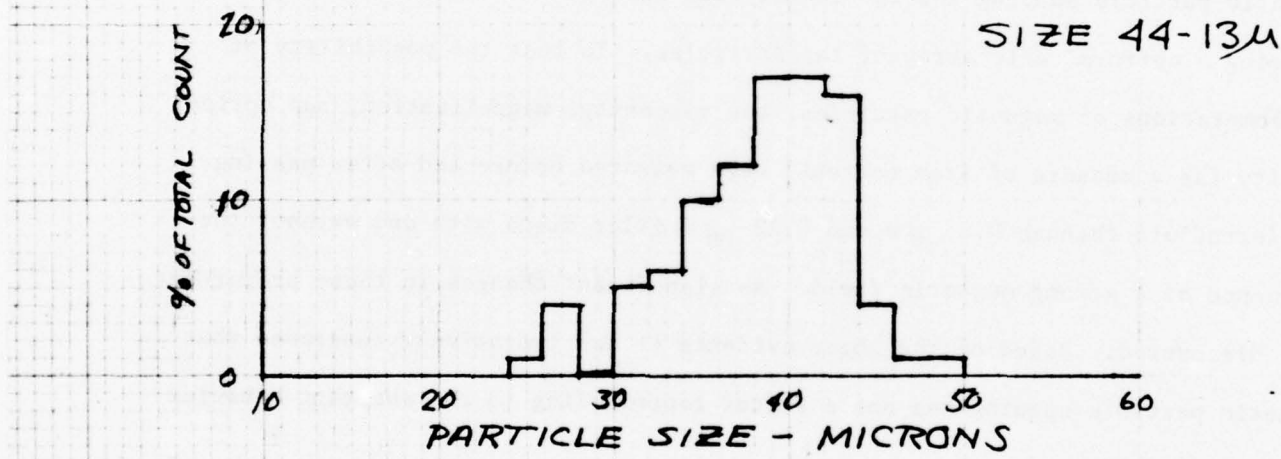
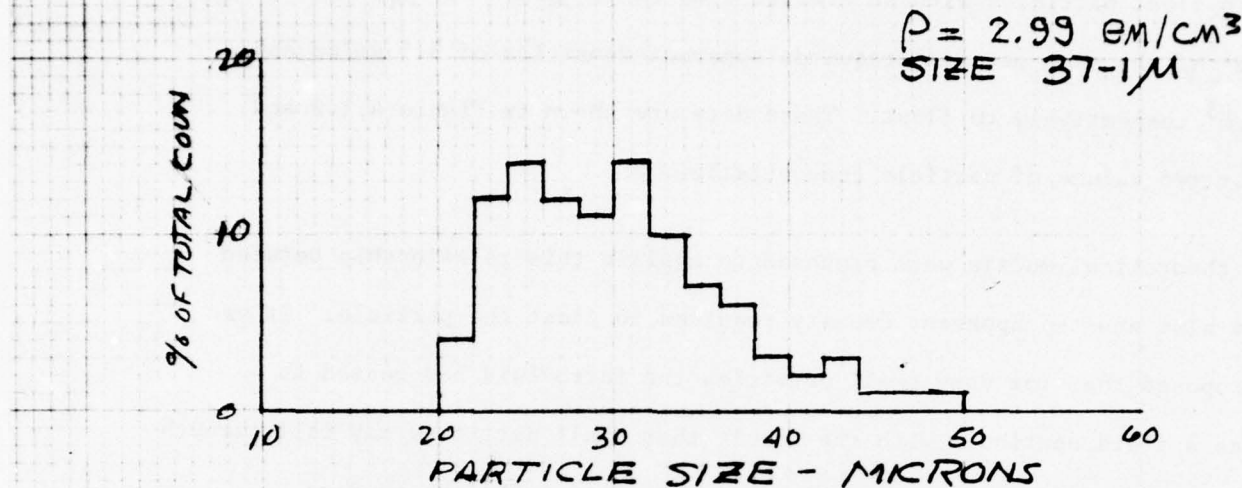


FIG 4.1.2 FLOTATION CHARACTERISTICS  
OF GLASS MICROBEADS  
DENSITY 2.99 GM/CM<sup>3</sup>  
PARTICLE CONCENTRATION,  $\epsilon_v$ , .003

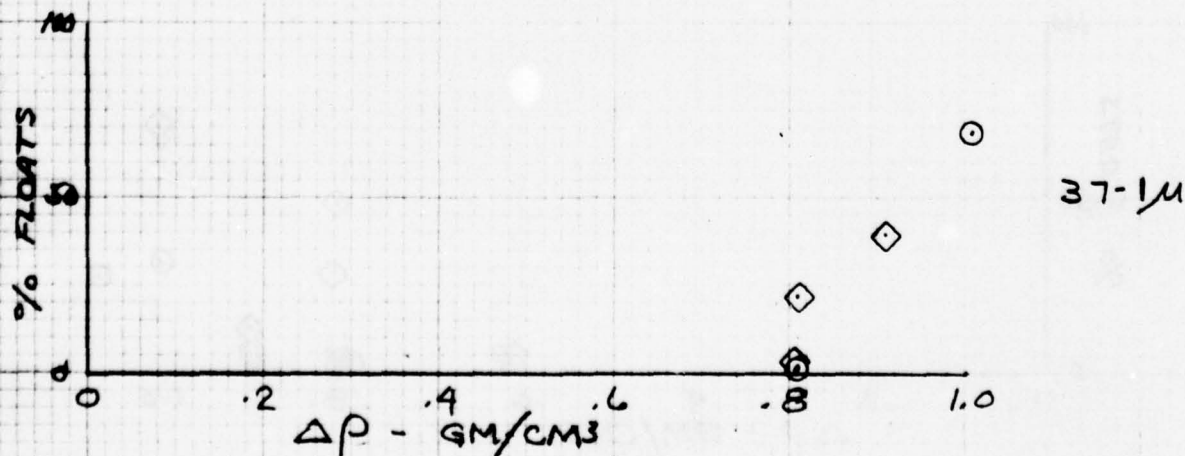
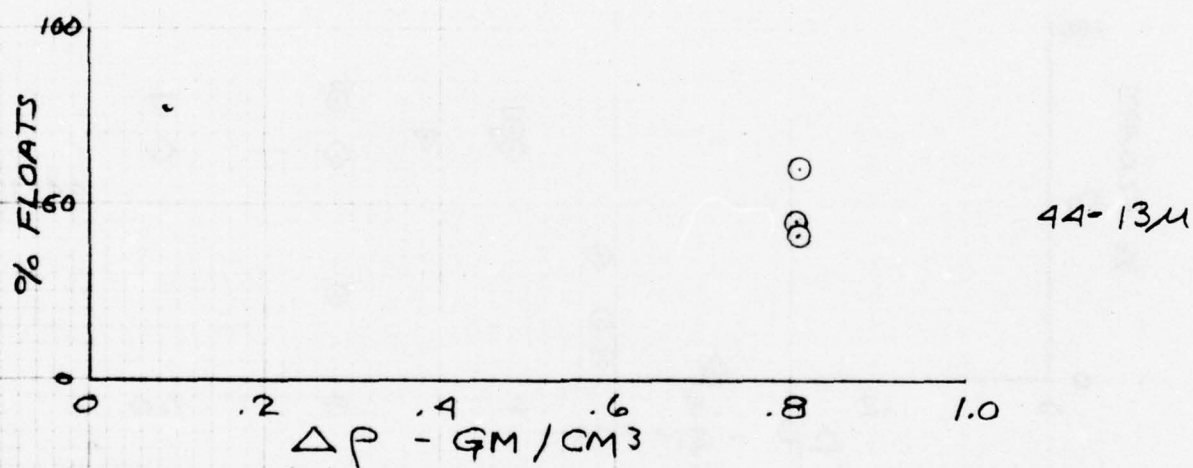
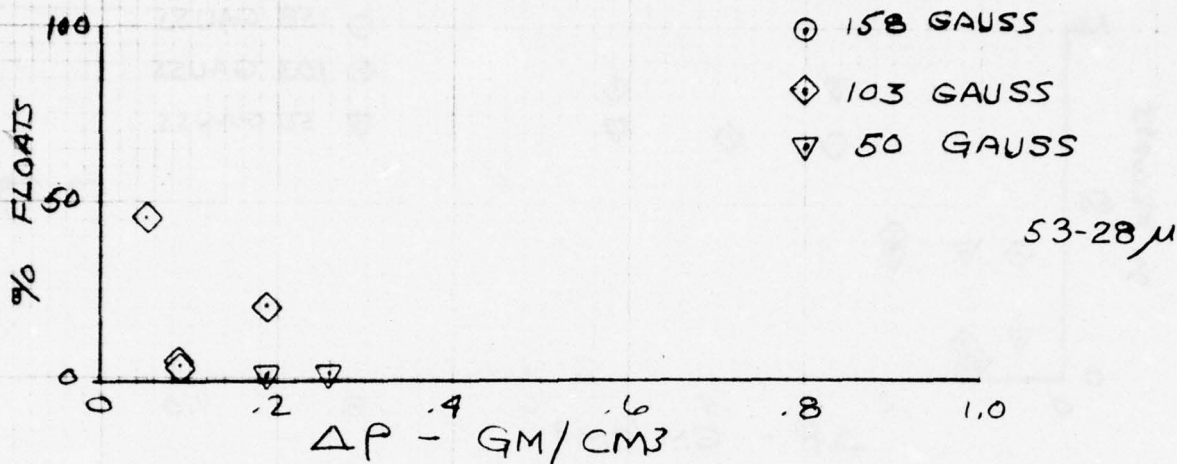
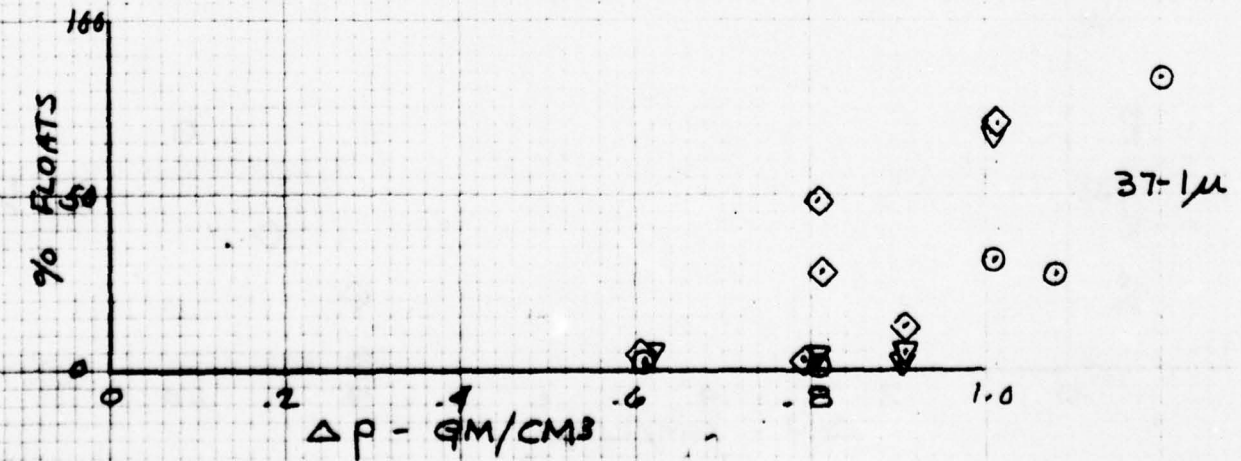
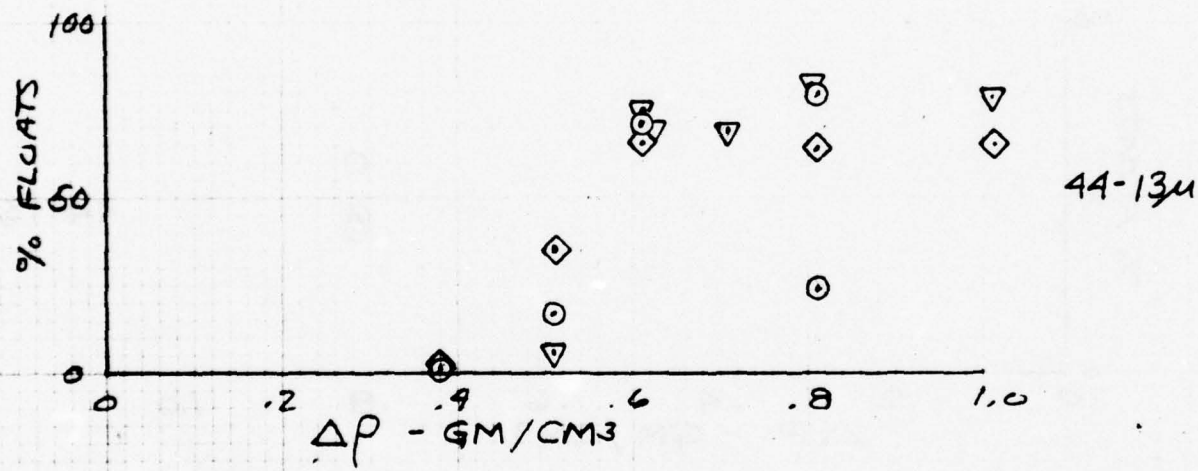
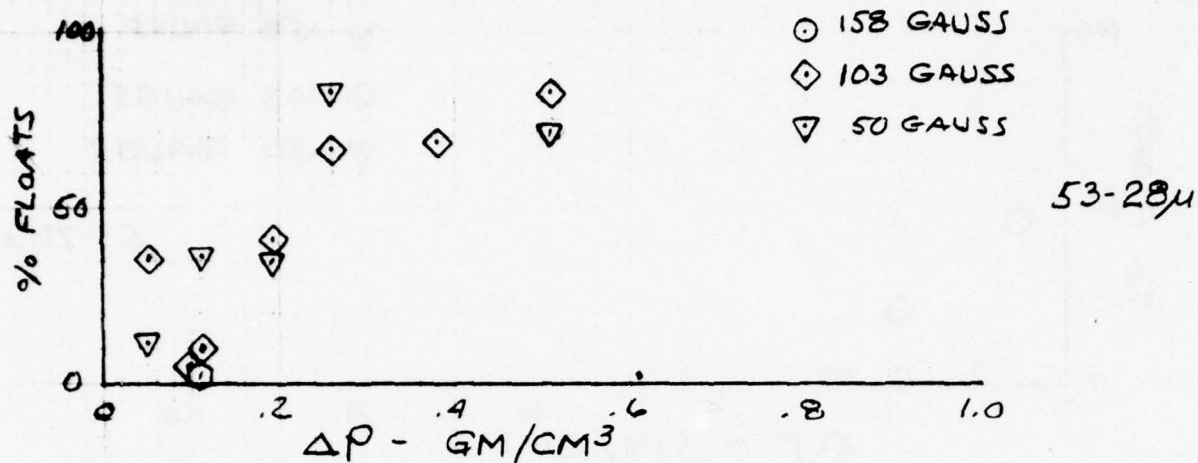


FIG 4-113 FLOTATION CHARACTERISTICS  
OF GLASS MICROBEADS  
DENSITY 2.99 GM/CM<sup>3</sup>  
PARTICLE CONCENTRATION,  $\Sigma v$ , .012



a small layer of constant thickness grows relatively smaller compared to particle volume as particle size increases. In this fashion large particles would be relatively unaffected by the magnetic forces and small particles would be greatly effected.

From this information one might expect the ferrofluid pool to operate as a sort of magnetic sieve separating small particles from large particles. That such was not the case was indicated by examination of the float and sink fraction when operating at an apparent density where transition from particle sinking to flotation occurred where it was determined that the particle size distribution of the sink and float fractions were identical. In fact, operating with a powder having a bimodal size distribution peaking at 30  $\mu\text{m}$  and 70  $\mu\text{m}$  the size distributions of the float and sink fractions were identical. Also, because it was noticed that there was never complete recovery of the input material in the float fraction the middle fraction of the ball valve was examined where it was found that the middle fraction often contained a significant quantity of the input material.

To explain this behavior it is assumed that large particles, which would be expected to float could be overwhelmed by a large number of attached smaller particles having an effective density heavier than large particle. To account for the presence of fine particles in the float fraction we may assume that fine particles could attach to large particles in smaller numbers such that the composite density is greater than the apparent density of the medium. Similarly agglomerates of intermediate densities may be created which would hover within the magnetic volume.

As discussed later in Section 4.2, similar flotation experiments were conducted with liquid oxygen with no evidence of the particle size apparent density behavior was with ferrofluids. Because liquid oxygen is an elemental liquid in contrast with ferrofluids which are colloidal suspensions of tiny particles, this result lends credibility to the assumption of magnetic particle - non-magnetic particle interaction.

It was thought, based on previous theoretical calculations, that the interaction force between small particles would set a lower limit on the size of the particles that could be separated by ferrofluid levitation. This low limit on particle size was considered to be something less than  $10 \mu\text{m}$ . Now, it seemed reasonable to assume that the particle interaction force was operable on particles of much larger size such that particles of a range of sizes could conglomerate and react as a single particle of varying density depending upon the amount of adsorbed magnetic particles.

To illustrate the influence of particle interaction on flotation characteristics consider the following experiments which were originally thought to be successful separations of binary mixtures of fine powders. The separations involved equal parts by volume mixture of silicon carbide particles ( $\rho = 3.18 \text{ gm/cm}^3$  9-44  $\mu\text{m}$ ) and silicone dioxide ( $\rho = 2.65 \text{ gm/cm}^3$  A.P.S. 3  $\mu\text{m}$ ). The technique used in the apparently successful experiments was to introduce carefully weighed amounts of each material separately into the half-filled ball value which was used as the separatory vessel. The ball value was then filled and the magnet energized to a predetermined current to obtain the desired apparent density. In all cases the silicon dioxide was introduced first. The results were excellent separations of the components. Later repeats, differing only in the manner of introducing the powders failed to yield enrichment of any fraction. In these experiments the powders were premixed mechanically or agitated within the separation vessel before separation. The conclusion drawn here is that in the case of the supposedly successful separations the particles had the opportunity to selectively conglomerate with other particles of like material and then respond properly as a sink or float. It is of interest to note that the

silicone dioxide particles which were introduced first and which ultimately reported in the float fraction had conglomerated and then risen through the silicon carbide sink fraction without becoming seriously contaminated.

Later experiments, conducted in the transparent liquid oxygen confirmed the particle interaction effect (which should be independent of the magnetic medium). Fine powders which would be predicted by Stokes' Law to require several hours to traverse the depth of the separation chamber under the prevailing conditions of apparent density, particle size and viscosity were detected in a matter of minutes at the bottom of the chamber.

Recognizing the importance of particle interaction in obtaining successful separations of particle mixtures having different densities a new separation apparatus was designed and built. This apparatus permits separation experiments to be conducted at particle concentrations three or four orders of magnitude lower than previously giving average particle spacings 10 to 20 times larger than in the original experiments greatly decreasing the possibility of particle collisions and interaction. Of course, there still exists the statistical possibility of some interaction of unlike materials with a resulting misclassification of the resulting conglomerate of composite density. This misclassification can be minimized in one fraction by biasing the apparent density of the magnetic medium to favor the other fraction. This apparatus differs from the previous separation chamber in that involves a continuous process as opposed to a batch process. Even if it were successful in enriching only one fraction, successive iterations of the process would enrich the other fraction.

The apparatus is illustrated schematically in Fig. 4.1.4 and consists basically of an open-ended trough of non magnetic material placed between the pole faces of the laboratory magnet. After the magnet was energized, a quantity of ferrofluid was poured into the trough where it assumed the shape shown in the Figure. The body of a hypodermic syringe was positioned as shown with the tip of its needle located at the approximate center of the working volume of the magnet. A very dilute suspension of the particles to be separated was placed in the syringe where it was held by the magnetic forces. These forces generated a magnetic pressure and slowly forced the ferrofluid and suspended particles into the center of the separatory vessel. At low enough concentrations each particle should enter the decision zone of the separatory chamber as individual particles and react as either a float or sink and leave to report to the proper fraction. If conglomeration should occur after leaving the decision point it would be among like particles and should not effect the quality of the separation. Float particles would rise to the top of the ferrofluid pool and then move forward and rearward on the surface of the ferrofluid under the influence of the magnetic gradients in the Z direction. The float particles were retained in aluminum foil catch pans positioned near the top edges of the ferrofluid pool as shown.

In an actual separation, about 10 mg each of silicon carbide powder ( $\rho = 3.18 \text{ gm/cm}^3$ , 33-9  $\mu\text{m}$ ) and glass microbeads ( $\rho = 3.99 \text{ gm/cm}^3$ , 44-13  $\mu\text{m}$ ) were placed in approximately one liter of ferrofluid and maintained in suspension by continuously stirring. About 20 cc of this mixture was introduced at intervals of about 4 minutes to maintain a constant flow of material into the chamber. As the fluid level rose in the trough the excess fluid was removed from regions of high fluid density near the magnet shims where few

FIG 4.1.4 FINE PARTICLE  
SEPARATION APPARATUS FOR  
LOW PARTICLE CONCENTRATION

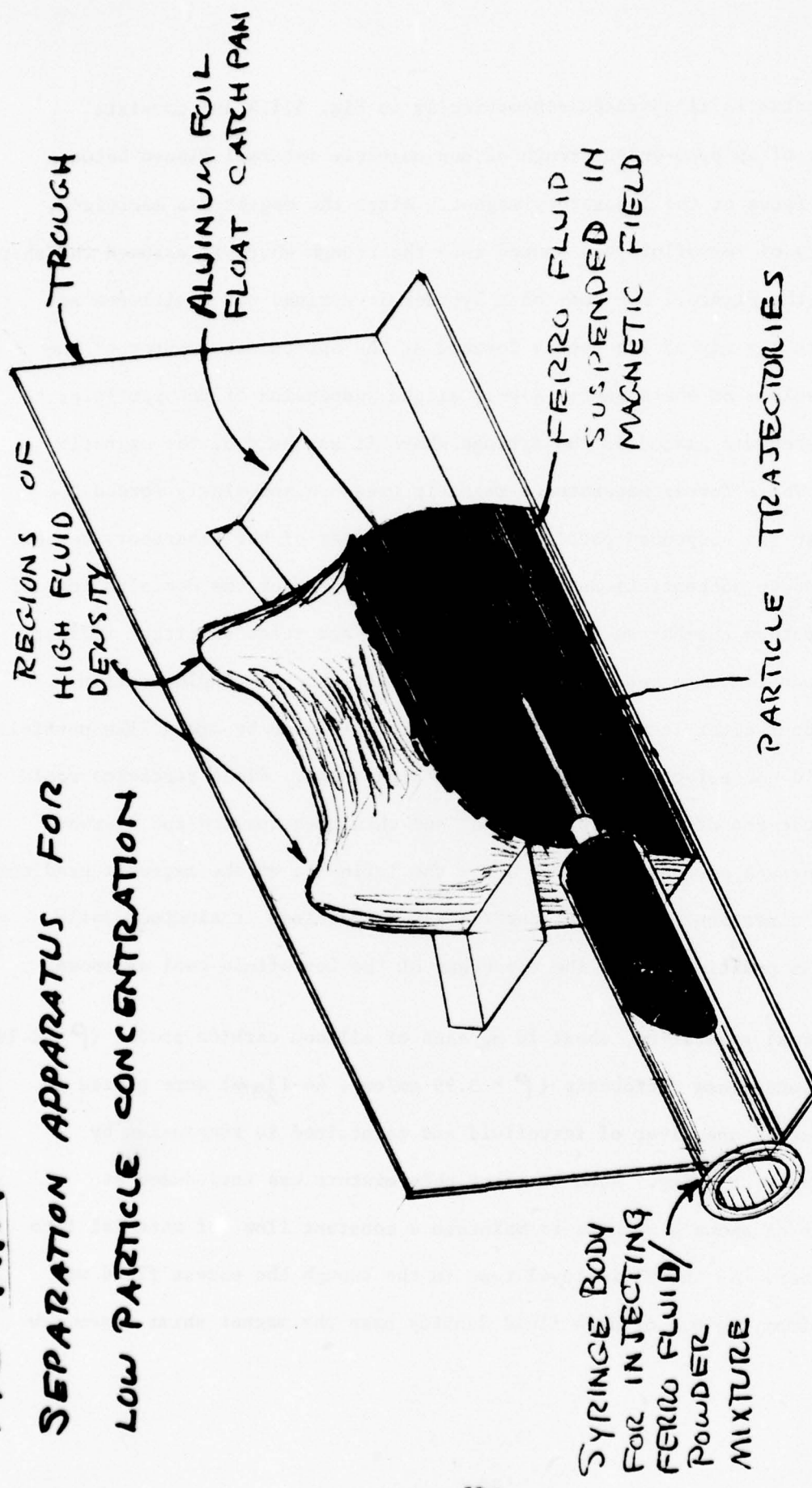
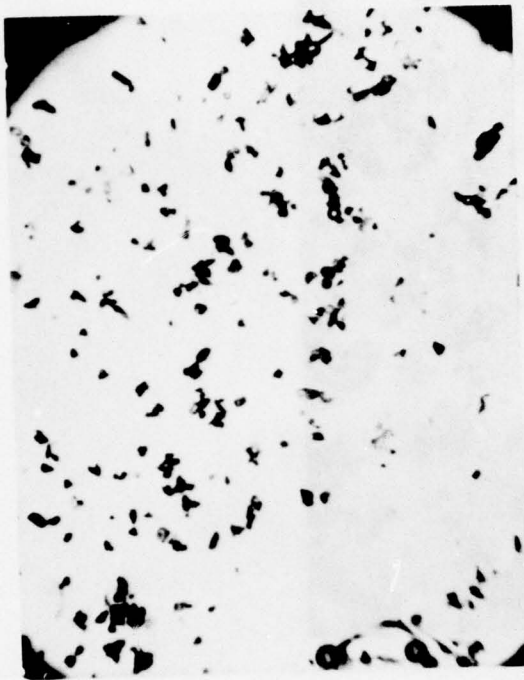
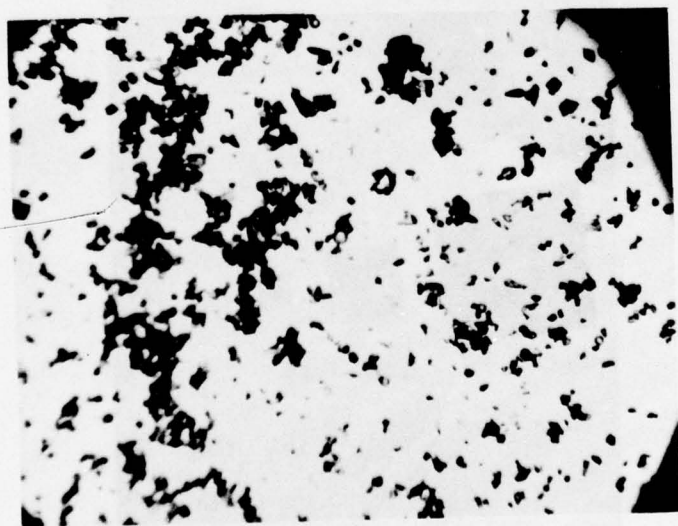


FIG 4.1.5

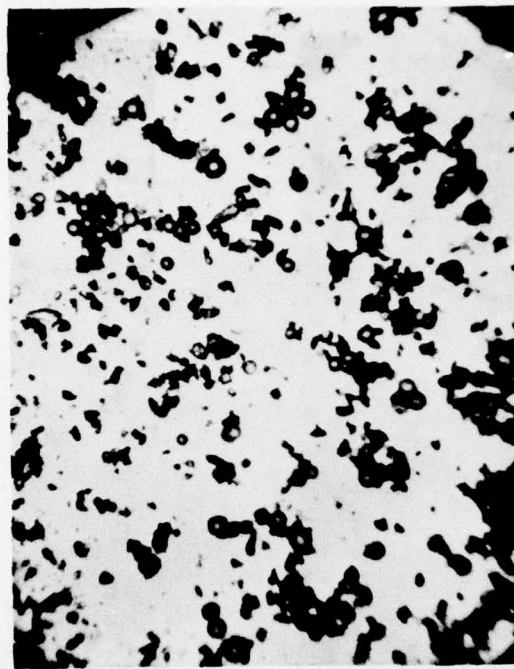


FRONT FLOAT FRACTION

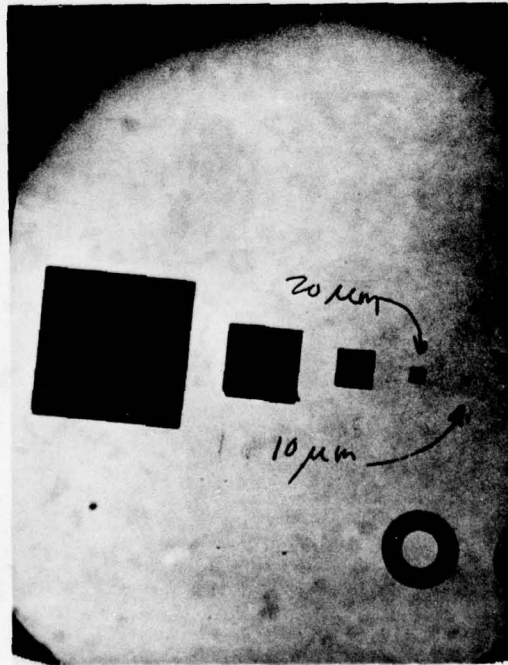


REAR FLOAT FRACTION

FIG. 4.1.6



SINK FRACTION



MICROSCOPE CALIBRATION

particles should penetrate. For this experiment the apparent density of the magnetic medium was adjusted to be about  $3.6 \text{ gm/cm}^3$  or roughly midway between the densities of the particles to be separated.

The calculated volumetric particle concentration for these experiments was about  $5 \times 10^{-6}$ . The actual effective concentration was somewhat less, however, due to the settling out of some of the larger particles in the fixed syringe. This settling of coarse particles could be eliminated by providing internal ridges on the syringe and cause it to rotate almost until the moment of injection.

The results of the experiments were quite encouraging and are shown in Figs. 4.1.5 and 4.1.6. The float fraction consisted of an estimated 10-15% of the material originally placed in suspension. This fraction was about 99% pure silicon carbide. The remaining material recovered in the sink fraction was not perceptibly enriched but it is thought that repeatedly reprocessing the sink fraction would yield an increasingly pure sink fraction. The presence of the light material in the sink fraction is attributed to the previously described apparent density - particle size phenomenon.

The design of this apparatus is particularly conducive to automatic unattended processing of the particles to be separated. Operation at even lower particle concentrations is possible by operating for long periods of time to accumulate sufficient quantities of the designed materials or by operating several parallel separations, even in the same magnet gap.

At this point in the program experiments with ferrofluids were suspended to evaluate liquid oxygen as the separation medium.

#### 4.2 Liquid Oxygen

The initial experiments with liquid oxygen were conducted in a closed-ended, insulated trough which proved satisfactory for operation with large objects. However, when working with fine powders it became necessary to greatly reduce the thermal transfer through the insulation to eliminate or minimize the bubble generation and convective currents. To circumvent the necessity of constructing an evacuated Dewar-type vessel shaped to fit the magnet pole faces, a separation chamber design using a sacrificial barrier of liquid oxygen was constructed. This device also employed inner baffles which served the dual purpose of diverting bubbles and currents from the working volume and as a removable depository for the sink and float fractions. The apparatus is shown in Figure 4.2.1.

Calibration of the chamber was accomplished by observing the behavior of small, 1/8", objects of known density within the liquid oxygen. Unlike an opaque ferrofluid which permitted observation of the calibration devices only on the surface of the ferrofluid, the transparent liquid oxygen allowed the calibration object to be viewed within the volume of the separation chamber, hovering at various levels as the magnet current and apparent density of the fluid was varied.

The calibration verified that liquid oxygen is a paramagnetic liquid, its magnetization increasing linearly with magnetic field strength. Experimental data for the determination of the magnetization curve for liquid oxygen is shown on Fig. 4.2.2. The slope of this curve,  $dM/dH$  is  $\chi$ , the magnetic susceptibility of the liquid. The experimental data are seen to agree well with the published value of susceptibility, which is also plotted in this figure. Combining the data above with the measured field intensity vs. magnet current characteristics of Fig. 4.2.3 one can generate a calibration graph of apparent density of the liquid oxygen as a function of magnet current for several levels corresponding to the top and bottom

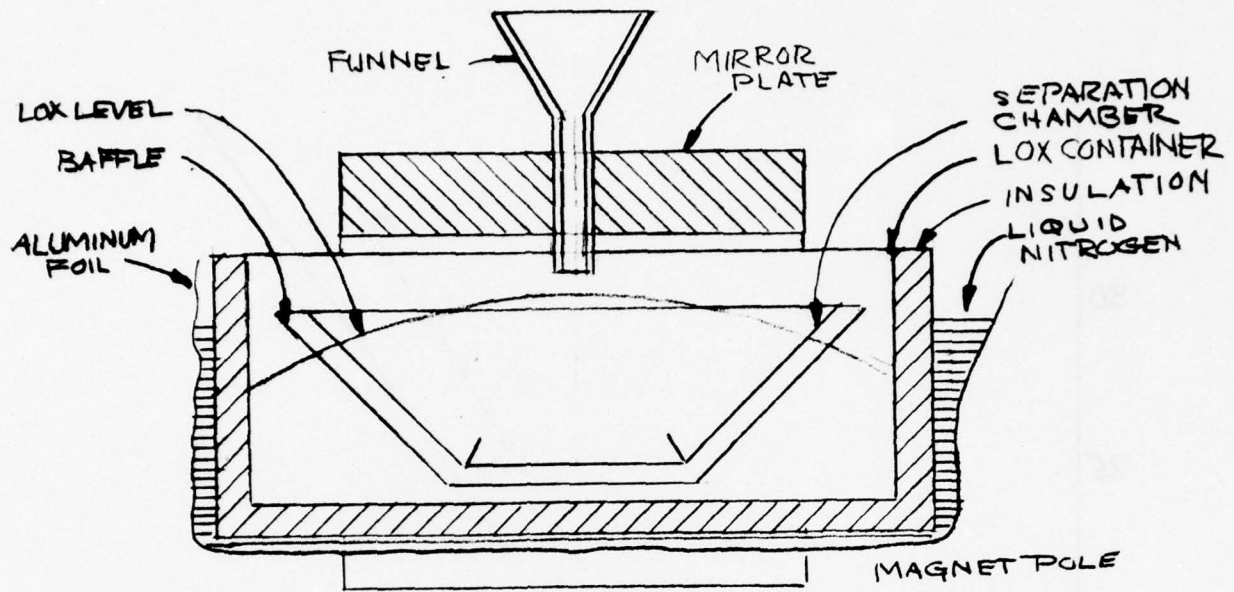


FIG. 2A CROSS SECTION OF LIQUID OXYGEN SEPARATION APPARATUS

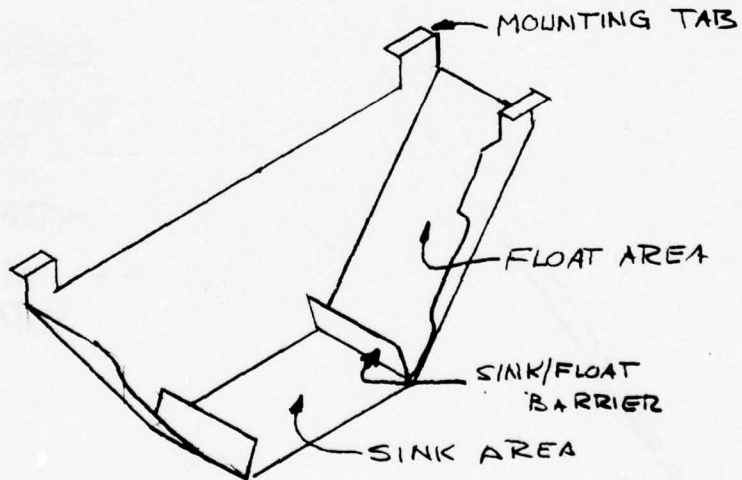


FIG 4.2.1 ISOMETRIC VIEW OF SEPARATION CHAMBER

FIGURE 2 MAGNETIZATION DATA FOR LIQUID OXYGEN

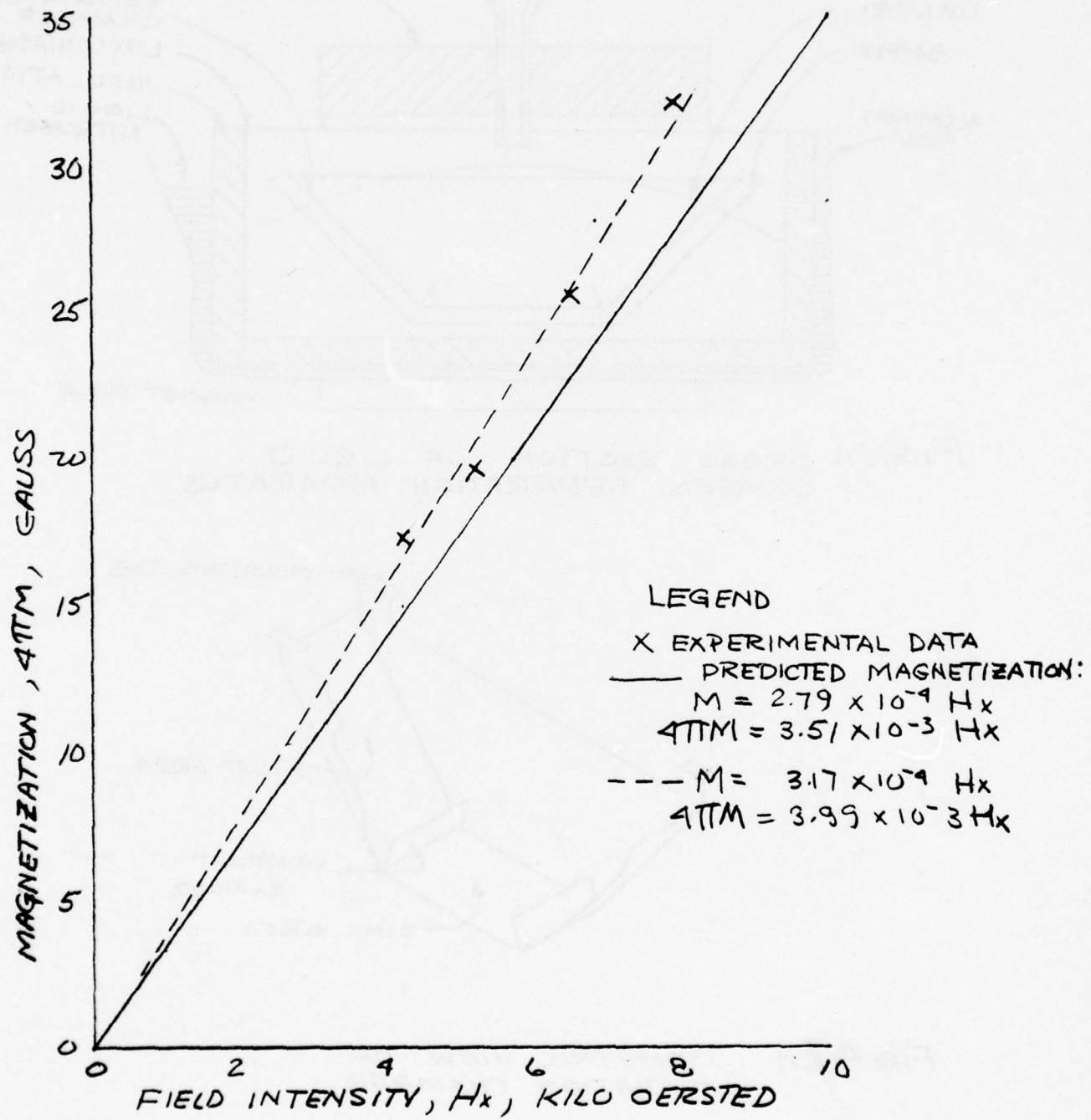
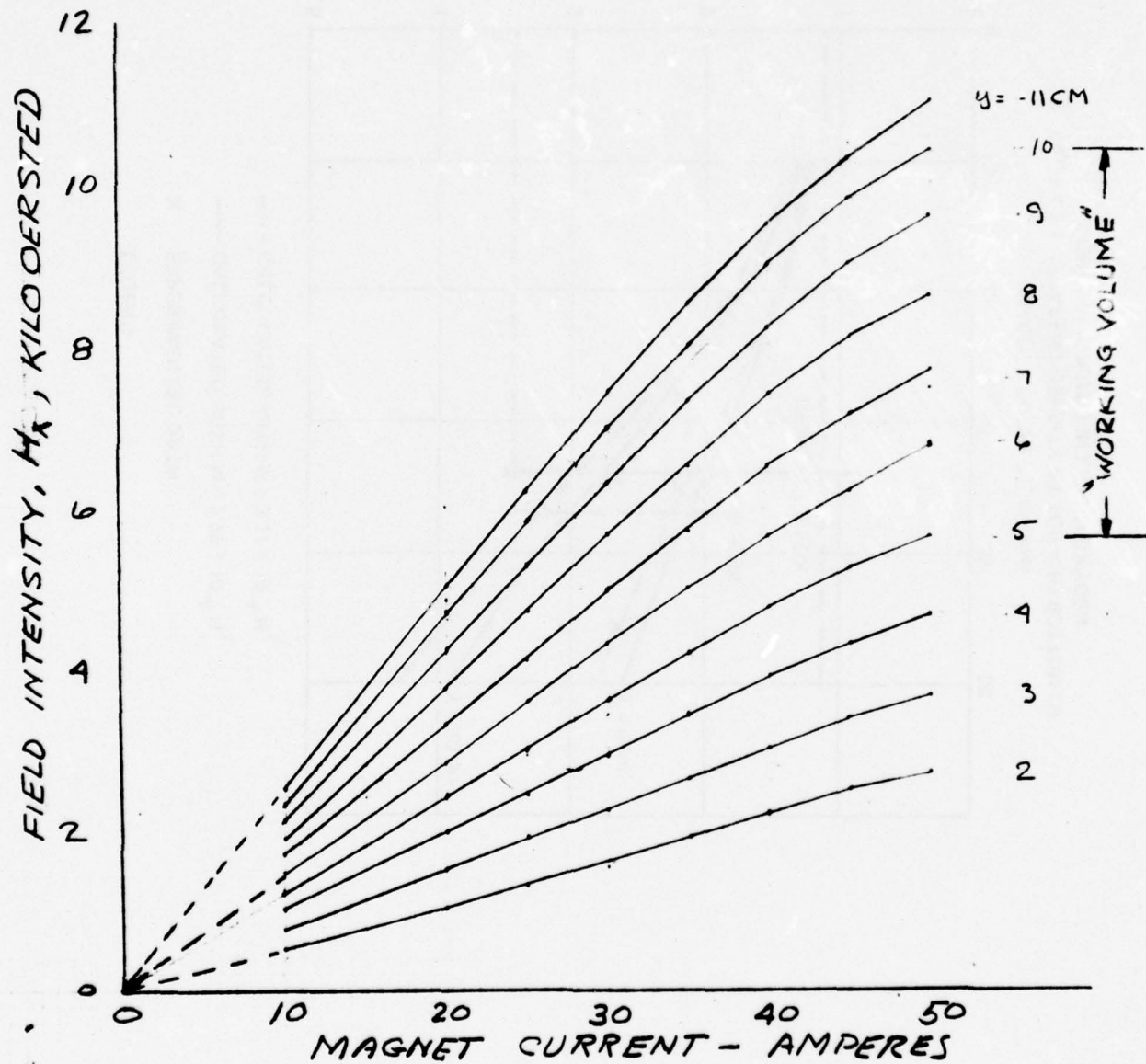


FIG 423 MEASURED FIELD INTENSITY OF  
LABORATORY MAGNET  $Z=0$ ,  $X=0$



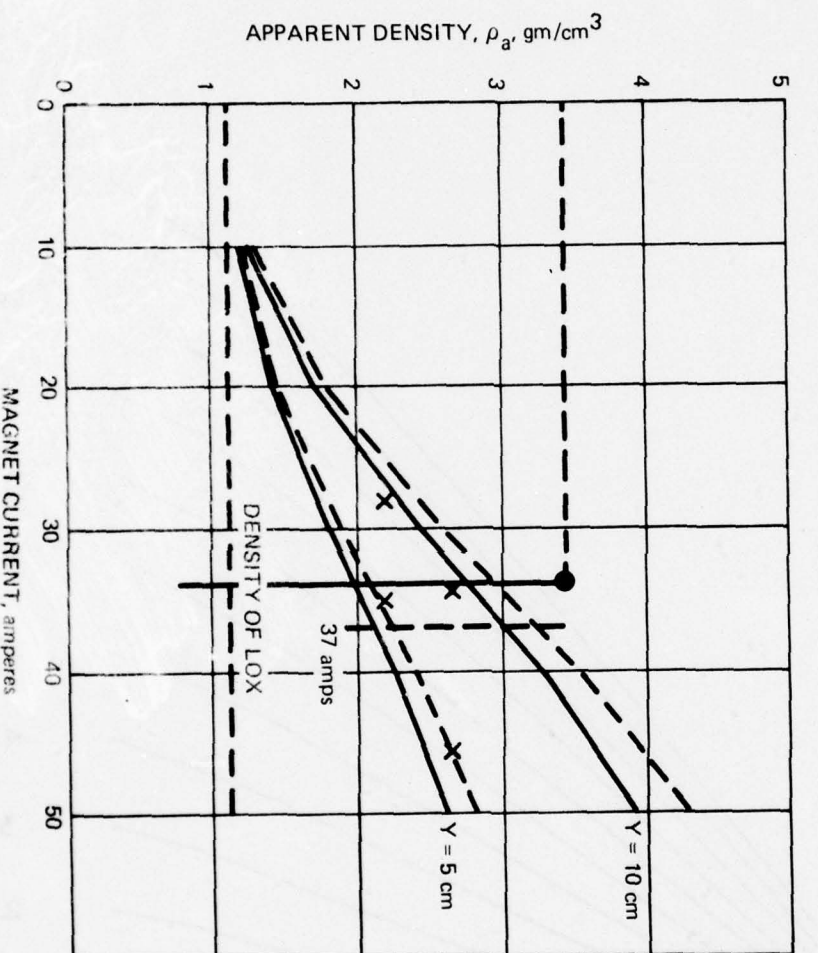


Figure 4.2.4 APPARENT DENSITY AT TOP AND BOTTOM OF WORKING VOLUME IN LIQUID OXYGEN

of the separation chamber as shown in Fig. 4.2.4. Apparent density at intermediate levels may be obtained by interpolation.

The excellent visibility afforded by the liquid oxygen gives a graphic appreciation of the forces, other than vertical, operating on objects within the working volume of the fluid. For instance, an object released near the pole faces can be seen to move very rapidly to the center plane of the magnet and then sink or float as dictated by the densities of the medium and object. Additionally there is another force, of considerably smaller magnitude than the centering force which acts to move objects in and out of the magnet gap. At low magnet currents, say below 30 amperes, the force is directed inward. Above this value of current the force is increasingly stronger, and changes sense or polarity such that at maximum magnet current, 50 amperes, there is a considerable outward force on an object to expel it from the working volume of the magnet fluid. In addition this effect is not symmetrical from front to rear, items introduced considerably to the rear of magnet center,  $Z = 0$ , tend to exit to the front at high magnet currents.

The above observed behavior is a result of the imperfect compensation for magnetic fringing provided by the magnet shim pads at various field strengths. Flatter horizontal magnetic gradients may be provided within the central zone of the magnet by using a magnetic having wider pole faces. It should be recognized, however that a small, consistent exit force is desirable to minimize particle crowding within the separation chamber and to provide a means of removing the light float fraction from the separation chamber.

It has been noted that when introducing a quantity of fine powder into the separation chamber that the powder, after spreading over the surface of the liquid oxygen, would move toward the center of separation chamber, spread out in a line in the Z direction and then descend to the bottom as a narrow curtain or veil of the particles.

Several methods were used to introduce the powders into the liquid oxygen in the separation chamber. At first the powders were merely sprinkled on the surface of the liquid oxygen through a funnel positioned through the mirror plate. Upon hitting the liquid oxygen surface the relatively warm fine particles could be seen to disperse quite rapidly over the surface of the liquid oxygen before separating into fractions.

Later the powder mixtures were first placed in a small test tube contained in an insulated sheath. By removing the test tube from the sheath and touching the test tube with a gloved hand it was possible to generate violent bubbling action within the test tube which, it was hoped would stir up and disperse the particles.

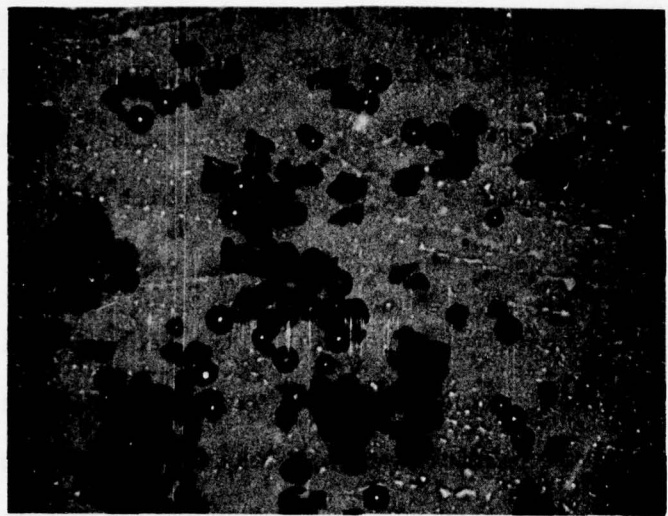
An ultrasonic probe, capable of operation at the temperature of liquid oxygen, was obtained to disperse the particles in liquid oxygen before pouring the liquid oxygen into the partly empty separation chamber.

It was found that operating the magnet without its mirror plate did not significantly degrade the magnetic gradient in the separation chamber so the ultrasonic probe was used directly in the chamber to disperse the powder mixtures to be separated.

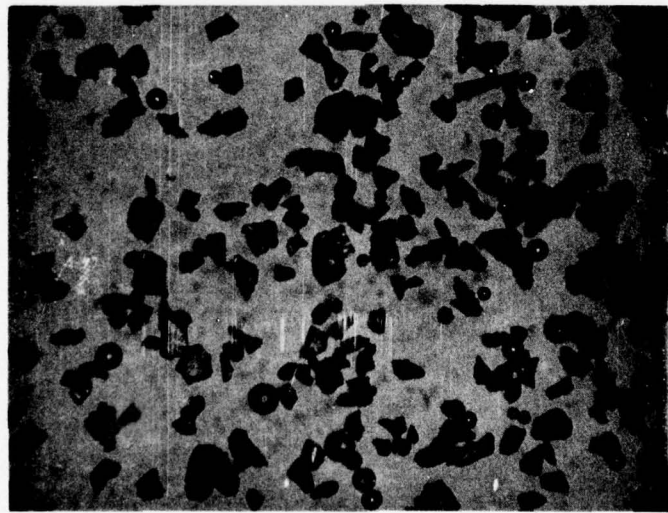
All of the above methods of particle dispersion yielded essentially identical results: A relatively pure sink fraction containing as much as 15% of the input material and a float fraction that was not perceptibly enriched. The finer particles

yielded poorer results. For example, Figures 4.2.5 and 4.2.6 show the results of separations of particle mixtures in the 10-15  $\mu$  size range with good enrichment of the sink fraction and a reasonable yield. Using a mixture of finer particles such as mixture A of Fig. 4.2.7 (Glass microbeads,  $\rho = 3.98 \text{ gm/cm}^3$ , 5-10  $\mu$  and silicon dioxide  $\rho = 2.65 \text{ gm/cm}^3$  A.P.S. 9  $\mu$ ) gives a good enrichment of the sink fraction (Fig. 4.2.8) but with a poor yield of about 2-3% of the input quantity (about 5% of the material which should have reported to the sink fraction).

It is possible that a contributing factor to the poor yield in the sink fractions is a vertical convection current within the liquid oxygen due to excessive heat leak into the separation chamber even with the sacrificial barrier of liquid oxygen. It has been noted that a small open Dewar flask will retain liquid oxygen in the separation chamber is dissipated in about two hours indicating the relatively high rate of heat transfer into the separation.

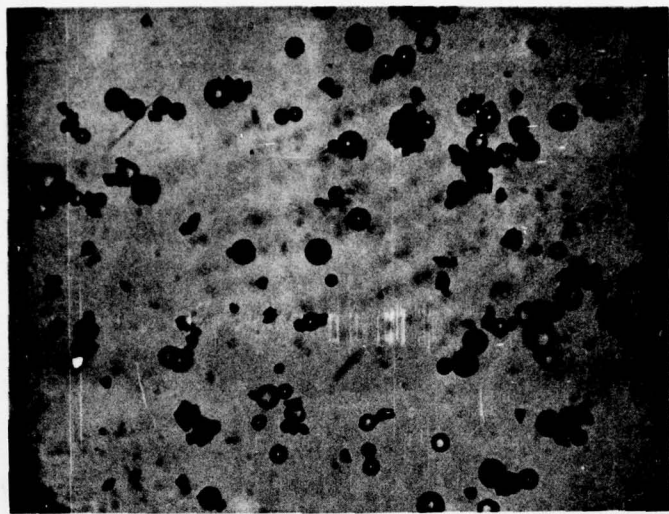


FLOATS

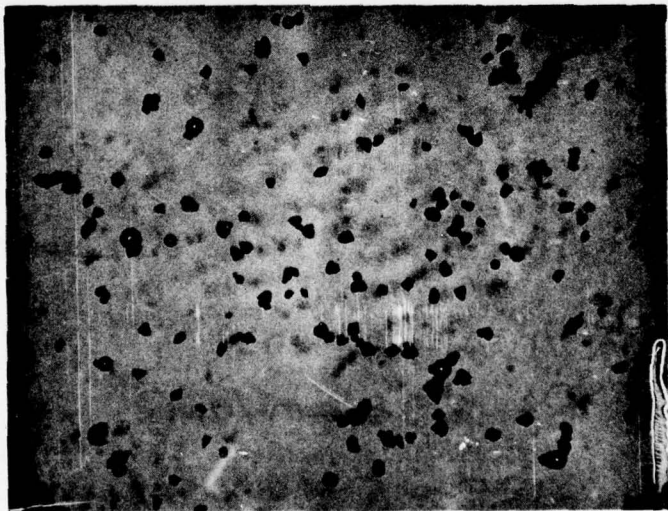


SINKS

FIG 4.2.5 RESULTS OF THE SEPARATION  
IN LIQUID OXYGEN OF ALUMINUM  
OXIDE ( $\rho = 3.98$ , 35-17 $\mu\text{m}$ , A.P.S 21 $\mu\text{m}$ )  
AND GLASS MICROBEADS ( $\rho = 2.42 \text{ gm/cm}^3$ ,  
37-14 $\mu\text{m}$ , A.P.S 28 $\mu\text{m}$ )

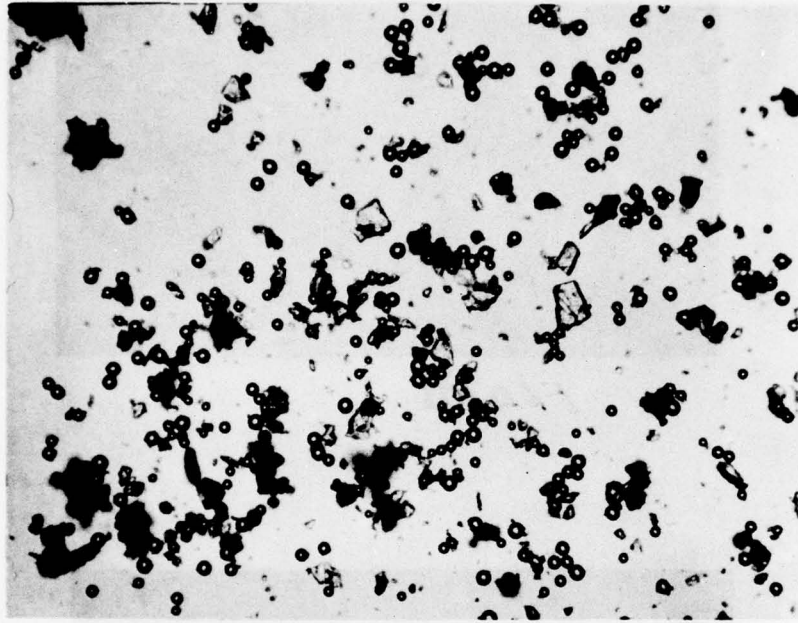


FLOATS



SINKS

FIG. 4.2.6 RESULTS OF THE SEPARATION  
IN LIQUID OXYGEN OF DIAMOND PARTICLES  
( $\rho = 3.51$ , 12-22  $\mu\text{m}$  A.P.S. 15  $\mu\text{m}$ ) AND  
GLASS MICROBEADS ( $\rho = 2.42$ , 37- $\mu\text{m}$   
A.P.S 28  $\mu\text{m}$ )



→ ← 10  $\mu$ m

200 X MIXTURE "A"

APPROX. 50-50 BY VOLUME

GLASS MICROBEADS

$\rho = 2.65 \text{ gm/cm}^3$

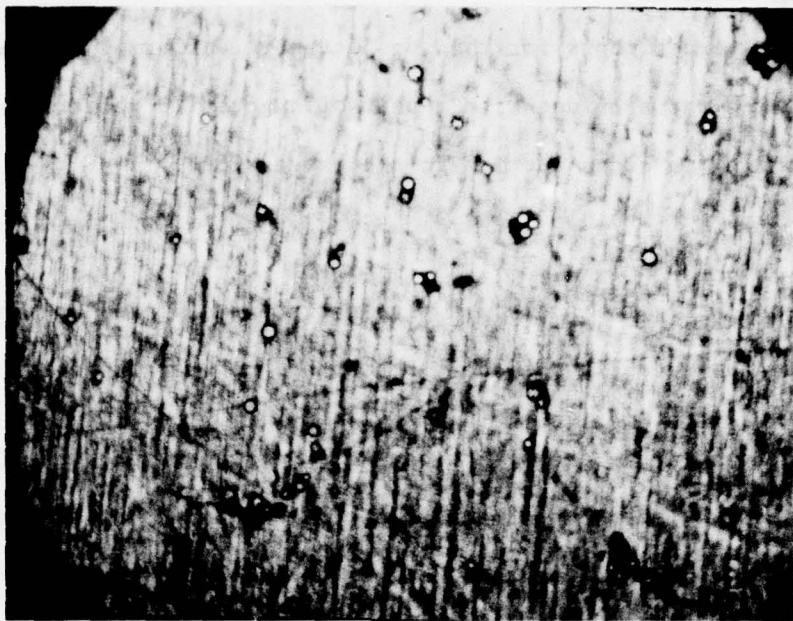
SIZE  $\sim 5-10 \mu\text{m}$

$\text{SiO}_2$

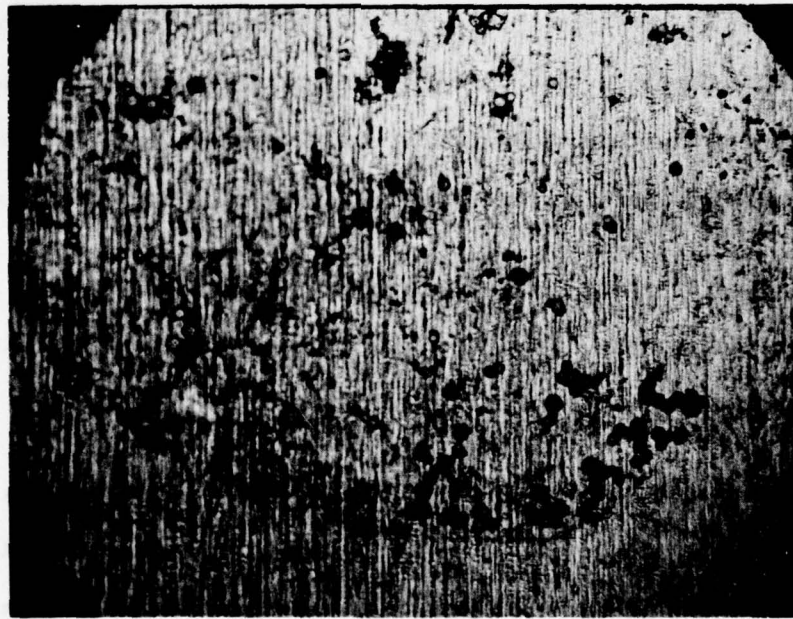
$\rho = 2.65 \text{ gm/cm}^3$

SIZE (AVG) 9  $\mu\text{m}$

FIG 4.2.7



3/31 SINK FRACTION  $I = 33A$  200 $\times$   
 $19\text{ }\mu$



9/1 SINK FRACTION  $I = 33A$  200 $\times$   
ESTIMATED 2-3% OF INPUT QTY  
 $E_V \approx 10^{-5}$

FIG 4.2.8

## 5.0 Magnet Design

The initial experiments for this project were performed on a small laboratory magnet which was provided with a pair of hyperbolic pole faces roughly corresponding in cross section to the expression

$$XY = \pm 4$$

where X and Y are in inches. A mirror plate was placed at the origin to eliminate the necessity of construction and upper pair of poles.

Fig. 5.1.1 shows the cross sectional view of the magnet and mirror plate where it may be seen that around the central portion of the magnetic the contour of the magnetic agrees well with the mathematical expression.

Above and below this "working zone" the magnet is truncated to minimize the total magnetic flux in the flux return path thus minimizing the amount of iron necessary to prevent saturation.

The purpose of the hyperbolic pole configuration is to provide a linear magnetic gradient on the axis of the magnet. Measurements made of the field strength within the gap have shown that the linearity of the magnetic gradient in the working zone has not been effected by the truncation of the magnetic poles.

Also included on Fig. 5.1.1 are data on the coils which provide the magnetomotive force for this magnet.

At a coil current of 50 amperes, limited by the power supply, the maximum field strength in the gap is about 10,000 gauss, which is well below the saturation flux of the iron pole structure of about 20,000 gauss.

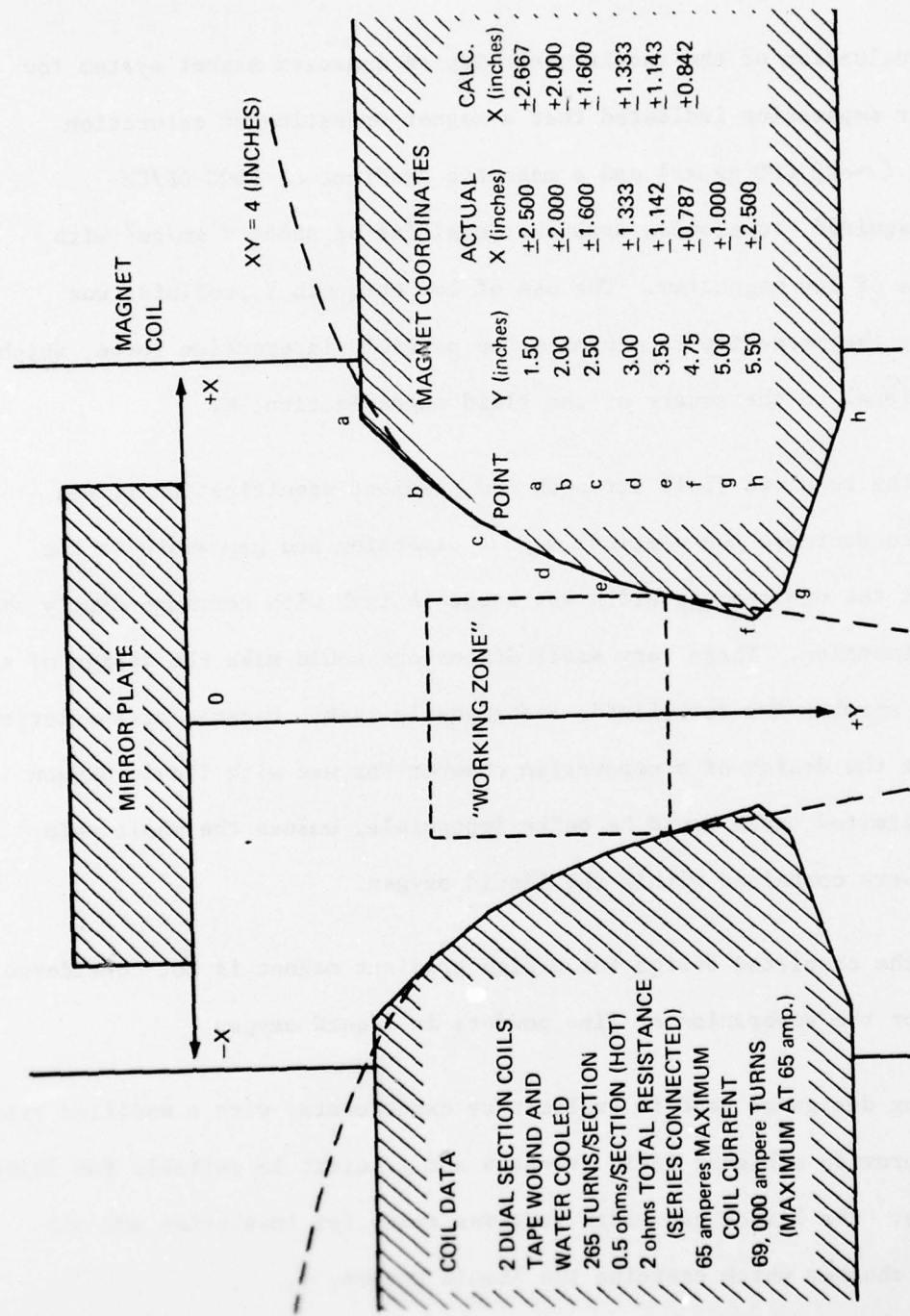


Figure 5.1.1 SEPARATION MAGNET SPECIFICATIONS

By redesigning this coil to double the ampere-turns it would be possible to double the field strength and gradient available in the magnet gap.

An early evaluation of the requirements for an improved magnet system for fine powder separation indicated that a magnet operating at saturation flux level ( $\sim 20,000$  gauss) and a magnetic gradient of 5000 OE/CM would be required to provide apparent densities of about  $7 \text{ gm/cm}^2$  with ferrofluids of low magnetism. The use of low strength ferrofluids was dictated by the necessity to minimize the particle interaction force, which is proportional to the square of the fluid magnetization,  $M$ .

To obtain the required field strength and gradient specification it was necessary to decrease the vertical magnet dimension and gap width to the extent that the minimum gap width was about .4 inch with correspondingly small vertical dimension. These very small dimensions would make the design of a separation chamber for ferrofluids a formidable task. Because of insulation requirement the design of a separation chamber for use with liquid oxygen in such a limited space would be quite impossible, unless the whole pole structure were contained within the liquid oxygen.

Therefore the completed design for a high gradient magnet is not considered suitable for the separation of fine powders in liquid oxygen.

The existing design as used in preliminary experiments, with a modified coil design to provide a higher field strength and gradient is suitable for future experiments. The 2 inch gap width provides space for insulation and the separation chamber which contains the liquid oxygen.

## 6.0 CONCLUSIONS AND RECOMMENDATIONS

### 6.1 Conclusions

Magnetic fluids, such as ferrofluids and liquid oxygen operating in a gradient magnetic field, are capable of floating objects more dense than any other liquid media and therefore represent a potentially valuable tool for use in the separation of mixtures of various non-magnetic materials according to their densities. Unfortunately, there are undesirable side-effects associated with these fluids which cannot be ignored if successful separations are to be accomplished.

The force on a non-magnetic particle in a gradient magnetic field is approximately equal to the product of the magnetization,  $M$ , of the fluid and the magnetic gradient,  $\nabla T$ . A magnet with hyperbolic pole faces can generate a magnetic field having a linear vertical magnetic gradient. By filling the gap of the magnet with a suitable magnetic liquid and aligning the axis of the magnet with the direction of gravity an adjustable magnetic force can be generated on a non-magnetic particle such that the particle may be made to float or sink selectively in the medium. In addition to the vertical magnetic gradient the hyperbolic magnet configuration has horizontal gradients which result in horizontal forces on a particle. In a magnet of practical pole width there is a diminution of field strength near the pole edges due to fringing effects. This may be countered somewhat by pads of magnetic material attached to the edges of the pole faces to reinforce the magnetic field in this area by shortening the gap. It has been found, however, that a small outward magnetic force is desirable to aid in removal of floating particles from the medium.

The other horizontal gradient is such that all non-magnetic particles in the magnetic liquid within the magnet gap tend to move to the center of the magnet. The magnitude of this gradient and its proportional horizontal force is a

function of the position of a particle within the magnetic volume. The horizontal magnetic force is related to the vertical magnetic force by the expression

$$F_x = \frac{x}{y} F_y$$

From this expression we see, for example that a particle at X,Y coordinates (1,2) experiences an inward force 1/2 as great as the levitation force. The situation is worsened by the fact that the vertical levitation force (including the buoyancy force of the liquid) is opposed by gravitational force such that the net vertical force is quite small and in a typical separation situation the horizontal force is predominant for particles some distance from the center line of the magnet. The result of the above action is that all particles tend to congregate on the vertical plane of symmetry of the magnet increasing the opportunities of particle interaction and misclassification.

It had been predicted and confirmed by experimental evidence that there is a force of attraction, of magnetic origin, between particles of like and unlike materials which may be greater than the sink/float forces on the particles with a resultant misclassification of the conglomerate of intermediate density. This attractive force,  $F_{ss}$ , stems from the distortion of the magnetic field caused by the presence of the non magnetic particles in the field. This force varies as the square of the fluid magnetization, M, the sixth power of the particle diameter, D, and inversely as the fourth power of the particle spacing, a:

$$F_{ss} = \frac{(4\pi M)^2}{96} \frac{D^6}{a^4}$$

Thus the interparticle force is lessened by using the lowest fluid magnetization possible and by increasing the interparticle spacing.

In addition, there appears to be an interaction between fine particles and colloidal ferrite particles of the ferrofluid such that very fine non-magnetic particles gain some magnetic properties and appear to be heavier than their true density. It has been tentatively theorized that a ferrite layer of constant thickness attaches to all particles regardless of size. For small particles, say  $< 10 \mu\text{m}$ , the surface area to volume ratio is such that the adsorbed ferrite layer can change the effective density of the particle by as much as 50%. The effect diminishes with increasing particle size until the effect is undetectable for particles larger than about  $100 \mu\text{m}$ . From the above effective density - particle size relationship one might assume that in operating a powder having a wide range of particle sizes in ferrofluid would result in a separation of the particles according to size - a sort of magnetic sieve. That this is not the case is attributed to the particle interaction forces since it was observed in flotation experiments of particle having a wide range of sizes that at the apparent density transition point from floating to sinking the particles recovered in the float and sink fractions had essentially identical particle distributions. It appears that the power mixtures respond according to the average particle size of the mixture.

The fact that this effective density - particle size relationship was not present in experiments conducted with liquid oxygen lends credence to the assumption of ferrite non-magnetic particle interaction, since liquid oxygen is a homogeneous, elemental fluid.

Early experiments were performed at magnetic field strength high enough to cause magnetic saturation in the ferrofluid used with the result that the magnetization of the fluid was constant (but variable by dilution) and a pool of constant

density was generated for separation of items by density into sink and float fractions. In this case the apparent density of the ferrofluid on the magnet center line was

$$\rho_a = \rho_f + \frac{MT}{g}$$

in which the natural density of the fluid,  $\rho_f$ , was augmented by a magnetic "density" proportional to the product of the fluid magnetization, M, and the magnetic gradient,  $T$ .

It was proposed to manufacture a ferrofluid having considerably smaller particle size so that at high field strength the ferrofluid would not saturate and the fluid magnetization would increase somewhat linearly with field strength, H, so that the apparent density of this medium varied as the vertical dimension Y:

$$\rho_a = \rho_f + \frac{\chi T^2 y}{g}$$

Here,  $\chi$  is the slope of the magnetization curve  $dM/dH$ . A ferrofluid of this type was never manufactured but the effect was observed in experiments with liquid oxygen, a non-saturating paramagnetic liquid.

The most successful separations experiments of the program involved the separation of a binary mixture of closely sized particles using a technique in which a very dilute suspension of the particles was injected into a ferrofluid pool such that each particle entered the decision point on the centerline of the magnet unencumbered by other particles and moved to the proper reporting point. Conglomeration of like particles after the decision point would not effect the efficiency of the separation. These experiments resulted in a very pure float fraction with about 25% of the light material recovered in the floats. The sink fraction was considerably enriched.

In summary, then, there are several factors which adversely effect the separation of mixtures of material according to density.

1. There is a particle to particle interaction force which causes misclassification by creating an agglomerate of intermediate density.
2. A ferrite to non-magnetic particle interaction which causes misclassification by altering the effective density of particles.
3. A high particle concentration is conducive to particle interaction.
4. The effective particle concentration is increased by the centering forces on the particles.

## 6.2 RECOMMENDATIONS

The design of a system for the successful separation, by density of mixtures of fine particles involves the evaluation and optimization of a number of conflicting and counteracting factors.

The use of liquid oxygen as the magnetic medium has been demonstrated to eliminate the very undesirable change in effective density experienced in ferrofluid on particles smaller than about  $100 \mu M$  and is considered to be superior to ferrofluids for this important reason. The low boiling point and high volatility of liquid oxygen are not considered to be insuperable problems.

Liquid oxygen is a paramagnetic material and therefore must generate a density gradient in the separation chamber. The magnitude of the density gradient is dictated by separation chamber and magnet design. The use of a density gradient column offers the possibility of attaining more than two density fractions as the result of a separation depending on the gradient and depth of the chamber.

A fluid of low magnetization is desirable to minimize the particle interaction force. In order to achieve the required apparent density however, would necessitate an increase in the magnetic gradient, which in turn increases the centering forces and opportunities for particle interaction.

For these reasons it is thought that the separation apparatus which offers the greatest chance for success is an adaptation of the injection technique used somewhat successfully with ferrofluids. The use of liquid oxygen would eliminate the undesirable variation of the effective density of the particles with size.

By injecting particles on the centerline of the magnet from a well stirred or agitated suspension essentially one particle at a time, each particle can make its sink/float decision unhindered by other particles and unaffected by the centering forces. In this way the untoward effects of the centering and particle interaction forces are eliminated. If particle agglomeration should occur it would be after the sink/float decision has been made and the interaction should be between like particles which would not effect the quality of the separation.

The injection of the particles would be accomplished by the magnetic force of attraction on the liquid oxygen which would be drawn into the magnet gap carrying the non magnetic particles into the center of the separation chamber against the horizontal pressure gradient associated with the horizontal magnetic gradient. Heavy particles would sink to the bottom of the separation chamber and remain there. Light particles would float to the surface and then move forward and backward under the influence of the small magnetic gradients in the Z-direction to suitable catch trays positioned in the magnetic liquid. Particles of intermediate density will be similarly propelled along levels of constant density to be retained in compartmented trays.

The material throughput rate for a single injection of particles is probably quite low. This situation could be improved considerably by the use of multiple injection of particles, from the same reservoir, along the center line of the magnet. In addition, the process described above is essentially a continuous process with respect to the input of material and may be operated, unattended, for extended periods of time.

The separation of mixtures of fine particles according to density is considered feasible using liquid oxygen as the magnetic medium. Additional experimental effort is required in the areas of fine particle handling, dispersion and introduction.

## APPENDIX A

### 1.0 Calculation of the Force on a Magnetic Dipole in a Magnetic Field.

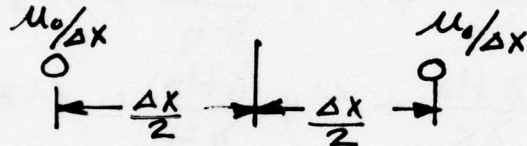
1.1 The force on a magnetic pole  $m$  (unit poles) in a magnetic field  $\vec{H}$  (Oersteds) is given by

$$\vec{F} = m \vec{H} \text{ dynes}$$

To calculate the force on a dipole  $\vec{\mu}$  decompose it into its component part.

$$\vec{\mu} = \hat{i}\mu_x + \hat{j}\mu_y + \hat{k}\mu_z$$

The  $x$  component of the dipole  $\mu_x$  can be considered to be two poles of strength  $(\mu_x/\Delta x)$  and  $(-\mu_x/\Delta x)$  separated by a distance  $\Delta x$ .



The force on the two poles is given by

$$F_x^{(1)} = \left(\frac{\mu_x}{\Delta x}\right) H_x \left(x + \frac{\Delta x}{2}, y, z\right)$$

$$F_x^{(2)} = \left(\frac{-\mu_x}{\Delta x}\right) H_y \left(x - \frac{\Delta x}{2}, y, z\right)$$

Thus the force on the dipole can be written

$$F_x(x, y, z) = \left(\frac{\mu_x}{\Delta x}\right) \left[ H_x \left(x + \frac{\Delta x}{2}, y, z\right) - H_x \left(x - \frac{\Delta x}{2}, y, z\right) \right]$$

Taking the limit as

$$\Delta x \rightarrow 0$$

The  $y$  and  $z$  directed forces on this dipole are similarly calculated as:

$$F_y = \mu_x \frac{\partial H_y}{\partial x}$$

$$F_z = \mu_x \frac{\partial H_z}{\partial x}$$

1.2 By symmetry<sup>(1)</sup> one can deduce that the forces on  $M_y$  and  $M_z$  are given by

$$F_x = M_y \frac{\partial H_x}{\partial y}$$

$$F_x = M_z \frac{\partial H_x}{\partial z}$$

$$F_y = M_y \frac{\partial H_y}{\partial y}$$

$$F_y = M_z \frac{\partial H_y}{\partial y}$$

$$F_z = M_y \frac{\partial H_z}{\partial y}$$

$$F_z = M_z \frac{\partial H_z}{\partial z}$$

1.3 Combining the results of 1.1 and 1.2

$$F_x = M_x \frac{\partial H_x}{\partial x} + M_y \frac{\partial H_x}{\partial y} + M_z \frac{\partial H_x}{\partial z}$$

$$F_y = M_x \frac{\partial H_y}{\partial x} + M_y \frac{\partial H_y}{\partial y} + M_z \frac{\partial H_y}{\partial z}$$

$$F_z = M_x \frac{\partial H_z}{\partial x} + M_y \frac{\partial H_z}{\partial y} + M_z \frac{\partial H_z}{\partial z}$$

1.4 Examining the x-component of force one sees that

$$F_x = \left( M_x \frac{\partial}{\partial x} + M_y \frac{\partial}{\partial y} + M_z \frac{\partial}{\partial z} \right) H_x$$

$$\text{or } F_x = (\vec{\mu} \cdot \nabla) H_x$$

(1) let  $x \rightarrow y$ ,  $y \rightarrow z$  and  $z \rightarrow x$

1.5 Thus one can write the force on a dipole in a magnetic field as

$$\vec{F} = (\vec{\mu} \cdot \nabla) \vec{H}$$

where  $\vec{\mu} \cdot \nabla$  is a scalar operator operating on each component of the vector field  $\vec{H}$ . Thus the force in the x direction is determined by the operator  $\vec{\mu} \cdot \nabla$  operating on the x component of the magnetic field  $H_x$ .

$$F_x = (\vec{\mu} \cdot \nabla) H_x$$

$$F_y = (\vec{\mu} \cdot \nabla) H_y$$

$$F_z = (\vec{\mu} \cdot \nabla) H_z$$

## 2.0 Calculation of the Force on a Magnetic Particle in a Magnetic Field

### 2.1 Case I magnetized (saturated) particle of volume $V$

$$\vec{\mu} = M_s V$$

2.1.1 The saturated particle will align itself with the magnetic field such that

$$\vec{\mu} = M_s \frac{\vec{H}}{|\vec{H}|} = M_s \frac{\vec{H}}{|\vec{H}|}$$

Therefore the form on a saturated particle is given by

$$\vec{F} = (\vec{\mu} \cdot \nabla) \vec{H} = (M_s \frac{\vec{H}}{|\vec{H}|} \cdot \nabla) \vec{H}$$

### 2.1.2 For simplicity consider the two dimensional case

$$\vec{F} = M_s \left[ \left\{ \frac{\vec{i} H_x + \vec{j} H_y}{|\vec{H}|} \right\} \cdot \left\{ \vec{i} \frac{\partial}{\partial x} + \vec{j} \frac{\partial}{\partial y} \right\} \right] (\vec{i} H_x + \vec{j} H_y)$$

$$= M_s \frac{1}{|\vec{H}|} (H_x \frac{\partial}{\partial x} + H_y \frac{\partial}{\partial y}) (\vec{i} H_x + \vec{j} H_y)$$

$$F_x = M_s \frac{1}{|\vec{H}|} \left\{ H_x \frac{\partial H_x}{\partial x} + H_y \frac{\partial H_x}{\partial y} \right\}$$

$$F_y = M_s \frac{1}{|\vec{H}|} \left\{ H_x \frac{\partial H_y}{\partial x} + H_y \frac{\partial H_y}{\partial y} \right\}$$

The force on a saturated particle in a magnetic field is sometimes given as proportional to the gradient of the magnitude of the magnetic field  $\vec{H}$ . To test this assumption one can calculate  $\nabla|\vec{H}|$ .

$$\begin{aligned}\nabla|\vec{H}| &= \left(\hat{x}\frac{\partial}{\partial x} + \hat{y}\frac{\partial}{\partial y}\right)(H_x^2 + H_y^2)^{\frac{1}{2}} \\ &= (H_x^2 + H_y^2)^{-\frac{1}{2}} \left[ \hat{x} \left\{ H_x \frac{\partial H_x}{\partial x} + H_y \frac{\partial H_y}{\partial x} \right\} \right. \\ &\quad \left. + \hat{y} \left\{ H_x \frac{\partial H_x}{\partial y} + H_y \frac{\partial H_y}{\partial y} \right\} \right]\end{aligned}$$

$$[\nabla|\vec{H}|]_x = \frac{1}{|\vec{H}|} \left\{ H_x \frac{\partial H_x}{\partial x} + H_y \frac{\partial H_y}{\partial x} \right\}$$

$$[\nabla|\vec{H}|]_y = \frac{1}{|\vec{H}|} \left\{ H_x \frac{\partial H_x}{\partial y} + H_y \frac{\partial H_y}{\partial y} \right\}$$

Comparing the last two equations with the force equations one can see that the force on a saturated particle is not proportional to  $\vec{H}$  unless

$$\frac{\partial H_x}{\partial y} = \frac{\partial H_y}{\partial x}$$

But as will be discussed in section 3.0 the magnetic field strength is defined as the negative gradient of a scalar potential  $\phi$

$$\begin{aligned}\vec{H} &= -\nabla \phi \\ &= -\hat{x} \frac{\partial \phi}{\partial x} - \hat{y} \frac{\partial \phi}{\partial y} - \hat{z} \frac{\partial \phi}{\partial z}\end{aligned}$$

or -  $H_x = -\frac{\partial \phi}{\partial x}$   
 $H_y = -\frac{\partial \phi}{\partial y}$   
 $H_z = -\frac{\partial \phi}{\partial z}$

Thus

$$\frac{\partial H_x}{\partial y} = -\frac{\partial}{\partial y} \left( \frac{\partial \phi}{\partial x} \right) = -\frac{\partial}{\partial x} \left( \frac{\partial \phi}{\partial y} \right) = \frac{\partial H_y}{\partial x}$$

The physics of the magnetic field therefore imposes the relationship

$$\vec{F} = \mu_s \nabla |\vec{H}|$$

or in words the force on a saturated magnetic particle is equal to the dipole moment of the particle  $\mu_s$  times the gradient of the magnitude of the magnetic field.  $\vec{H}$

## 2.2 Case II unsaturated particle of volume $V$

$$\vec{\mu} = \vec{M} V$$

2.2.1 The magnetization  $M$  of a paramagnetic particle is dependent on its demagnetizing factor<sup>(2)</sup> which is geometry dependent and its susceptibility  $\chi$ . The field internal to an ellipsoidal particle in a magnetic field  $H_0$  is given by

$$H_i = H_0 - \frac{N}{4\pi} (4\pi M)$$

where  $\frac{N}{4\pi}$  is the demagnetizing factor (for a sphere  $\frac{N}{4\pi} = \frac{1}{3}$ )

but  $M = \chi H_i$  therefore

$$M = \frac{\chi H_0}{1 + \chi N}$$

(2) R.M. Bozorth, "Ferromagnetism" page 10.

AD-A035 639

AVCO CORP LOWELL MASS SYSTEMS DIV

MAGNETIC FLUID DENSITY SEPARATION SYSTEM FOR FINE POWDERS. (U)

AUG 76 E P MCQUAID

F/G 14/2

F08606-74-C-0064

NL

UNCLASSIFIED

2 of 2  
ADAO35639



END

DATE  
FILMED  
3 - 77

Therefore the dipole moment of a paramagnetic particle in a magnetic field is given by

$$\vec{\mu} = (\text{volume}) \frac{\chi \vec{H}}{1 + \chi N}$$

For the purpose of this calculation let

$$\kappa = (\text{volume}) \chi / (1 + \chi N)$$

$$\text{therefore } \vec{M} = \kappa \vec{H}$$

2.2.2 Combining the results from paragraph 1.5 and 2.2.1 one finds that the force on a paramagnetic particle is given by

$$\begin{aligned} \vec{F} &= (\vec{\mu} \cdot \nabla) \vec{H} \\ &= (\kappa \vec{H} \cdot \nabla) \vec{H} \end{aligned}$$

To relate this to the gradient of the field one must again expand into components.

$$F_x = \kappa \left\{ H_x \frac{\partial H_x}{\partial x} + H_y \frac{\partial H_x}{\partial y} + H_z \frac{\partial H_x}{\partial z} \right\}$$

$$F_y = \kappa \left\{ H_x \frac{\partial H_y}{\partial x} + H_y \frac{\partial H_y}{\partial y} + H_z \frac{\partial H_y}{\partial z} \right\}$$

$$F_z = \kappa \left\{ H_x \frac{\partial H_z}{\partial x} + H_y \frac{\partial H_z}{\partial y} + H_z \frac{\partial H_z}{\partial z} \right\}$$

Now the gradient of the magnitude of the field is given by

$$\begin{aligned} \nabla |\vec{H}| &= \vec{x} \frac{\partial}{\partial x} (H_x^2 + H_y^2 + H_z^2)^{\frac{1}{2}} \\ &\quad + \vec{y} \frac{\partial}{\partial y} (H_x^2 + H_y^2 + H_z^2)^{\frac{1}{2}} \\ &\quad + \vec{z} \frac{\partial}{\partial z} (H_x^2 + H_y^2 + H_z^2)^{\frac{1}{2}} \\ &= \frac{\vec{x}}{|\vec{H}|} \left\{ H_x \frac{\partial H_x}{\partial x} + H_y \frac{\partial H_y}{\partial x} + H_z \frac{\partial H_z}{\partial x} \right\} \\ &\quad + \frac{\vec{y}}{|\vec{H}|} \left\{ H_x \frac{\partial H_x}{\partial y} + H_y \frac{\partial H_y}{\partial y} + H_z \frac{\partial H_z}{\partial y} \right\} \\ &\quad + \frac{\vec{z}}{|\vec{H}|} \left\{ H_x \frac{\partial H_x}{\partial z} + H_y \frac{\partial H_y}{\partial z} + H_z \frac{\partial H_z}{\partial z} \right\} \end{aligned}$$

Thus along the curve defined by the equation  $xy = a$  (first and third quadrants) the magnetic scalar potential is given by

$$\phi(x, y) = \phi_0$$

and along the curve defined by the equation  $xy = a$  (second and forth quadrants) the magnetic scalar potential is given by:

$$\phi(x, y) = -\phi_0$$

A magnetostatic potential must satisfy Laplace's equation

$$\nabla^2 \phi = 0$$

It is easily shown that:

$$\nabla^2 \phi = \left( \frac{\partial^2}{\partial x^2} + \frac{\partial^2}{\partial y^2} + \frac{\partial^2}{\partial z^2} \right) \frac{\phi_0}{a} xy = 0$$

Now the magnetic field strength  $\vec{H}$  (in the absence of currents) is defined as the negative gradient of the magnetic scalar potential

$$\vec{H} = -\nabla \phi = -\left[ \hat{x} \frac{\partial \phi}{\partial x} + \hat{y} \frac{\partial \phi}{\partial y} + \hat{z} \frac{\partial \phi}{\partial z} \right] \phi$$

Thus

$$H_x = -\frac{\partial \phi}{\partial x} = -\frac{\phi_0}{a} y$$

and

$$H_y = -\frac{\partial \phi}{\partial y} = -\frac{\phi_0}{a} x$$

For the purpose of this discussion it is convenient to write  $\phi_0/a$  as  $T$  therefore

$$\phi = T x y$$

$$H_x = -T y$$

$$H_y = -T x$$

From the definition of the magnetic field as the negative gradient of a scalar magnetic potential one has:

$$H_x = -\frac{\partial \phi}{\partial x}, \quad H_y = -\frac{\partial \phi}{\partial y}, \quad H_z = -\frac{\partial \phi}{\partial z}$$

Therefore

$$\frac{\partial H_x}{\partial y} = \frac{\partial H_y}{\partial x}, \quad \frac{\partial H_x}{\partial z} = \frac{\partial H_z}{\partial x}, \quad \frac{\partial H_z}{\partial y} = \frac{\partial H_y}{\partial z}$$

and the force on an unsaturated (i.e. paramagnetic) particle

can be written

$$\vec{F} = \kappa |H| \nabla |H|$$

which is easily shown to be

$$\vec{F} = \frac{1}{2} \kappa \nabla |H|^2$$

or

$$\vec{F} = \frac{\kappa}{2} \nabla \{ H_x^2 + H_y^2 + H_z^2 \}$$

In words, the force on an unsaturated (paramagnetic) particle is proportional to the gradient of the magnetic field squared.

$$\vec{F} = \frac{\kappa}{2} \nabla (H \cdot H)$$

### 3.0 The magnetic Field in a quadrupolar magnet

The pole pieces of a quadrupolar magnet have a hyperbolic geometry. Thus a pole surface is defined by a portion of the curve.

$$xy = a$$

If one energizes the poles shown in Figure 1 the magnetic scalar potentials of the poles are  $\phi_1 = \phi_3 = -\phi_2 = -\phi_4 = \phi_0$

One can therefore write the magnetic scalar potential in the region enclosed by the poles as

$$\phi(x, y) = \frac{\phi_0}{a} xy$$

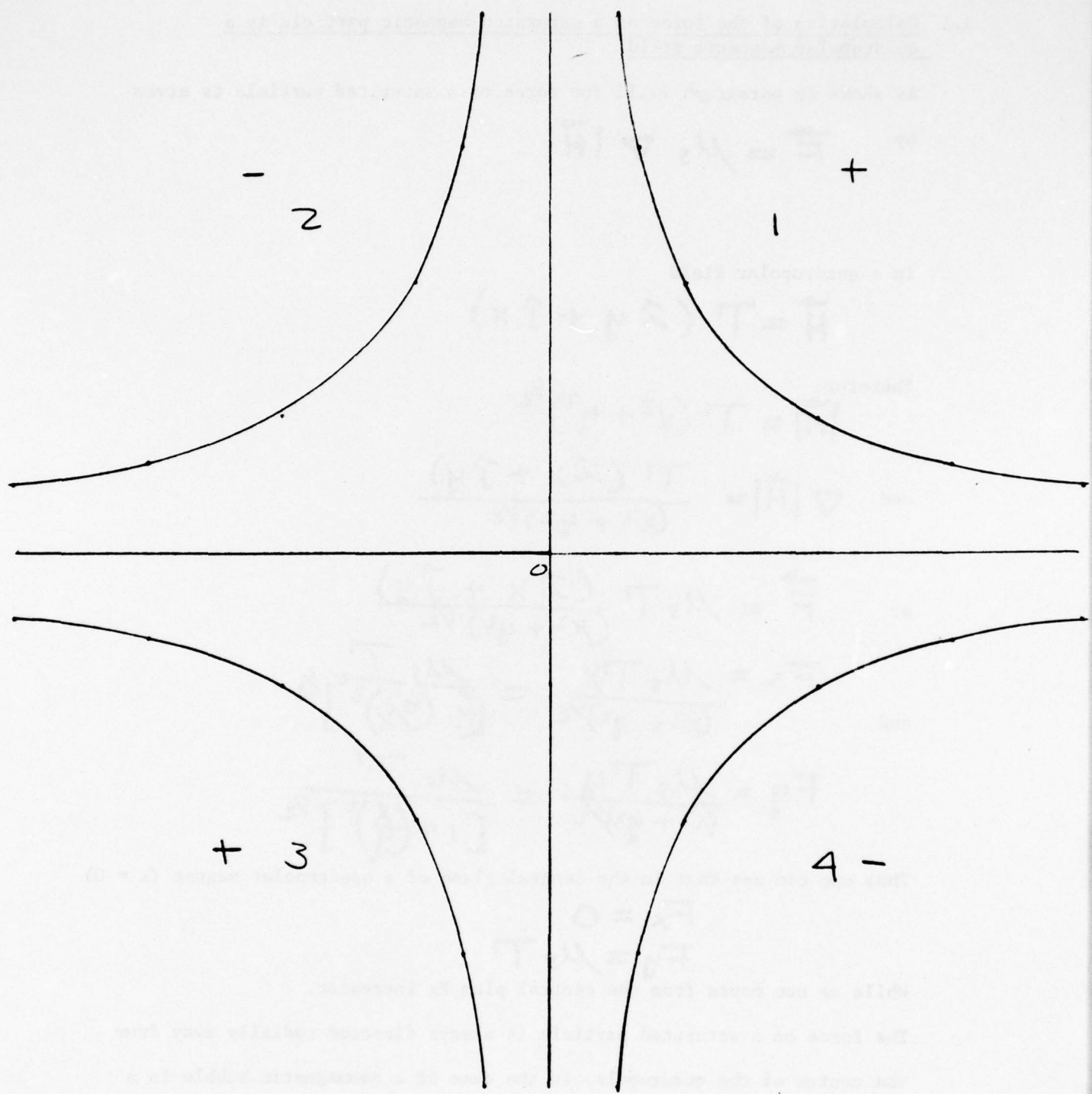


Fig A-1

3.1 Calculation of the force on a saturated magnetic particle in a quadrupolar magnetic field

As shown in paragraph 2.12 for force on a saturated particle is given

by  $\vec{F} = \mu_s \nabla |\vec{H}|$

in a quadrupolar field

$$\vec{H} = T (\hat{i}y + \hat{j}x)$$

Therefore

$$|\vec{H}| = T (x^2 + y^2)^{1/2}$$

and  $\nabla |\vec{H}| = \frac{T (\hat{i}x + \hat{j}y)}{(x^2 + y^2)^{1/2}}$

or  $\vec{F} = \mu_s T \frac{(\hat{i}x + \hat{j}y)}{(x^2 + y^2)^{1/2}}$

and  $F_x = \frac{\mu_s T x}{(x^2 + y^2)^{1/2}} = \frac{\mu_s T}{[1 + (y/x)^2]^{1/2}}$

$$F_y = \frac{\mu_s T y}{(x^2 + y^2)^{1/2}} = \frac{\mu_s T}{[1 + (x/y)^2]^{1/2}}$$

Thus one can see that in the central plane of a quadrupolar magnet ( $x = 0$ )

$$F_x = 0$$

$$F_y = \mu_s T$$

While as one moves from the central plan  $F_x$  increases.

The force on a saturated particle is always directed radially away from the center of the quadrupole. In the case of a nonmagnetic bubble in a saturated ferrofluid the force is always directed radially toward the center of the quadrupole.

3.2 Calculation of the force on an unsaturated (paramagnetic) particle in a quadrupolar magnetic field

As shown in paragraph 2.2.2 the force on a paramagnetic particle is given by

$$\vec{F} = \frac{\kappa}{2} \nabla (\vec{H} \cdot \vec{H})$$

In the case of a quadrupolar field.

$$\vec{H} = T(\hat{x}y + \hat{y}x)$$

and:  $\vec{H} \cdot \vec{H} = T^2(x^2 + y^2)$

thus:  $\nabla(\vec{H} \cdot \vec{H}) = 2T^2(-x + \hat{y}y)$

therefore:  $\vec{F} = \kappa T^2(\hat{x}x + \hat{y}y)$

or  $F_x = \kappa T^2 x$

$$F_y = \kappa T^2 y$$

Where  $\kappa$  was defined in paragraph 2.2.1 as

$$\kappa = (\text{volume of particle}) \chi / (1 + \chi N)$$

where

$\chi$  = susceptibility of the material

$N$  = the demagnetizing factor for the sample particle

$$(\frac{N}{4\pi}) = \frac{1}{3} \text{ for a spherical particle}$$

As in the case of the saturated particle, the force on a paramagnetic particle is directed radially away from the center of the quadrupolar field. In the case of a bubble in a paramagnetic liquid the force is directed radially toward the center of the quadrupole.

## APPENDIX B

### SECOND ORDER EFFECTS IN FLUIDMAGNETIC BUOYANCY

R. A. Curtis\*  
Systems Division, AVCO Corporation

---

\*Permanent address: Purdue University, School of Aeronautics and  
Astronautics, West Lafayette, Indiana.

## ABSTRACT

A non-magnetic solid object placed in a magnetically responsive fluid in the presence of a magnetic field gradient experiences a net buoyancy force of magnetic origin. A procedure is developed to account for the effects of magnetic field distortion due to the difference of magnetic permeability between the fluid and the solid and non-zero dependence of fluid magnetization of magnetic field strength. This procedure gives an expression for the magnetic buoyancy force correct to first order in the dimensionless magnetization of the fluid and in the dimensionless variation of fluid magnetization across the object. Calculations are performed for a sphere, cylinder and plate in an applied magnetic field where the field and field gradient are either aligned or at right angles in order to give an indication of the range of force variation due to a change of shape and due to a change of applied field geometry. Variations on the order to 10% can be expected in typical applications.

## INTRODUCTION

Fluids which have a strong magnetic polarization have been developed. Such fluids, called ferrofluids, behave as true fluid continua in a variety of circumstances although they demonstrate special characteristics arising from their magnetic properties. One such characteristic leads to the phenomenon of fluidmagnetic buoyancy. This term refers to the force experienced by a non-magnetic body when placed in a ferrofluid in the presence of a magnetic field gradient. It has been shown by Rosensweig (1) that the magnetic buoyancy force  $F_M$  exerted on such a non-magnetic body of volume  $V$  is given by

$$F_M = -VMVH \quad (1)$$

where  $M$  is the magnetization of the ferrofluid and  $VH$  is the gradient of the magnitude of the magnetic field. This force exists in addition to the normal buoyancy force which exists in the presence of gravity. One way of interpreting the magnetic buoyancy force is suggested by an analogy with gravitational buoyancy. Thus, consider a region of stationary ferrofluid in equilibrium in the presence of a magnetic field gradient in the absence of gravity. Now the ferrofluid can be viewed as a collection of magnetic dipoles each of which experiences the well-known dipole force in the presence of a magnetic field gradient. Thus the fluid

in any small subvolume must experience a force which is the summation of these dipole forces. But since the fluid is in equilibrium, this magnetic force is balanced by surface forces exerted by the surrounding fluid. Now if we imagine the fluid in this subvolume to be replaced by some nonmagnetic solid then this solid will experience this surface force above, a force which arises from the magnetic characteristics of the surrounding fluid. This analogy for fluidmagnetic buoyancy, descriptive as it is, fails to account for the local distortion of the magnetic field caused by the presence of the non-magnetic region. In addition there is a second factor which will have to be considered, namely the variation of fluid magnetization with magnetic field. This variation, which is always present, will give a further distortion of the surface force distribution over that predicted by the gravitational buoyancy analogy. These two effects will appear as corrections to the result stated in equation (1). The two corrections noted here, due to field distortion and to variation of magnetization with magnetic field, have analogues in the case of gravitational buoyancy although the effects are quite small. The gravitational field distortion is, of course, extremely small and the variation of fluid density with pressure given an extremely small effect in liquids. In fluidmagnetic buoyancy, though, the related magnetic effects can be significant.

## 1. FERROHYDROSTATICS

In a ferrofluid at rest there exists a balance of mechanical (pressure) and electromagnetic stresses such as to satisfy the following equation (2)

$$-\frac{\partial P}{\partial X_i} + \frac{\partial T_{ij}}{\partial X_j} = 0 \quad (2)$$

where  $P$  is the mechanical pressure and  $T_{ij}$ , the Maxwell stress tensor, is given by

$$T_{ij} = \frac{1}{4\pi} \{ H_i B_j - (\oint B dH) \delta_{ij} \}$$

The subscripts here represent the Cartesian tensor notation;  $H_i$  is the magnetic field;  $B_i$  is the magnetic induction;  $B$  and  $H$  denote the magnitudes of vectors  $B_i$  and  $H_i$  respectively. Notice that this expression for the force balance uniquely separates the mechanical stress from the magnetic stress. This separation is possible (3) if the fluid magnetization, defined by the constitutive equation

$$\underline{M} = \frac{1}{4\pi} (\underline{B} - \underline{H}) \quad (3)$$

has the following form

$$\underline{M} = M(T, H) \hat{e}_H \quad (4)$$

where  $M$  is the magnitude of the magnetization vector,  $T$  is the fluid temperature, and  $\hat{e}_H$  is a unit vector in the direction of the magnetic field.

We will assume that the magnetization has no temperature dependence. Then equations (2), (3), and (4) combined with the equation  $\nabla \cdot \underline{B} = 0$  give

$$-\nabla P - [1 + 4\pi \frac{M}{H}] [\underline{H} \times (\nabla \times \underline{H})] = 0 \quad (5)$$

If the fluid is non-conducting, Ampere's Law requires that  $\nabla \times \underline{H} = 0$  so we can conclude that the mechanical pressure, under the stated conditions, is uniform throughout the fluid.

The force exerted on a solid surface in contact with the ferrofluid is not determined solely by the mechanical pressure but has contributions from the magnetic forces which act on the fluid and are transmitted at the interface to the solid. The force exerted by the fluid on the wall, which will be referred to as  $P_w$  (it is a normal force and can thus be represented as a pressure as will be shown below), is different from the sum of the mechanical pressure and the magnetic potential ( $\int M dH$ )

by a term which represents the magnetic force exerted on the magnetic "charge" ( $\underline{M} \cdot \hat{n}$ ) which naturally exists at the interface. The specific form of this surface term follows from equation (2) as applied to a pillbox located at the interface such that one of its ends is located just inside the fluid and the other end is located just at the edge of the fluid. It is recognized in discussing this pillbox that the fluid magnetization varies continuously in approaching the interface from a finite value just inside the fluid to a value of zero as we reach the portion of the interface where there is no longer any fluid. The pillbox is imagined to become small such that its height is always small relative to the diameter of its end face. Integrating equation (2) across this imaginary pillbox using the divergence theorem to convert the volume integrals to surface integrals we have

$$(P_w - P) n_i = \{ T_{ij} n_j \} \quad (6)$$

where  $n_i$  is the unit normal vector to the interface (pointing into the fluid) and the bracket denotes the change of the enclosed quantity from just outside to just inside the fluid. Evaluating the right-hand side of equation (6) using the Maxwell stress (equation 2) gives

$$\{ T_{ij} n_j \} = \{ H_i B_j n_j \} - \{ n_i \int B dH \} \quad (7)$$

Applying the two Maxwell equations ( $\nabla \cdot \underline{B} = 0$  and  $\nabla \times \underline{H} = 0$ ) across the pillbox establishes that

$$\{T_{ij} n_j\} = \left( \int M dH \right) \hat{n} + 2\pi (\underline{M} \cdot \hat{n})^2 \hat{n}$$

Notice that there is no tangential component to this magnetic force, a consequence of the condition  $\underline{M} \times \underline{H} = 0$  implied by equation (4). Thus,

$$P_w = P + \int_0^H M dH + 2\pi (\underline{M} \cdot \hat{n})^2 \quad (8)$$

The second term on the right represents the integrated effect of the magnetic body force acting throughout the volume of the fluid and the last term represents the magnetic force acting on the surface "charge" layer at the interface. The net force exerted by the fluid on a submerged object is then given by

$$\underline{F}_m = - \int_S P_w \hat{n} dA \quad (9)$$

where the integration extends over the surface of the object in question.

Since in the electrically non-conducting fluid situation with temperature-independent magnetization considered here the mechanical pressure is constant, the evaluation of  $\underline{F}_m$  involves

the determination of the magnetic fields at the surface of the non-magnetic object. Thus we need to solve the magnetostatics problem in the fluid and in the non-magnetic solid. In the solid magnetic field satisfies

$$\begin{aligned}\bar{\nabla} \cdot \underline{H} &= 0 \\ \bar{\nabla} \times \underline{H} &\approx 0\end{aligned}\tag{10}$$

so that the magnetic field can be derived from a potential which satisfies Laplace's equation. In the fluid the appropriate field equations are

$$\begin{aligned}\bar{\nabla} \times \underline{H} &= 0 \\ \bar{\nabla} \cdot \underline{H} + 4\pi \nabla \cdot \underline{M} &= 0\end{aligned}\tag{11}$$

Using equation (4) the latter equation becomes

$$(1 + \frac{4\pi M}{H}) \nabla \cdot \underline{H} + (\underline{H} \cdot \nabla) \frac{4\pi M}{H} = 0\tag{12}$$

Our interest here will be restricted to the solutions of equations (11) in the case where the fluid is nearly saturated (corresponding to sufficiently high magnetic fields). Thus the magnetization can be expressed as a function of  $H$  as

$$M = M_0 + \left(\frac{\partial M}{\partial H}\right)_0 (H - H_0)\tag{13}$$

where  $M_o$  is the value of magnetization corresponding to  $H_o$  and where it will be assumed that  $(\frac{\partial M}{\partial H})_o$  is a constant, independent of  $H$ . Our attention will, furthermore, be restricted to a consideration of magnetic fields which possess a gradient ( $\Gamma$ ). The quantity  $\Gamma$  can be viewed as the field gradient in the absence of the fluid as will be clarified later.

Notice that equation (12) is non-linear. The solution depends on the following dimensionless quantities

$$\rho \equiv \frac{4\pi M_o}{H_o} ; \quad \delta \equiv 4\pi (\frac{\partial M}{\partial H})_o ; \quad \epsilon \equiv \frac{\Gamma a}{H_o} \quad (14)$$

where  $a$  is a measure of the size of the non-magnetic object (radius of a sphere, for example);  $\epsilon$  measures the percentage change in the applied magnetic field over a distance characteristic of the submerged object. It will be assumed that  $\rho$ ,  $\delta$ , and  $\epsilon$  are small quantities. The magnetic field then will be expanded in ascending powers of these smallness parameters. Thus,

$$\underline{H} = \underline{H}_o + \epsilon \underline{H}_o \underline{h}_1 + \rho \underline{H}_o \underline{h}_2 + \epsilon \rho \underline{H}_o \underline{h}_3 + \epsilon \delta \underline{H}_o \underline{h}_4 + \rho \delta \underline{H}_o \underline{h}_5 + \dots \quad (15)$$

where  $\underline{H}_o$  is a constant and the  $\underline{h}_i$  are dimensionless functions of position and have magnitudes of order one. The term  $\epsilon \underline{h}_1$  represents the (applied) field gradient;  $\rho \underline{h}_2$  represents the field due to the distribution of "charge" at the surface of the

non-magnetic body. There is no term linear in  $\delta$  since the  $\delta$  correction (equation 13) always appears multiplied by another smallness parameters. Representing the magnitude of the magnetic field by

$$H = H_0 [1 + \epsilon h'_1 + \rho h'_2 + O(\epsilon\rho)] \quad (16)$$

equation (12) becomes

$$[1 + \rho + O(\epsilon\rho)] \nabla \cdot \underline{H} - (\rho - \delta) \epsilon H_0 (\hat{e}_{H_0} \cdot \nabla) h'_1 + O(\rho^2) = 0 \quad (17)$$

The magnetic field will be calculated here correct to  $O(\epsilon\rho, \epsilon\delta)$ . The term of order  $\epsilon$  gives the lowest order contribution to the force i.e. equation (1). The term  $\epsilon\rho$  will give the lowest order effect due to the finite magnetization of the fluid, the term  $\epsilon\delta$  will give the lowest order effect due to the departure from complete saturation. For the symmetric bodies considered here (sphere, cylinder, plate with

short dimension aligned with the principal component of the magnetic field gradient) even terms, such as  $\epsilon^2$ , will integrate to zero when inserted into the expression for  $F_m$ . As a consequence size effects (the size appears only in  $\epsilon$ ) will not appear as a lowest order correction - size appears as a correction at least of  $O(\epsilon^2)$ .

Inserting equations (15) and (16) into equation (17) gives the following equations for the  $\underline{h}_1$

$$\nabla \cdot \underline{h}_1 = 0$$

$$\nabla \cdot \underline{h}_2 = 0$$

$$\nabla \cdot \underline{h}_3 + (\hat{e}_{H_0} \cdot \nabla) \underline{h}_1' = 0 \quad (18)$$

$$\nabla \cdot \underline{h}_4 + (\hat{e}_{H_0} \cdot \nabla) \underline{h}_1' = 0$$

$$\nabla \times \underline{h}_1 = 0, \text{ all } i$$

Thus  $\underline{h}_1$  and  $\underline{h}_2$  can each be found using a potential which satisfies Laplace's equation. This is not true, however, for  $\underline{h}_3$  and  $\underline{h}_4$ . The procedure for constructing the field, correct to  $O(\epsilon\rho)$ , is best illustrated by an example as is provided in the next section.

## 2. SPECIFIC EXAMPLES OF SINGLE PARTICLE FLUIDMAGNETIC BUOYANCY

### A. Right Circular Cylinder in Aligned Field Case

Consider an infinitely long non-magnetic right circular cylinder of radius  $a$  placed in a ferrofluid in a region in which the magnetic field and magnetic field gradient are aligned (i.e., the cross-product of the field and field-gradient is zero to  $O(\epsilon)$ ). Cartesian and

cylindrical coordinate systems with their origins at the center of the cylinder will be used. The polar angle  $\theta$  is measured from the direction of the applied magnetic field.

As a more intuitive approach to constructing the magnetic field than that outlined in the previous section consider the following: a magnetic field with an associated field gradient is produced in the region occupied by the fluid and cylinder in the absence of both the fluid and cylinder (this represents  $\underline{H}_0$  and  $\underline{h}_1$ ); the influence of the fluid is then added (giving contributions to the terms  $\underline{h}_3$  and  $\underline{h}_4$ ); and finally the field associated with the magnetic "charge" layer associated with the cylinder is added (giving  $\underline{h}_2$  and additional terms  $\underline{h}_3$  and  $\underline{h}_4$ ). Thus an acceptable field in the absence of fluid and cylinder is given by:

$$\underline{H} = (\underline{H}_0 + \Gamma x) \hat{i} + (-\Gamma y) \hat{j}$$

In the presence of the fluid this field must be corrected by a term  $\underline{h}_3$  (which is not divergence free). An acceptable correction is given by:

$$\underline{H} = [\underline{H}_0 + \Gamma(1 + \rho - \delta)x] \hat{i} + [-\Gamma y] \hat{j}$$

Finally, consider the effect on this field of adding the cylinder. The presence of the cylinder introduces additional fields ( $\underline{h}_2$  and  $\underline{h}_3$ ) which are divergence- and curl-free (the part of  $\underline{h}_3$  which is not divergence free was accounted for in the previous step). The exact form of  $\underline{h}_3$  and  $\underline{h}_4$  is dictated by the necessity of satisfying the magnetic boundary conditions  $\{\underline{B} \cdot \hat{e}_r\} = 0$  and  $\{\hat{e}_\theta \times \underline{H}\} = 0$  at the surface of the cylinder. The field inside the cylinder must be

divergence- and curl-free. Consider then,

$$\underline{H}_{in} = (H_1 + B'x)\hat{i} + (-B'y)\hat{j}$$

where  $H_1$  and  $B'$  are constants. The boundary conditions can be satisfied to  $O(\epsilon\rho)$  provided  $\underline{h}_2$  is a dipole of strength  $(1/2)\rho H_0 a^2$  oriented in the  $x$ -direction and the additional term in  $\underline{h}_3$  is due to a quadrupole of strength  $(1/8)(\rho+\delta)\epsilon H_0 a^3$ . The dipole and quadrupole terms are derived from the following potentials:

$$\phi_{Dipole} = \frac{\mu \cos \theta}{r}$$

$$\phi_{Quad} = \frac{n}{r^2} (\cos^2 \theta - \sin^2 \theta)$$

Corresponding to these values, the values of  $H_1$  and  $B$  are:

$$H_1 = H_0 + 2\pi M_0$$

$$B = \Gamma \left( 1 + \frac{3}{4} \epsilon - \frac{1}{4} \delta \right)$$

The field in the fluid at the surface of the cylinder is then given by:

$$\begin{aligned} \frac{H}{H_0} = & [\cos \theta - \frac{1}{2} \rho \cos \theta + \epsilon (\cos^2 \theta - \sin^2 \theta) \\ & + \epsilon \rho (\frac{3}{4} \cos^2 \theta + \frac{1}{4} \sin^2 \theta) + \frac{1}{4} \epsilon \delta (-\frac{5}{4} \cos^2 \theta + \sin^2 \theta)] \hat{e}_r \\ & - [\sin \theta + \frac{1}{2} \rho \sin \theta + 2\epsilon \sin \theta \cos \theta \\ & + \frac{3}{2} \epsilon \rho \sin \theta \cos \theta - \frac{1}{2} \epsilon \delta \sin \theta \cos \theta] \hat{e}_\theta \end{aligned} \quad (19)$$

Knowing this magnetic field distribution, the net force on the cylinder can be calculated using equation (9). Thus, the force is

given by, after some algebraic manipulations,

$$\mathbf{F}_m = -M_0 \Gamma V (1 + \rho - \frac{1}{2} \delta) \mathbf{j} \quad (20)$$

### B. Results for Additional Geometries

To give an indication of the range of second-order effects possible in fluidmagnetic buoyancy calculations similar to those presented in the previous section have been carried out for the following additional cases: cylinder in a crossed geometry (magnetic field and field gradient at right angles); a sphere and a flat plate in the aligned and crossed field geometry. The plate is stably aligned when its short axis is aligned in the direction of the gradient of the magnitude of the magnetic field.

The results of these calculations are summarized in the following table:

|          | ALIGNED $\nabla H \uparrow \uparrow \underline{H}$ | CROSSED $\nabla H \uparrow \uparrow \underline{H}$ |
|----------|--|--|
| CYLINDER | $-M_0 \Gamma V (1 + \rho - \frac{\delta}{2})$      | $-M_0 \Gamma V (1 + \frac{1}{2} \delta)$           |
| SPHERE   | $-M_0 \Gamma V (1 + \rho - \frac{2}{3} \delta)$    | $-M_0 \Gamma V (1 + \frac{1}{3} \delta)$           |
| PLATE    | $-M_0 \Gamma V (1 + \delta)$                       | $-M_0 \Gamma V (1 + \rho)$                         |

Table 1: Summary of Force Corrections Due to Finite Magnetization ( $\rho$ ) and Incomplete Saturation ( $\delta$ ).

The shape dependence is clearly seen, for instance, in the absence of the finite magnetization correction from the cylinder and sphere in the crossed geometry although it does appear for the plate in this geometry. It will also be observed that the sign of the finite magnetization correction changes for the cylinder and sphere between the aligned and crossed geometry.

To give an idea of the magnitudes of these corrections in practice, consider the following typical set of parameters for fluid-magnetic buoyancy:

$$H_0 = 10^3 \text{ oe} ; 4\pi M_0 = 10^2 \text{ oe} ; \frac{1}{M_0} \left( \frac{\partial M_0}{\partial H} \right) = 10^{-4} \text{ (oe)}^{-1}$$

giving  $\rho = .10$  ;  $\delta = .01$  . Thus, for example, a variation of about 10% in the buoyancy force could be expected between, say, a sphere and a plate in either the aligned or the crossed geometry.

#### REFERENCES

1. Rosensweig, R. E., AIAA J., 4 (1966) 1751.
2. Curtis, R. A., Phys. Fluids, 14 (1971) 2096.
3. Chu, B., Phys. Fluids, 2 (1959) 473.

APPENDIX C

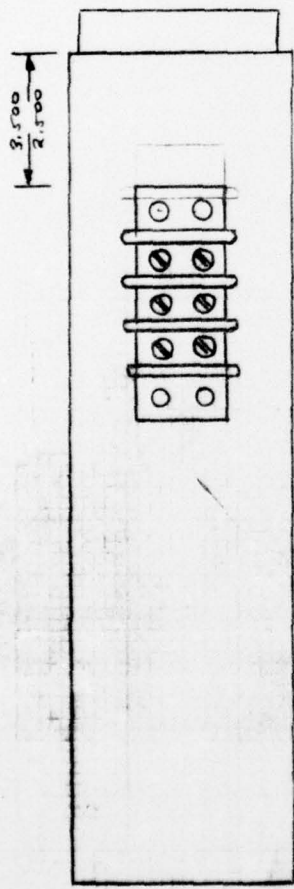
HIGH GRADIENT MAGNETIC DESIGN

1- WINDING: 220 TURNS OF COPPER (.010)  
SHEET WET WOUND WITH .001 KRAFT PAPER  
AND POLYESTER RESIN. (CHARGE OR SPECIFIC  
REIN LEFT TO THE VENDOR)

2- COOLING PLATE TO BE MOUNTED AT ONE  
END OR IN THE CENTER, CHARGE OR LOCATION  
IS LEFT TO THE VENDOR

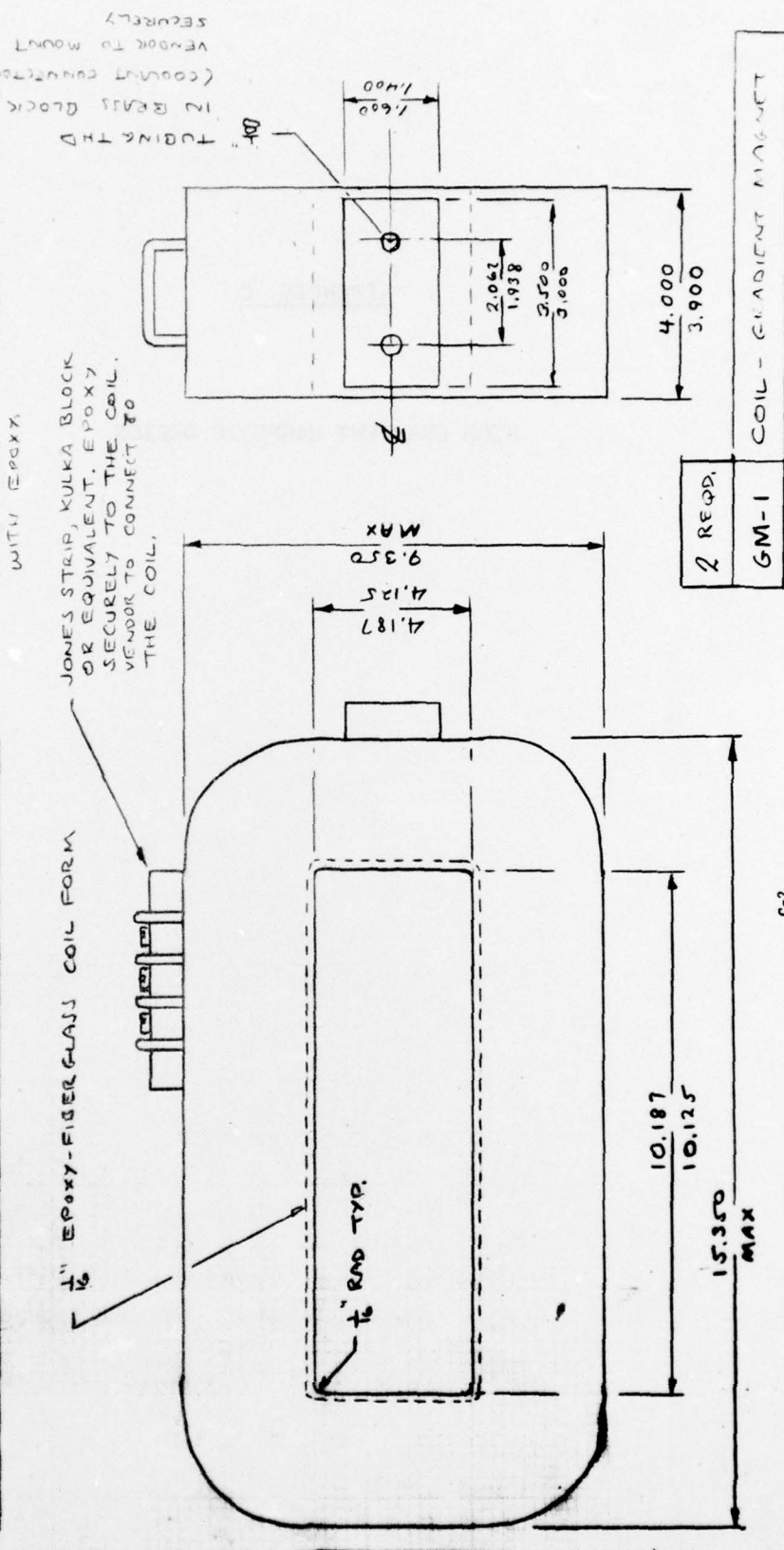
3- SUPPLIED VENDOR: OGALLALA ELECTRONICS  
MFG. CO., OGALLALA, NEBR.

4- EXTERIOR OF THE COIL TO BE WOUND  
WITH GLASS TAPE AND INSULATORS  
WITH EPOXY.

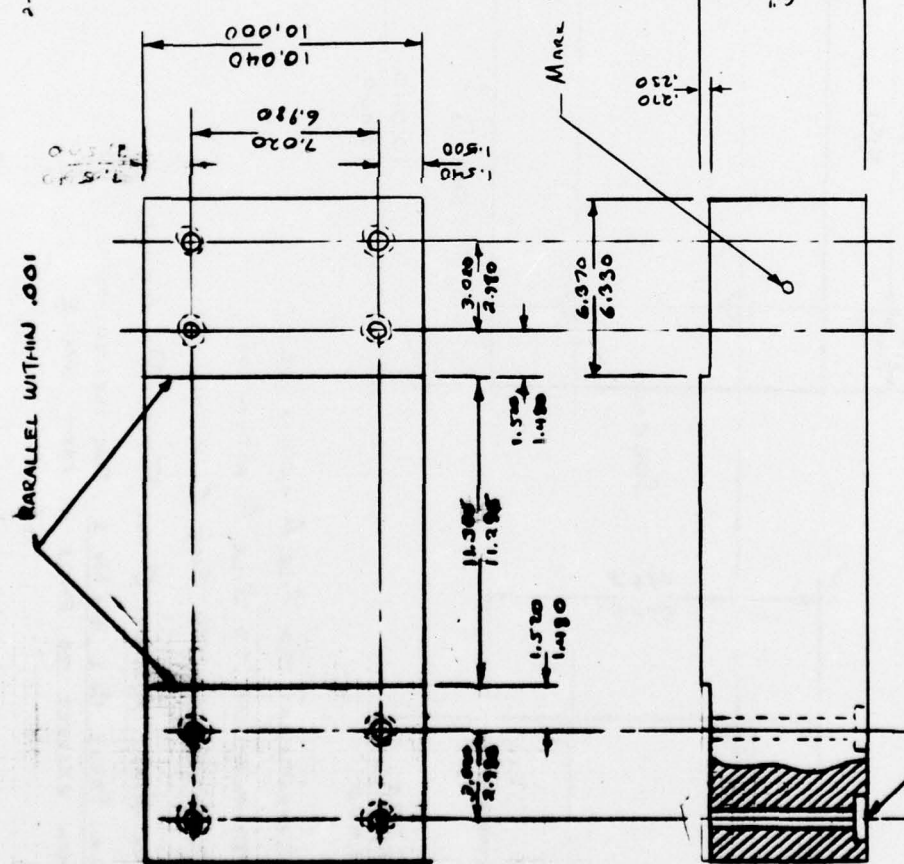


1/2" EPOXY-GLASS COIL FORM

JONES STRIP, KULKA BLOCK  
OR EQUIVALENT, EPOXY  
SECURELY TO THE COIL.  
VENDOR TO CONNECT TO  
THE COIL.



1- MATE'L: HOT ROLLED  
PUNTE  
2- SUGGESTED VENDOR: RYDERSON STEEL  
ALLSTON, MASS.

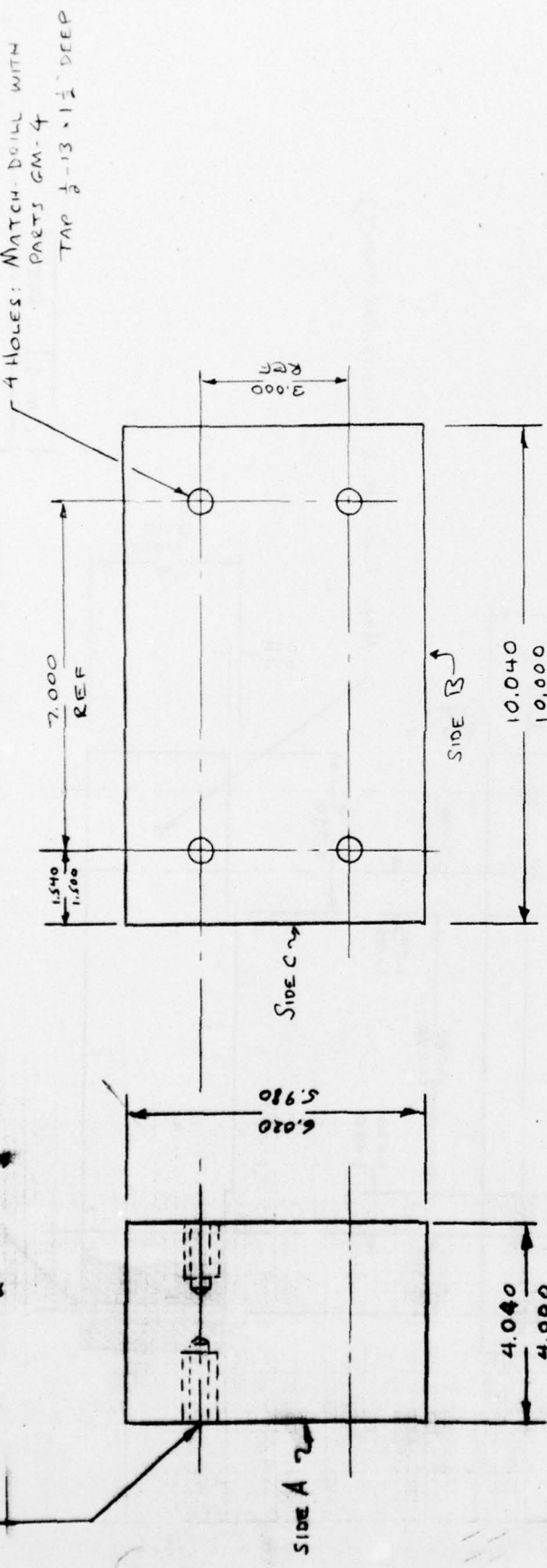


GM-2 1 REQD.

Base Plate - GM-2

C-3

4 HOLES: MASONITE DOME W/ 1/2" DEEP  
TAP  $\frac{1}{2} - 13 \times 1\frac{1}{2}$ " DEEP

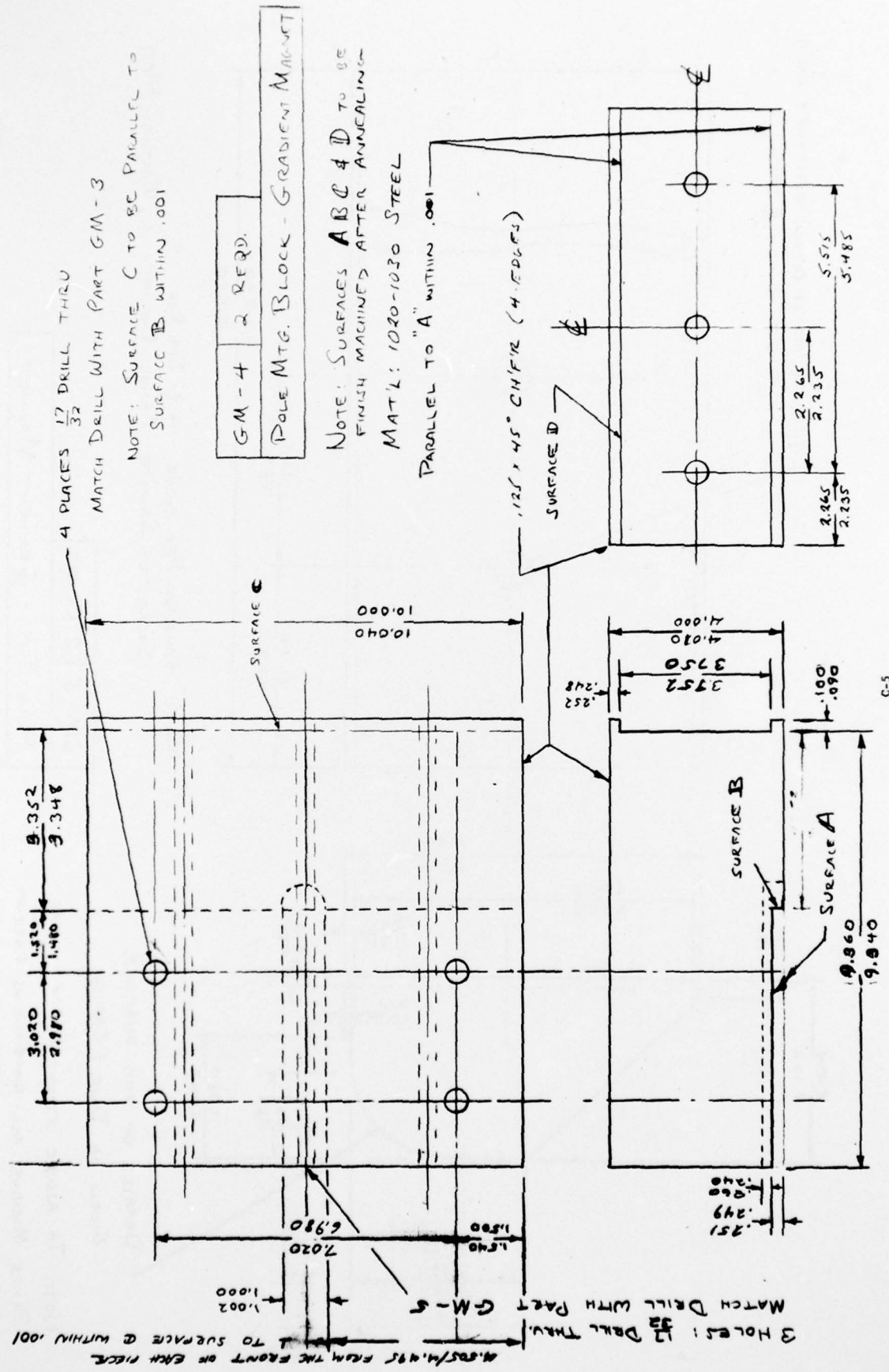


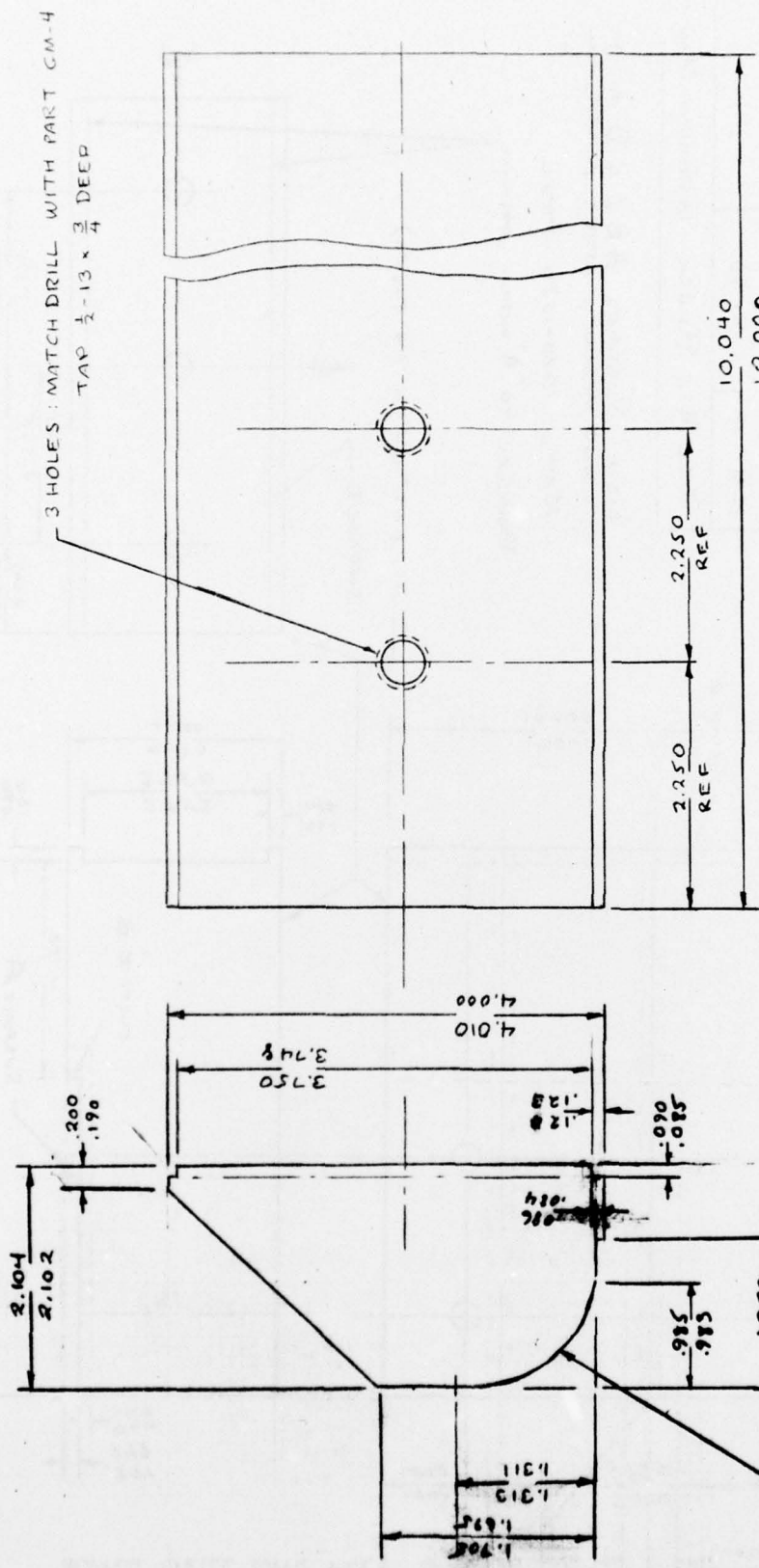
SIDE B PERPENDICULAR TO SIDE A WITHIN .001  
SIDE C PERPENDICULAR TO SIDE A WITHIN .001  
SIDE B PERPENDICULAR TO SIDE C WITHIN .001

NOTE: MARK SIDES A, B AND C FOR FUTURE REFERENCE  
MARK PARTS NO. 1 AND NO. 2 FOR IDENTIFICATION  
WITH RESPECT TO ENDS OF PART GM-2

MAT'L: HOT ROLLED 1020-1030 STEEL  
PLATE  
SUGGESTED VENDOR: RICHMOND STEEL,  
ALLSTON, MASS.

|  |        |
|--|--------|
| GM-3                                   | 2-REQD |
| POLE SUPPORT BLOCK - C-101017 M1A1-NFT |        |





MATÉ: VANADIUM PERMENDUR - 4  $\frac{1}{2}$  " Dia. Rod  
SUGGESTED SOURCE: ARNOLD ENGINEERING, Waltham, Mass.

DETAILS OF THIS SURVEY

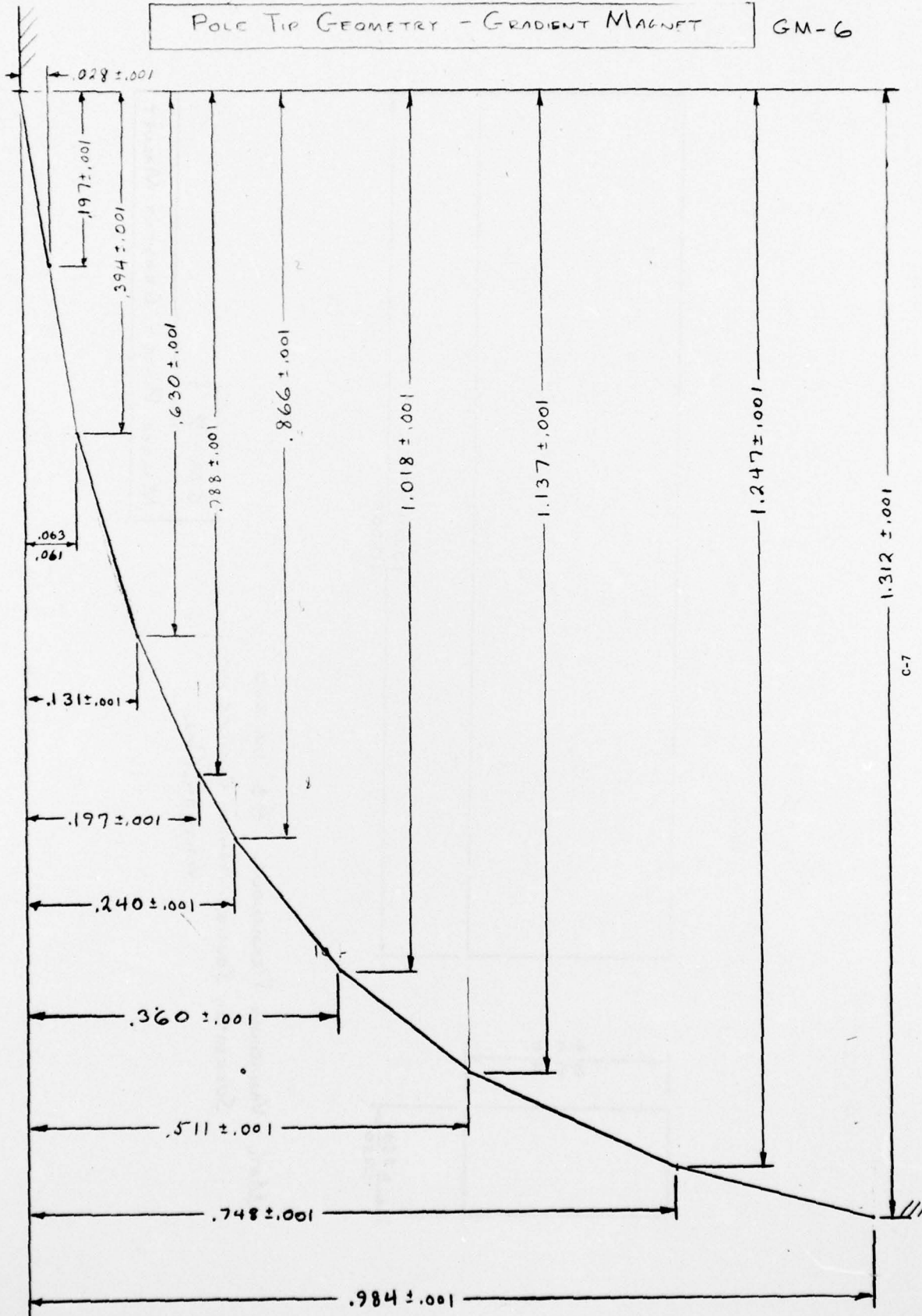
NOTE: TO ASSURE SYMMETRY OF THESE PARTS MACHINE ALL DIMENSIONS EXCEPT THE LENGTH 10.040/10.000 ON ONE PLATE.

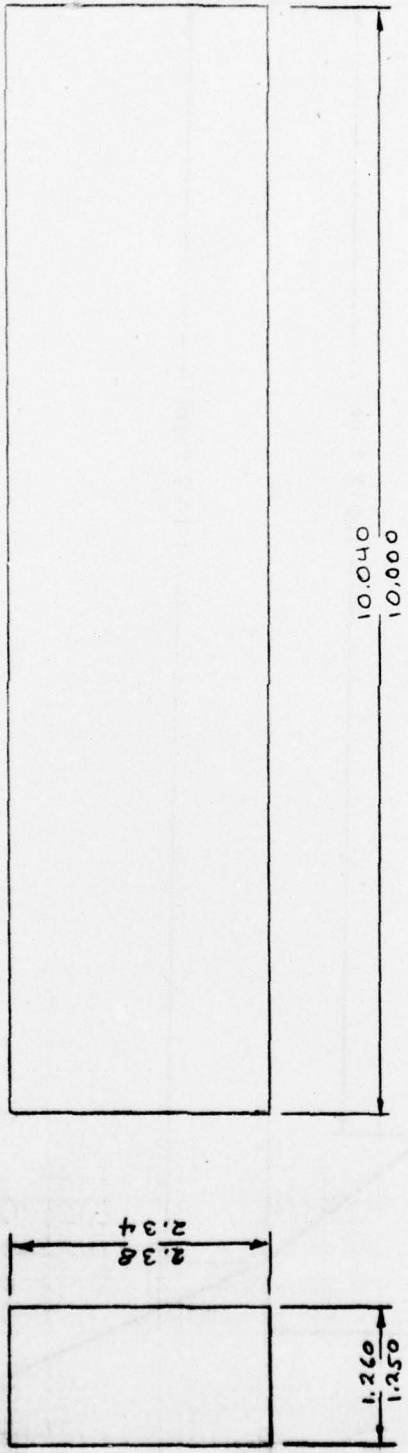
GM-5 2 RECORD

## Pole Tip - Gradient Magnet

Pole Tip Geometry - Gradient Magnet

GM-6

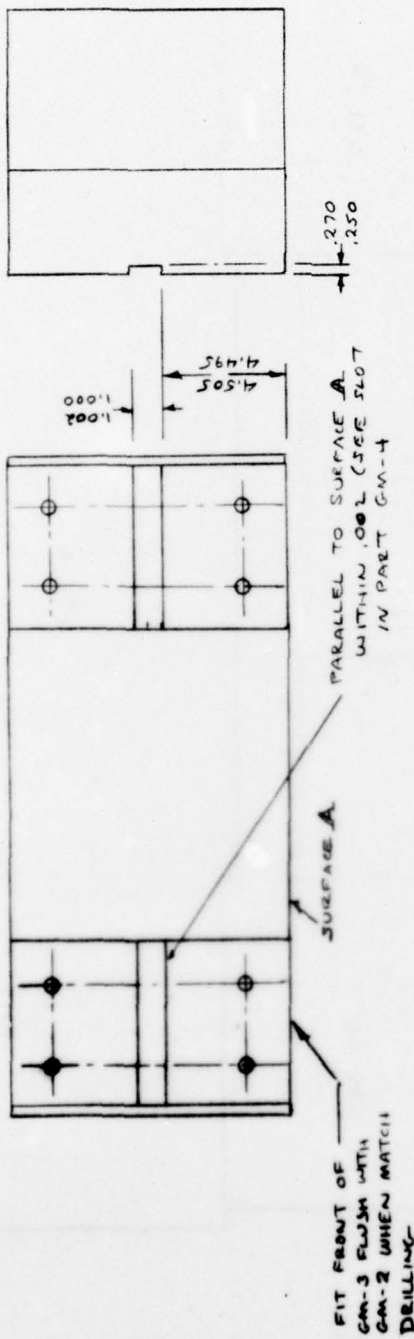




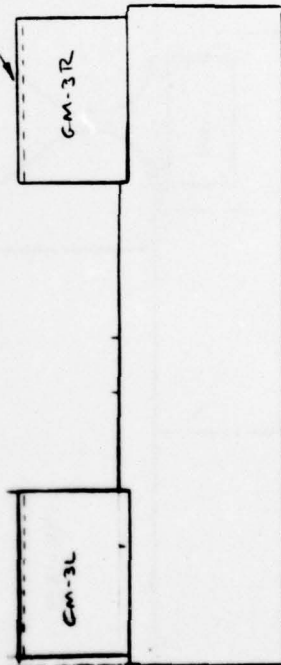
Mat: Vanadium Permendur : 4  $\frac{1}{2}$ " dia. rod  
 SUGGESTED SOURCE: Arnold Engineering,  
 Waltham, Mass

GM-7

Mirror Plate - Gradient Magnet

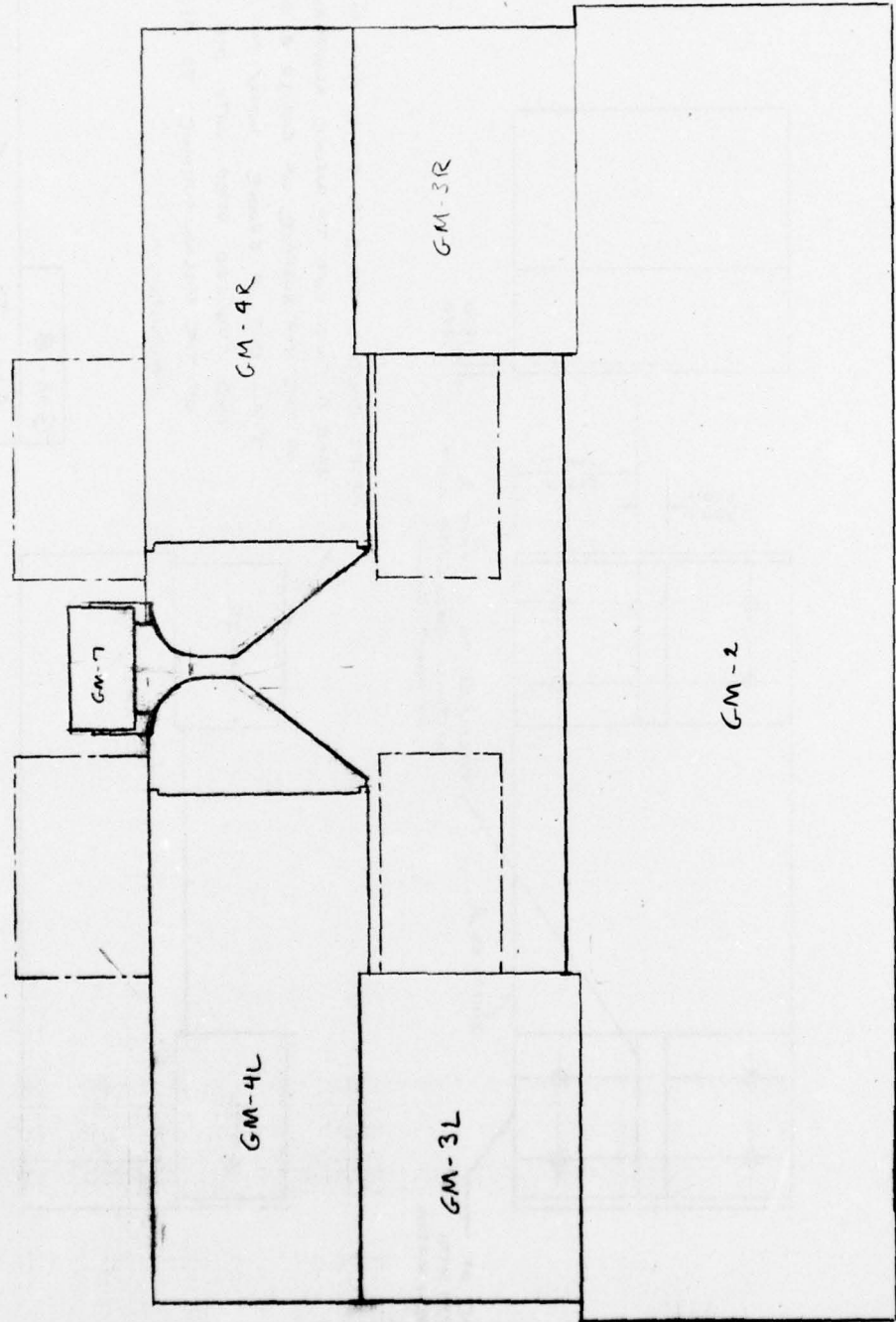


AFTER BOLTING GM-3 TO GM-2 AND PINING  
TAKE A FINISH CUT TO INSURE ALIGNMENT  
OF THE TOP SURFACE OF GM-3R & GM-3L  
THEN CUT A CROOVE 1.002/1.000 WIDE  
AND .770/.250 DEEP WITH ONE SETTING  
OF THE MILLING MACHINE TO A LINE  
PARALLEL TO A LINE



GM-8

Assy. Due. - Graduate Mfg. RT



GM-9 Assn Dwg. - C-100017 - 11/1967

c-10

